

FINAL REPORT

**ECOSYSTEM LEVEL ALTERATIONS IN SOIL NUTRIENT CYCLING:
AN INTEGRATED MEASURE OF CUMULATIVE EFFECTS OF ACIDIC DEPOSITION ON
A MIXED CONIFER FOREST
IN SOUTHERN CALIFORNIA**

Contract No. 92-335

March 4, 1996

Submitted to:

**Dr. John R. Holmes
Chief, Research Division
California Air Resources Board
Sacramento, CA 95812**

Prepared by:

**P.R. Miller, M.A. Poth, A. Bytnerowicz and M.E. Fenn
USDA Forest Service, Pacific Southwest Research Station
Riverside, CA 92507**

and

**P.J. Temple
Statewide Air Pollution Research Center
University of California
Riverside, California 92521**

and

**J.C. Chow, J.G. Watson, C. Frazier and M. Green
Energy and Environmental Engineering Center**

**D.W. Johnson
Biological Sciences Center**

at the

**Desert Research Institute
University of Nevada
Reno, Nevada 89506**

EXECUTIVE SUMMARY

This project was proposed and approved as a supplement to ARB Contract No. A032-180, "Assessment of Acidic Deposition and Ozone Effects on Conifer Forests in the San Bernardino Mountains." The final report for A032-180 was submitted in March 1996. The four tasks to be completed by this project (ARB Contract No. 92-335) were: (1) Continue dry deposition monitoring at Barton Flats for several months during the summer of 1994; (2) Calibrate the Nutrient Cycling Model (NuCM) for the Barton Flats area and run simulations to examine some possible effects of five levels of nitrogen deposition over a 40 yr period; (3) Determine the relationship between stomatal conductance and ozone uptake for Jeffrey pines of three size classes during diurnal and seasonal cycles; and provide a one-time assessment of the variability of stomatal conductance at several Sierra Nevada sites; (4) Conduct an intensive sampling study during July 18-31, 1993 in order to examine the fine structure of events or processes including, meteorology, atmospheric chemistry, pollutant flux to foliage, tree physiology, and the efflux of CO₂ and NO from soils.

The investigators elected to include the data from the additional dry deposition monitoring in the summer of 1994 as part of the report for Contract No. A032-180. The only portion of that work included in this report was the data from the intensive sampling period (summarized below).

The Nutrient Cycling Model (NuCM) was formerly appropriate for humid forests of the eastern United States but this project succeeded in calibrating it for Barton Flats, a "dry" ponderosa pine ecosystem. The model was used to simulate the effects of varying levels of atmospheric N deposition ranging from 0.14 to 6.83 kmol ha⁻¹ yr⁻¹ (1.9 to 95.6 kg ha⁻¹ yr⁻¹). Simulation results indicated a significant increase in NO₃⁻ leaching, reduced N retention, and a cessation of growth response to N input at deposition levels greater than 2.73 kmol ha⁻¹ yr⁻¹ (38.2 kg ha⁻¹ yr⁻¹). Increasing simulated N deposition levels from 0.14 to 0.68 and 1.37 kmol ha⁻¹ yr⁻¹ (1.9 to 9.5 and 19.5 kg ha⁻¹ yr⁻¹) reduced base cation leaching because of an anion shift from NO₃⁻ to HCO₃⁻ and SO₄²⁻ caused by lower soil solution pH. Increasing deposition levels resulted in reduced exchangeable base cation levels in the soil, especially at the highest deposition level (6.83 kmol ha⁻¹ yr⁻¹) and especially with respect to K⁺.

These simulation results are not offered as quantitative predictions of what specific response will occur at a specific N deposition loadings but rather as indicators of what is expected with changing N loadings based upon our best current knowledge of nutrient cycling within this ecosystem. The results of these simulations clearly identify key indicators of long-term deposition effects and suggest several hypotheses that could be tested in either a field or laboratory setting.

Average monthly O₃ flux to pines was calculated for daylight hours for each of the summer months of 1992 to 1994. Rates of stomatal conductance as measured for water vapor were converted to rates of conductance for O₃ and the average daily rate of conductance was calculated for each month. Flux of O₃ to foliage was calculated as average daily O₃ concentration times daily conductance rate. Ozone flux to pine foliage was highly variable, both from year-to-year and within the year. Ozone flux to foliage was highest in June, and declined rapidly after June particularly in a dry year such as 1994. From 60% to 70% of total annual ozone uptake occurred in the months of May, June, and July. Flux of ozone to foliage of mature pine trees averaged 30% lower than fluxes to seedlings and saplings during peak periods in early summer. Later in the summer

and in dry years, ozone flux to mature trees was equal to or only slightly lower than flux to foliage of other age classes of trees. Total amount of precipitation in the previous winter was associated with total ozone uptake in 1992 (high precipitation) and 1994 (low precipitation), but not in 1993, a year of high precipitation but low ozone uptake. These estimates of stomatal conductance and ozone flux also suggest that flux rates of other pollutants which enter the leaf through the cuticle and to some extent through the stomata, including HNO_3 , NH_3 , and NO_2 , would follow the same seasonal pattern as ozone. We are now able to compare this physiologically-based estimate of seasonal ozone flux to foliage of Jeffrey pine at Barton Flats with the purely physical estimate of flux simulated by the Big Leaf Model (Draft Final Report for Contract No. A032-180). This task is sizeable and is recommended for future study.

The one-time survey of environmental factors controlling stomatal conductance of pines at Sierra Nevada sites associated with the interagency project (Forest Ozone Response Study) found significant variation among sites, among plots, and among trees within plots. No geographical trends were observed. The best predictor of rates of conductance was needle length, which may be a good surrogate indicator of site conditions favoring tree growth. The sample size needs to be larger in order to increase confidence in this conclusion.

The intensive study during July 18-31, 1993 was carried out in order to observe as many processes as possible in finer time resolution. The day-to-day weather during the two week period was very typical of previous summers. No rain occurred so only air concentrations and dry deposition of acidic species and ozone could be measured or estimated. For example, at the monitoring station the sampling of particulate matter and reactive gas species was done for the morning period (0600 to 1200 PST), afternoon 1200 to 1800 PST and nighttime (1800 to next day 0600 PST). The lowest concentrations for the intensive monitoring period all occurred during the morning period, with the exception of $\text{PM}_{2.5}$ chloride and gaseous ammonia, sulfur dioxide, and nitric acid concentrations. It implies that $\text{PM}_{2.5}$ mass and ions vary significantly during the daytime and much of the information was not attainable by acquiring an integrated 12-hour sample, as was the normal sampling schedule for the remainder of this study and Contract No. A032-180. Comparisons of the two-week data set with earlier data showed that the air chemistry and meteorology was representative of the summer of 1992 and 1993.

During the intensive study dry deposition fluxes of nitrate and ammonium to foliage of container-grown ponderosa pines were similar at all three plots. Among ponderosa pine, white fir and California black oak, the highest deposition flux was to foliage of black oak. The measurement of stomatal conductances of seedling, sapling and mature Jeffrey pines over a diurnal period showed that 0900 to 1200 conductances were appropriate for estimating ozone flux for the entire daylight period. Carbon dioxide fluxes from soils were comparable to rates observed in other forest and chaparral soils. Nitric oxide fluxes exceeded those of eastern forests by an order of magnitude.

This project along with Contract No. A032-180 have provided an infrastructure for continued monitoring of the responses to climate, ozone, and acidic pollutants by the mixed conifer forests at Barton Flats. Additional products include an extensive database, published protocols and quality assurance objectives, and models that assist in estimating pollutant deposition to the forest canopy and long-term effects on nutrient cycling.

TABLE OF CONTENTS

EXECUTIVE SUMMARY	i
TABLE OF CONTENTS	iv
LIST OF TABLES	vi
LIST OF FIGURES	vii
1.0 INTRODUCTION	1-1
2.0 SIMULATED EFFECTS OF N DEPOSITION RATES ON GROWTH AND NUTRIENT CYCLING IN A PONDEROSA PINE FOREST	
2.1 Introduction	2-1
2.2 Site and Methods	2-1
2.2.1 Field Site	2-1
2.2.2 NuCM Model Calibration	2-2
2.3 Results	2-4
2.4 Discussion	2-5
2.5 Summary and Conclusions	2-6
2.6 Acknowledgments	2-6
2.7 References	2-7
3.0 PATTERNS OF GAS EXCHANGE AND OZONE UPTAKE IN PINES AT BARTON FLATS	
3.1 Introduction	3-1
3.2 Objective	3-1
3.3 Methodology	3-1
3.4 Results and Discussion	3-2
3.4.1 Pattern of Precipitation and Conductance	3-2
3.4.2 Diurnal Curves of Stomatal Conductance	3-4
3.4.3 Ozone Flux to Pine Foliage	3-4
3.5 Conclusions	3-5
3.6 References	3-6
APPENDIX A Environmental Evaluation of Foliar Injury Observation Plots in Forest Ozone Response Project	3-16

4.0	INTENSIVE STUDY: DAY TO DAY DESCRIPTION OF METEOROLOGY, POLLUTANT CONCENTRATIONS, POLLUTANT DEPOSITION AND TREE RESPONSES FROM JULY 18 TO 31, 1993	
4.1	Introduction	4-1
4.2	Methods	4-1
4.3	Results	4-2
4.3.1	Description of Weather and Ozone during the Intensive Study	4-2
4.3.1.1	Comparison of Meteorological Variables and Ozone for the July 18-31 Periods of 1992, 1993 and 1994 at the Barton Flats Monitoring Station	4-2
4.3.1.2	Meteorological and Ozone Measurements in the Forest Canopy at Plot # 2 During July 18-31, 1993	4-2
4.3.2	Dry Deposition Measurements at the Monitoring Station	4-3
4.3.3	Diurnal Variations of Particulate Nitrate, Nitric Acid, Particulate Ammonium, and Ammonia	4-3
4.3.4	Measurement of Greenhouse Gas Efflux from Soils at Plot 2	4-4
4.3.5	Dry Deposition to Foliage at Plots 1, 2 and 3	4-4
4.3.6	Diurnal Variation of Stomatal Conductance during July 20-22, 1993	4-4
4.4	Discussion	4-5
4.5	Summary	4-6
4.6	References	4-7

LIST OF TABLES		
2-1	Simulated net ecosystem balances of N, P, Ca, K, Mg and S under varying N deposition scenarios ($\text{kmol ha}^{-1} 40 \text{ yrs}^{-1}$).	2-10
2-2	Simulated nutrient distribution after 40 years under varying N deposition scenarios (kmol ha^{-1} and $\text{kmol ha}^{-1} \text{ yr}^{-1}$).	2-11
3-1	Annual ozone uptake in one-year-old foliage of three age classes of Jeffrey pines at Barton Flats, San Bernardino mountains, 1992 to 1994.	3-8
Appendix A Table 1.	Location of sites in Forest Ozone Response Study.	A-10
4-1	Contrast of 0600 to 1800 (PST) averages for temperature, relative humidity, solar radiation and ozone; total daily precipitation, and winds at 4 pm PST (the approximate time of the daily ozone peak) for the 07/18 to 07/31 periods of 1992, 1993 and 1994.	4-8
4-2	Statistical summary of gas/particle ambient concentrations acquired at the Barton Flats Station, CA, during the summer Intensive Study between 07/18/93 and 07/31/93.	4-9
4-3	Comparison of the averages of 15-17 gas/particle ambient daytime and nighttime concentrations acquired at Barton Flats between 06/01/94 to 08/31/94 with 13-14 daytime and nighttime samples obtained during the intensive sampling period between 07/18/93 and 07/31/93.	4-10
4-4	Deposition of nitrate and ammonium ($\mu\text{g m}^{-2} \text{ h}^{-1}$) to branches of mature trees at the forest floor level during the intensive study.	4-11
4-5	Deposition of sulfate to branches of mature trees at the forest floor level during the intensive study ($\mu\text{g m}^{-2} \text{ h}^{-1}$).	4-12

LIST OF FIGURES		
1-1	Schedule for completion of field work and analytical tasks.	1-2
2-1	Simulated nitrogen leaching at Barton Flats under various N deposition scenarios: 0.1 x = 0.14, 0.5 x = 0.68, 1 x = 1.37, 2 x = 2.73, and 3 x = 6.83 kmol ha ⁻¹ yr ⁻¹ (1.9, 9.5, 28.7, 38.2, and 95.6 kg ha ⁻¹ yr ⁻¹).	2-12
2-2	Simulated biomass at Barton Flats under various N deposition scenarios: 0.1 x = 0.14, 0.5 x = 0.68, 1 x = 1.37, 2 x = 2.73, and 3 x = 6.83 kmol ha ⁻¹ yr ⁻¹ (1.9, 9.5, 28.7, 38.2, and 95.6 kg ha ⁻¹ yr ⁻¹).	2-13
2-3	Simulated phosphorus leaching at Barton Flats under various N deposition scenarios: 0.1 x = 0.14, 0.5 x = 0.68, 1 x = 1.37, 2 x = 2.73, and 3 x = 6.83 kmol ha ⁻¹ yr ⁻¹ (1.9, 9.5, 28.7, 38.2, and 95.6 kg ha ⁻¹ yr ⁻¹).	2-14
2-4	Simulated potassium leaching at Barton Flats under various N deposition scenarios: 0.1 x = 0.14, 0.5 x = 0.68, 1 x = 1.37, 2 x = 2.73, and 3 x = 6.83 kmol ha ⁻¹ yr ⁻¹ (1.9, 9.5, 28.7, 38.2, and 95.6 kg ha ⁻¹ yr ⁻¹).	2-15
2-5	Simulated calcium leaching at Barton Flats under various N deposition scenarios: 0.1 x = 0.14, 0.5 x = 0.68, 1 x = 1.37, 2 x = 2.73, and 3 x = 6.83 kmol ha ⁻¹ yr ⁻¹ (1.9, 9.5, 28.7, 38.2, and 95.6 kg ha ⁻¹ yr ⁻¹).	2-16
2-6	Simulated magnesium leaching at Barton Flats under various N deposition scenarios: 0.1 x = 0.14, 0.5 x = 0.68, 1 x = 1.37, 2 x = 2.73, and 3 x = 6.83 kmol ha ⁻¹ yr ⁻¹ (1.9, 9.5, 28.7, 38.2, and 95.6 kg ha ⁻¹ yr ⁻¹).	2-17
2-7	Simulated base cation leaching at Barton Flats under various N deposition scenarios: 0.1 x = 0.14, 0.5 x = 0.68, 1 x = 1.37, 2 x = 2.73, and 3 x = 6.83 kmol ha ⁻¹ yr ⁻¹ (1.9, 9.5, 28.7, 38.2, and 95.6 kg ha ⁻¹ yr ⁻¹).	2-18
2-8	Simulated acid neutralizing capacity (ANC) leaching at Barton Flats under various N deposition scenarios: 0.1 x = 0.14, 0.5 x = 0.68, 1 x = 1.37, 2 x = 2.73, and 3 x = 6.83 kmol ha ⁻¹ yr ⁻¹ (1.9, 9.5, 28.7, 38.2, and 95.6 kg ha ⁻¹ yr ⁻¹).	2-19
2-9	Simulated soil solution nitrate concentrations in years 2 and 40 at Barton Flats under various N deposition scenarios: 0.1 x = 0.14, 0.5 x = 0.68, 1 x = 1.37, 2 x = 2.73, and 3 x = 6.83 kmol ha ⁻¹ yr ⁻¹ (1.9, 9.5, 28.7, 38.2, and 95.6 kg ha ⁻¹ yr ⁻¹).	2-20
2-10	Simulated soil solution pH in years 2 and 40 at Barton Flats under various N deposition scenarios: 0.1 x = 0.14, 0.5 x = 0.68, 1 x = 1.37, 2 x = 2.73, and 3 x = 6.83 kmol ha ⁻¹ yr ⁻¹ (1.9, 9.5, 28.7, 38.2, and 95.6 kg ha ⁻¹ yr ⁻¹).	2-21

2-11	Simulated soil base saturation at Barton Flats under various N deposition scenarios: 0.1 x = 0.14, 0.5 x = 0.68, 1 x = 1.37, 2 x = 2.73, and 3 x = 6.83 kmol ha ⁻¹ yr ⁻¹ (1.9, 9.5, 28.7, 38.2, and 95.6 kg ha ⁻¹ yr ⁻¹).	2-22
2-12	Simulated soil solution acid neutralizing capacity (ANC) concentrations in years 2 and 40 at Barton Flats under various N deposition scenarios: 0.1 x = 0.14, 0.5 x = 0.68, 1 x = 1.37, 2 x = 2.73, and 3 x = 6.83 kmol ha ⁻¹ yr ⁻¹ (1.9, 9.5, 28.7, 38.2, and 95.6 kg ha ⁻¹ yr ⁻¹).	2-23
2-13	Simulated soil solution sulfate concentrations in years 2 and 40 at Barton Flats under various N deposition scenarios: 0.1 x = 0.14, 0.5 x = 0.68, 1 x = 1.37, 2 x = 2.73, and 3 x = 6.83 kmol ha ⁻¹ yr ⁻¹ (1.9, 9.5, 28.7, 38.2, and 95.6 kg ha ⁻¹ yr ⁻¹).	2-24
2-14	Simulated soil solution total anion concentrations in years 2 and 40 at Barton Flats under various N deposition scenarios: 0.1 x = 0.14, 0.5 x = 0.68, 1 x = 1.37, 2 x = 2.73, and 3 x = 6.83 kmol ha ⁻¹ yr ⁻¹ (1.9, 9.5, 28.7, 38.2, and 95.6 kg ha ⁻¹ yr ⁻¹).	2-25
2-15	Simulated soil solution aluminum concentrations in years 2 and 40 at Barton Flats under various N deposition scenarios: 0.1 x = 0.14, 0.5 x = 0.68, 1 x = 1.37, 2 x = 2.73, and 3 x = 6.83 kmol ha ⁻¹ yr ⁻¹ (1.9, 9.5, 28.7, 38.2, and 95.6 kg ha ⁻¹ yr ⁻¹).	2-26
3-1	Maximum rates of stomatal conductance in one-year-old needles of three age classes of Jeffrey pines, and soil water content (0 to 15 cm) at the Barton Flats tower site in 1992.	3-7
3-2	Maximum rates of stomatal conductance in one-year-old needles of three age classes of Jeffrey pines, and soil water content (0 to 15 cm) at the Barton Flats tower site in 1993.	3-8
3-3	Maximum rates of stomatal conductance in one-year-old needles of three age classes of Jeffrey pines, and soil water content (0 to 15 cm) at the Barton Flats tower site in 1994.	3-9
3-4	Diurnal patterns of stomatal conductance in seedling, sapling, and mature Jeffrey pines at Barton Flats, based upon hourly measurements taken over 21-22 July 1993.	3-10
3-5	Mean monthly ambient ozone concentrations at Barton Flats, 1992 to 1994.	3-11
3-6	Monthly mean daily ozone flux to one-year-old foliage of seedling Jeffrey pine at Barton Flats, 1992 to 1994.	3-12
3-7	Monthly mean daily ozone flux to one-year-old foliage of sapling Jeffrey pine at Barton Flats, 1992 to 1994.	3-13

3-8	Monthly mean daily ozone flux to one-year-old foliage of mature Jeffrey pine at Barton Flats, 1992 to 1994.	3-14
Appendix A Figure 1	Average stomatal conductance for 1993 and 1992 foliage for each site of the Forest Ozone Response Study	A-11
Appendix A Figure 2	Average stomatal conductance for 1993 foliage from each plot at each FOREST site	A-12
Appendix A Figure 3	Average stomatal conductance for 1992 foliage from each plot at each FOREST site	A-13
Appendix A Figure 4	Relationship between stomatal conductance and needle length, across plots and sites for 1993 and 1992 foliage	A-14
4-1	Schedule for data gathering activities during the Intensive Study July 18-31, 1993	4-13
4-2	Daily course of temperature and ozone for the 07/18 to 07/31 periods of 1992, 1993 and 1994	4-14
4-3	Average ozone, relative humidity, wind speed and temperature at the Plot 2 scaffolding during the intensive study, July 18-31, 1993	4-15
4-4	Diurnal variations of a) $PM_{2.5}$ non-volatilized particulate nitrate, $PM_{2.5}$ volatilized particulate nitrate and nitric acid, and b) $PM_{2.5}$ non-volatilized particulate ammonium, $PM_{2.5}$ volatilized particulate ammonium and gaseous ammonia at the Barton Flats Station, CA, during the 1993 summer intensive study (M=06:00-12:00, A=12:00-18:00, N=18:00-06:00 the next day)	4-16
4-5	Summary of CO_2 and NO fluxes for the soils at Barton Flats, Plot 2	4-17
4-6	Deposition of nitrate to foliage of ponderosa pine seedlings located at the forest floor of Plots 1, 2 and 3, roof of the monitoring station and tower top (Plot 2) during July 23-30, 1993 period of the intensive study	4-18
4-7	Deposition of ammonium to foliage of ponderosa pine seedlings located at the forest floor of Plots 1, 2 and 3, roof of the monitoring station and tower top (Plot 2) during July 23-30, 1993 period of the intensive study	4-19
4-8	Deposition of sulfate to foliage of ponderosa pine seedlings located at the forest floor of Plots 1, 2 and 3, roof of the monitoring station and tower top (Plot 2) during July 23-30, 1993 period of the intensive study	4-20

1.0 INTRODUCTION

The plan for this project was based on the conclusions reached at a mid-project meeting to evaluate the progress of the preceding Air Resources Board-sponsored Contract No. A032-180: "Assessment of Acidic Deposition and Ozone Effects on Conifer Forests in the San Bernardino Mountains." Co-investigators proposed tasks which would lead to a more coherent interpretation of the existing data sets and fill some information gaps that were then apparent. The tasks resulting from these deliberations were:

1. Extend atmospheric chemistry and meteorological monitoring for one additional year, namely, 1994, to improve the estimate of year-to-year variation at Barton Flats.
2. Calibrate the Nutrient Cycling Model (NuCM) for the soils and vegetation of the Barton Flats area and run simulations using several scenarios of nitrogen deposition over a 40 year time span.
3. Determine the seasonal and diurnal trends of stomatal conductance in different size classes of ponderosa and Jeffrey pines, and the relationship of conductance to gaseous pollutant uptake at Barton Flats and also at several Sierra Nevada sites.
4. Conduct an intensive study providing more frequent observations of atmospheric chemistry, pollutant deposition and tree physiological responses during July 18-31, 1993.

The schedule for completion of field work for ARB Contract No. A032-180, and the four tasks described above, is shown in Figure 1-1. All data gathering work was completed on schedule in November 1994, but additional time was required to finish data analysis for tree response information collected in September 1994. A 6-month no-cost extension was granted which enabled the inclusion of all of the 1994 tree response data in this report.

It was more convenient for some investigators to report the results of the intensive study (Task 4) in the final report of Contract No. A032-180. Only summaries and conclusions will be included here, however, full details are available in the Contract No. A032-180 final report.

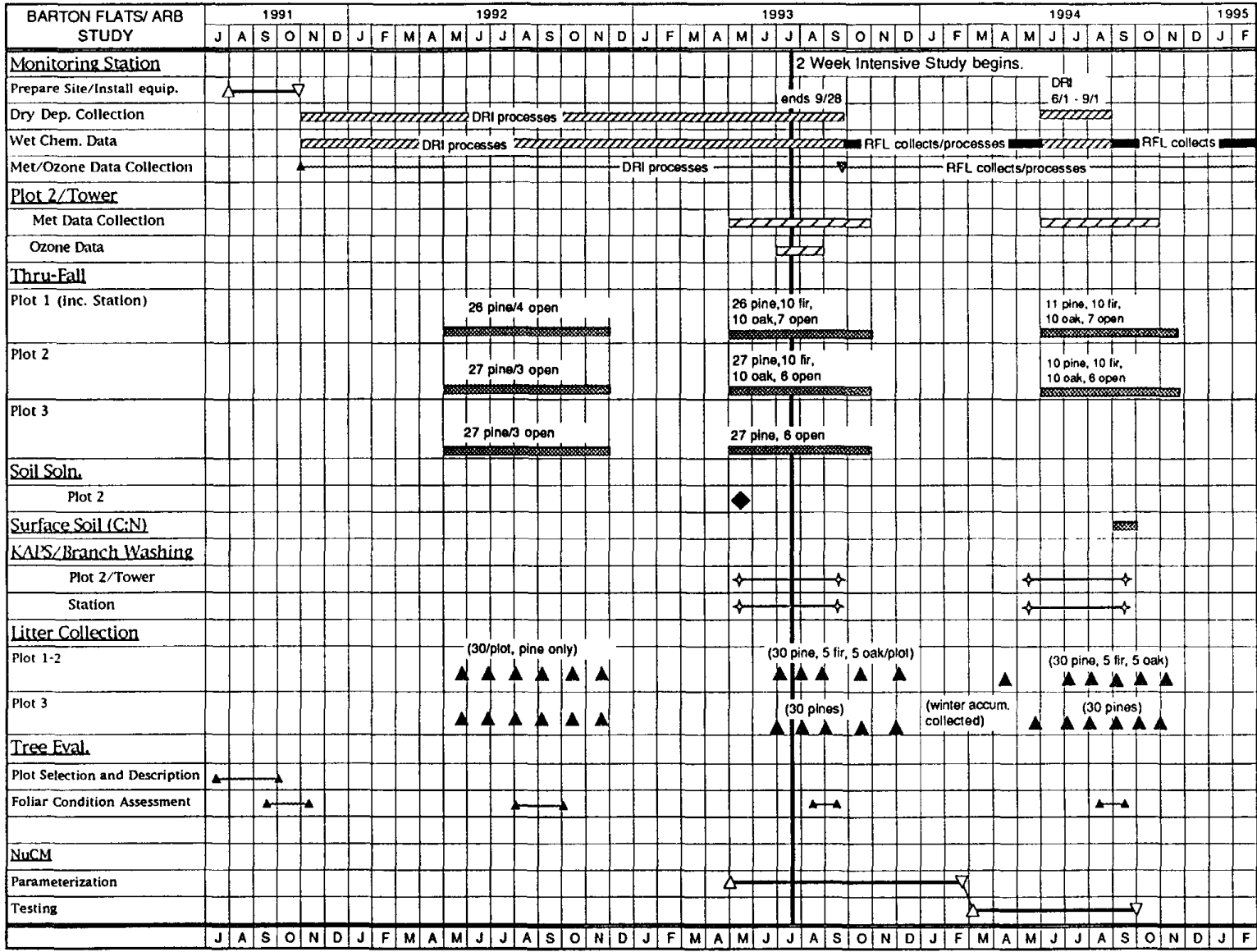


Figure 1-1. Schedule for completion of field work and analytical tasks.

2.0 SIMULATED EFFECTS OF N DEPOSITION RATES ON GROWTH AND NUTRIENT CYCLING IN A PONDEROSA PINE FOREST

Dale Johnson, Mark Poth, Mark Fenn, Paul Miller, and Andrzej Bytnerowicz

2.1 Introduction

In comparison to more humid regions, there is a paucity of information about nutrient cycling in forests of arid and semi-arid regions. There has been some nutrient cycling work in ponderosa pine (*Pinus ponderosa*) (e.g., Klemmedson, 1975; Hart and Firestone, 1989) and lodgepole pine (*Pinus contorta*) ecosystems (Fahey, 1983; Fahey and Knight, 1986), but these are relatively few in number compared to studies of more humid regions (e.g., Cole and Rapp, 1981; Johnson and Lindberg, 1991).

There are several reasons to increase our knowledge of nutrient cycles in semi-arid forests. First, this knowledge would allow intelligent assessments of forest management practices such as harvesting, burning, and site preparation as well as the effects of exogenous influences such as fire, air pollution, and climate change on these forests. Second, these forests act as filters for nutrients, especially nitrogen, which might otherwise enter the sensitive surface or groundwaters. In this context, there is considerable concern over the prospects for humid region forests becoming "nitrogen saturated" from atmospheric N inputs (Nilsson and Grennfelt, 1988; Schulze et al., 1989; Aber et al., 1989). Critical load calculations for N saturation have been made for many of these ecosystems which consider vegetation uptake and increment as the primary factors controlling forest ecosystem N retention and attribute little potential for soil N accumulation (Nilsson and Grennfelt, 1988; Schulze et al., 1989).

While N deposition rates in the semi-arid western US are typically low relative to the eastern US or Europe, there are notable exceptions. Fenn and Bytnerowicz (1993) report total N deposition rates ranging from 6 to 30.7 kg ha⁻¹ year⁻¹ in the San Bernardino mountains of southern California. Recent estimates of fog deposition suggest that total N inputs may exceed 50 kg ha⁻¹ yr⁻¹ at one site (Camp Pavika) (Fenn et al., submitted). These values bracket the range of N inputs in more humid forest ecosystems: Lovett (1991) reported N deposition values of 4-27 kg ha⁻¹ yr⁻¹ in the Integrated Forest Study (IFS) sites. Some of the IFS sites with high N deposition rates also have high soil solution nitrate concentrations and nitrate leaching rates: Van Miegroet et al. (1991) report soil nitrate leaching values of <1 to 26 kg ha⁻¹ yr⁻¹ for the Integrated Forest Study sites. The most "nitrogen saturated" of these sites - red spruce forests of the Great Smoky mountains of North Carolina - also have concentrations of Al in soil solution that approach thresholds for toxicity (Johnson et al., 1991). Elevated soil solution nitrate concentrations have also been found at the Barton Flats intensive study site in the San Bernardino mountains, where N deposition rates are at least 6 kg ha⁻¹ yr⁻¹. In order to gain some understanding of the potential effects of varying N inputs on ponderosa pine ecosystems, we have calibrated the Nutrient Cycling Model (NuCM) for the Barton Flats intensive study site and run simulations of N inputs ranging from near pristine (1.9 kg ha⁻¹ yr⁻¹) to heavily polluted (95.6 kg ha⁻¹ yr⁻¹) levels.

2.2 Site and Methods

2.2.1 Field Site

The San Bernardino mountains begin at the Cajon pass, which cuts between them and the San Gabriel mountains, approximately 80 kilometers east of Los Angeles. The San Bernardino mountains extend eastward for another 80 kilometers. Barton Flats, the site calibrated for these simulations, lies near the center of the mountain range. The elevation is 1946 m and mean annual precipitation of 540 mm (Arkley, 1977; Fenn and Dunn, 1989).

Meteorological data was obtained from the National Weather Service central archives (NOAA, NWS, Raleigh NC). The nearest complete data were from Norton Air Force Base in the city of San Bernardino which is at the foot of the San Bernardino mountains. Data were corrected for the difference in elevation between the study site at Barton Flats and Base. Annular denuder systems as described by Possanzini et al. (1983) and modified by Peake and Legge (1987) were used for collection of nitric acid (HNO₃) vapor, nitrous acid (HNO₂) vapor, ammonia (NH₃), and fine particles (< 2.2 μm diameter). The samples were collected for 24 hr periods.

Plant and soil analyses were done according to the methods described by Robarge and Fernandez (1986) with the exception of the method used for P determinations (Glaubig and Poth, 1993). Soil samples were taken from 15 soil pits dug in the Barton Flats area. Mean soil horizon values were used to parameterize the model. Means of plant nutrient concentrations for each of the three dominant tree species (*Pinus ponderosa* Laws., *Abies concolor*, *Quercus kelloggii*) were also used (n ≥ 5). Soil solution was collected by centrifugation and analyzed for anions via ion chromatography using a Dionex 4000i ion chromatograph and for cations via atomic absorption spectroscopy (Perkin-Elmer 5000).

2.2.2 NuCM Model Calibration

NuCM is a stand-level nutrient cycling model developed as part of the Electric Power Research Institute's Integrated Forest Study (Liu et al., 1991; Johnson and Lindberg, 1991). The forested ecosystem is represented as a series of vegetation and soil components. The model provides for both an overstory and understory, each of which can be divided into canopy, bole, and roots. Tree growth in the model is a function of user-defined stand developmental stage and the availability of nutrients and moisture. Using mass balance and transport formulations, the model tracks 16 solution-phase components including the major cations and anions (analytical totals), ANC (acid-neutralizing capacity), an organic acid analog, and total aluminum (Liu et al., 1991). The concentrations of hydrogen ion, aluminum and carbonate species, and organic acid ligands and complexes are then calculated based upon the 16 components. The acid-base characteristics of the forest soil solution are computed by the model to properly account for the influence of hydrogen-ion concentration on cation exchange and mineral weathering.

The model routes precipitation through the canopy and soil layers, and simulates evapotranspiration, deep seepage, and lateral flow. The soil includes multiple layers (up to ten), and each layer can have different physical and chemical characteristics. The movement of water through the system is simulated using the continuity equation, Darcy's equation for permeable media flow, and Manning's equation for free surface flow. Percolation occurs between layers as a function of layer permeabilities and differences in moisture content.

Nutrient pools associated with soil solution, the ion exchange complex, minerals, and soil organic matter are

all tracked explicitly. The processes which govern interactions among these pools include user-specified rates for decay, nitrification, anion adsorption, cation exchange and mineral weathering.

The model simulates the noncompetitive adsorption of sulfate, phosphate, and organic acid. Sulfate adsorption can be simulated in NuCM using either linear or Langmuir adsorption isotherms; the Langmuir isotherm was used in these simulations. As noted by Prenzel (1994), most models fail to incorporate pH-dependency into their formulations for soil sulfate adsorption; however, NuCM incorporates pH-dependent SO_4^{2-} adsorption into the Langmuir equation. Phosphate adsorption in the model is represented by a linear isotherm.

Cation exchange is represented by the Gapon equation because of empirical laboratory studies during IFS showing that the Gapon was more accurate and stable in predicting soil solution cation concentrations under varying ionic strengths (Richter et al., 1991). Mineral weathering reactions are described in the model using rate expressions with dependencies on the mass of mineral present and solution-phase hydrogen-ion concentration taken to a fractional power.

NuCM was calibrated for the Barton Flats site using data collected from the site for vegetation and soil nutrient concentrations, soil and litter mass, and soil solution concentrations. At the time of this exercise, no data for biomass from the Barton Flats site was available, so the data on a ponderosa pine stand from Klemmedson (1975) was used.

Procedures outlined in the User's Manual (Munson et al., 1992) were used in the calibration; details are described elsewhere (Liu et al., 1991; Johnson et al., 1993). Several model parameters which were of no great consequence to our particular ecosystem and for which no data were available (such as organic acid adsorption, phosphate adsorption, snowmelt characteristics, fractions of leachable nutrients in litter, etc.) were left as in the original model formulation (Liu et al., 1991).

Five N deposition scenarios were run: inputs of 1.96, 9.62, 19.2, 38.2, and 95.6 $\text{kmol ha}^{-1} \text{yr}^{-1}$ (1.9, 9.5, 19.2, 38.2, and 95.6 $\text{kg ha}^{-1} \text{yr}^{-1}$). These inputs were 0.1 x, 0.5 x, 1x, 2 x, and 5 x the baseline input value in the model of 1.37 $\text{kmol ha}^{-1} \text{yr}^{-1}$ for Barton Flats. Each simulation was run from the same initial conditions, with no input variable changed except N deposition. Simulations were run for 40 years each.

2.3 Results

As expected, increases in simulated N deposition resulted in increases in simulated NO_3^- leaching¹ (Table 2-1 and Figure 2-1). However, simulated NO_3^- leaching rates increased substantially only after N deposition rates became 2 x current rates or higher. Cumulative net ecosystem N retention was actually lower at 0.1 x N (63% of input) than at 0.5 x N or 1 x N (87 and 89% of input, respectively), even though NO_3^- leaching rates increased progressively with N deposition throughout these scenarios (Table 2-1). Apparently, the NO_3^- leaching rate at 0.1 x N was near a baseline level. Simulated vegetation and forest floor N contents increased progressively with N deposition from 0.1 to 1 x N, accounting for the retention of N in the ecosystem (Table 2-2). Between 0.1 and 1 x N, vegetation N content increased by $34.59 \text{ kmol ha}^{-1}$ (86%), forest floor N increased by $6.54 \text{ kmol ha}^{-1}$ (22%), and the sum of vegetation, forest floor and soil exchangeable N increased by $41.13 \text{ kmol ha}^{-1}$ (59%) (Table 2-2). At N deposition levels of 2 x N and 5 x N, net ecosystem retention decreased to 55 and 25% of input, respectively (Table 2-1). There were some increases in vegetation ($8.58 \text{ kmol ha}^{-1}$, or 11%) and forest floor ($1.52 \text{ kmol ha}^{-1}$, or 4%) N contents from 1 to 2 x N, but no further increases at 5 x N (Table 2-2). There was a large relative increase in exchangeable N from the 2 to the 5 x N scenarios ($8.14 \text{ kmol ha}^{-1}$, or 16,380%) but the absolute magnitude of this increase was too small to cause a large increase in ecosystem N retention (the sum of vegetation, forest floor, and exchangeable N increased by only 7%, all in the form of exchangeable N) (Table 2-2).

The patterns of simulated leaching and N retention closely corresponded to those in growth. Simulated growth increased substantially from the 0.1 to 0.5 and 1 x N scenarios, indicating N deficiency at less than 1 x N input (Figure 2-2). Growth rate also increased slightly from the 1 to 2 x N scenarios, but there was no further growth increase from the 2 to the 5 x N scenario. The N deposition scenarios caused relatively large reductions in P leaching due mostly to accumulation of P in vegetation and forest floor (Table 2-1 and Figure 2-3). However, P leaching rates were low in relation to ecosystem P pools, so that the changes in the latter with N deposition were very slight (< 0.5% variation among scenarios) (Table 2-2 and Figure 2-3). Soil exchangeable P pools were somewhat depleted due to uptake and accumulation in vegetation and forest floor pools, and there was a slight increase in soil exchangeable P from the 2 x N to the 5 x N scenario due to soil acidification and increased pH-dependent P adsorption (Table 2-2).

Increases in N deposition from 0.1 to 1 x N caused unexpected reductions in simulated K^+ , Ca^{2+} , Mg^{2+} , base cation, and ANC leaching rates (Table 2-1 and Figures 2-4 through 2-8). This was due to a complicated set of chemical interactions which resulted in lower total anion concentrations with increasing N deposition from 0.1 to 1 x N during winter months (October through February) when most leaching occurred. Figures 2-9 through 2-16 illustrate these interactions on a seasonal basis for years 2 and 40 of the simulations. Although summertime soil solution NO_3^- concentrations increased with increasing N deposition from 0.1 to 1 x N (Figure 2-9), this had little effect upon leaching rates because water flux was low during this period. Soil solution pH was reduced with increasing N deposition (Figure 2-10). The pH reductions were due to a combination of reduced base saturation (especially later in the simulation; Figure 2-11) and the "salt effect",

¹ Over 99% of total N leaching occurred as NO_3^- ; thus, NO_3^- leaching can be equated with total N leaching for all practical purposes.

whereby increases in mineral acid anion concentration (NO_3^- in this case) cause H^+ concentration to increase (Reuss and Johnson, 1986). These reductions in soil solution pH directly caused reductions in soil solution ANC (Figure 2-12) and indirectly caused reductions in soil solution SO_4^{2-} because of increased pH-dependent SO_4^{2-} adsorption (Figure 2-13). The net effect was a reduction in soil solution total anion (and cation) concentration with increasing N deposition from 0.1 to 1 x N during the winter months (Figure 2-14). At later stages of the simulations, there were also increases in soil solution Al concentrations (Figure 2-15), which caused further reductions in base cation leaching.

Although K^+ , Ca^{2+} , and Mg^{2+} leaching rates decreased from 0.1 to 1 x N for the reasons noted above, soil exchangeable K^+ , Ca^{2+} , Mg^{2+} pools decreased continuously from 0.1 to 5 x N deposition (Table 2-2). The decreases from 0.1 to 1 x N were due to uptake and accumulation in vegetation, which offset the reductions in leaching. As N deposition rates increased from 1 to 5 x N, base cation leaching rates increased again, and at 5 x N, there were large decreases in soil exchangeable base cation pools (Tables 2-1 and 2-2). The decrease in exchangeable pools was much larger for K^+ (decreased by 77% from 1 to 5 x N), than for Ca^{2+} and Mg^{2+} (decreased by 18 and 23%, respectively, from 1 to 5 x N) (Table 2-2).

2.4 Discussion

The NuCM simulations for Barton Flats produced some results that were expected and some that were unexpected. The reductions in N retention and increases in NO_3^- leaching with increasing N deposition were certainly expected; the only question was at what levels of N deposition the effects would occur. There was a continuous increase in NO_3^- leaching with N deposition, but the leaching rates were relatively low until N deposition increased beyond 1 x N ($19.2 \text{ kg ha}^{-1} \text{ yr}^{-1}$). At some level between 2 and 5 x N deposition (38.4 and $95.6 \text{ kg ha}^{-1} \text{ yr}^{-1}$), growth responses to N ceased and N retention remained constant. Thus, N "saturation" occurred at some point above $38.4 \text{ kg ha}^{-1} \text{ yr}^{-1}$, if N "saturation" is defined as the inability to accumulate further N. Below $38.4 \text{ kg ha}^{-1} \text{ yr}^{-1}$, a pronounced N deficiency occurred, as would also be expected as the norm in less polluted semi-arid forests of this type. The threshold at which N "saturation" occurs in a given simulation will vary with input values for vegetation N uptake (which in turn are determined by the maximum allowable growth and N concentrations in trees) and the degree of soil N retention. In the absence of any further data for these parameters in varying N deposition regimes, we have left them constant.

Although growth response to N occurred up through $38.4 \text{ kg ha}^{-1} \text{ yr}^{-1}$ (Figure 2-2), soil solution NO_3^- concentrations peaked at relatively high midsummer values ($> 150 \mu\text{mol}_e \text{ L}^{-1}$) even at the lowest N deposition scenario ($1.9 \text{ kg ha}^{-1} \text{ yr}^{-1}$). These peak NO_3^- concentrations would pose no serious threat for ground- or surface water pollution, however, because of the lack of water movement at that time. In practice, it may prove infeasible to collect soil solutions to check the simulation results during these dry periods because soil moisture tensions are very high.

The reductions in Ca^{2+} , Mg^{2+} , and K^+ leaching to reduced N deposition rates were unexpected. These reductions were an indirect result of complicated interactions among soil solution pH, base saturation, NO_3^- , SO_4^{2-} and HCO_3^- concentration which could only have been explored through simulation modeling. The general direction of the responses in soil solution pH, SO_4^{2-} , and HCO_3^- concentration are of course

consistent with the soil chemical theory built into the model, but the magnitudes of the responses and their interactions with NO_3^- and base cations were not intuitively predictable, very interesting, and worthy of testing either with field or laboratory column studies.

2.5 Summary and Conclusions

The results of these simulations suggest that reductions in N deposition to the Barton Flats site will result in the development of N deficiency, whereas increases will result in N saturation and groundwater pollution of NO_3^- . There is some suggestion from these simulations that N saturation will lead to K deficiencies because of large reductions in soil available pools. However, this cannot be given as a prediction because of the unknown rates of K weathering from soil primary minerals, for which there is no data. Increasing K weathering rates in the model would greatly slow the depletion of soil exchangeable K^+ pools.

The simulations suggest that reducing N deposition rates below $19.8 \text{ kg ha}^{-1} \text{ yr}^{-1}$ would cause increases in the rate of base cation leaching from soils due to increases in soil solution HCO_3^- and SO_4^{2-} concentrations. This interesting result was not intuitively predictable, and is worthy of testing either in the field or with laboratory column studies. Despite the reductions in K^+ , Ca^{2+} , and Mg^{2+} leaching, however, soil exchangeable K^+ , Ca^{2+} , Mg^{2+} pools decreased continuously from 0.1 to 5 x N deposition due to uptake and accumulation in vegetation.

The simulations indicate that summertime soil solution NO_3^- concentrations would remain elevated even under very low N deposition rates under this climate. In practice, however, these high soil solution NO_3^- values would be of little consequence because of the lack of soil moisture and may be impossible to verify because of the difficulty of obtaining soil solution samples at high moisture tensions.

Given the uncertainties inherent in both the model formulation and the data used to calibrate it, we must advise the reader not to use these simulation results as quantitative predictions of what specific response will occur at a specific N deposition load (for example, we cannot state that soil solution NO_3^- will increase to $100 \mu\text{mol L}^{-1}$ at an N loading of $1.37 \text{ kmole ha}^{-1} \text{ year}^{-1}$). Instead, we offer the results of these simulations as indicators of what is expected with changing N loadings based upon our best current knowledge of nutrient cycling within this ecosystem. From a scientific perspective, the results of these simulations present some interesting hypotheses that could be tested in either a field, or in some cases, a laboratory setting.

2.6 Acknowledgments

Research supported by the U.S. Forest Service, California Air Resources Board and the Nevada Agricultural Experiment Station. Many thanks are due Robin Peterson, Richard Susfalk, and Kastlie Beck for technical help.

2.7 References

- Aber, J.D., K.J. Nadelhoffer, P. Streudler, and J.M. Melillo. 1989. Nitrogen Saturation in Northern Forest Ecosystems. *Bioscience* 39:378-386.
- Cole, D.W., and M. Rapp. 1981. Elemental Cycling in Forest Ecosystems. Pages 341-409 in D.E. Reichle (ed.) *Dynamic Properties of Forest Ecosystems*. Cambridge University Press, London
- Cosby, B.J., G.M. Hornberger, J.N. Galloway, and R.F. Wright. 1985. Modeling the Effects of Acid Deposition: Assessment of a Lumped Parameter Model of Soil Water and Streamwater Chemistry. *Water Resour. Res.* 21:51-63.
- Davidson, E.A., J.M. Stark, and M.K. Firestone. 1990. Microbial Production and Consumption of Nitrate in an Annual Grassland. *Ecology* 71:1968-1975.
- Davidson, E.A. and W.T. Swank. 1987. Factors Limiting Denitrification in Soils from Mature and Disturbed Southeastern Hardwood Forests. *Forest Sci.* 33: 135-144.
- Fahey, T.J. 1983. Nutrient Dynamics of Aboveground Detritis in Lodgepole Pine (*Pinus Contorta* Ssp *Latifolia*) Ecosystems, Southeastern Wyoming. *Ecol.Monogr.* 53-51-72.
- Fahey, T.J. 1986. Lodgepole Pine Ecosystems. *Bioscience* 36:610-617.
- Hart, S.C., and M.K. Firestone. 1989. Forest Floor-Mineral Soil Interactions in the Internal Nitrogen Cycle of an Old -Growth Forest. *Biogeochemistry* 12:103-127
- Fenn, M.E., and P.H. Dunn. 1989. Litter Decomposition Across an Air Pollution Gradient in the San Bernardino Mountains. *Soil Sci. Soc. Am. J.* 53:1560-1567..
- Fenn, M.E., and A. Bytnerowicz. 1993. Dry Deposition of Nitrogen and Sulfur to Ponderosa and Jeffrey Pine in the San Bernardino National Forest in Southern California. *Environ. Pollut.* 81: 277-285.
- Fenn, M.E., M.A. Poth and D.W. Johnson (1996) Nitrogen Saturation in the San Bernardino Mountains of Southern California. *Forest Ecol. Manag.* 81:In Press
- Gessel, S.P., D.W. Cole, and E.C. Steinbrenner. 1973. Nitrogen Balances in Forest Ecosystems of the Pacific Northwest. *Soil Biol. Biochem.* 5:19-34.
- Gherini, S.A., L. Mok, R.J.M Hudson, G.F Davis, C.W. Chen, and R.A. Goldstein. 1985. The Ilwas Model: Formulation and Application. *Water, Air, and Soil Pollut.* 26:425-459.
- Glaubig, R. and M.A. Poth. 1993. Method for Total Phosphorus Determinations Innitric-Perchloric Digests of Pine Needles and Roots. *Commun. Soil Sci. Plant Anal.*, 24:2469-2477.
- Johnson, D.W., and J.T. Ball. 1990. Environmental Pollution and Impacts on Soils and Forests of North America. *Water, Air, and Soil Pollut.* 54: 3-20.
- Johnson, D.W., W.T. Swank,, and J.M. Vose. 1993. Simulated Effects of Atmospheric Sulfur Deposition on Nutrient Cycling in a Mixed Deciduous Forest. *Biogeochemistry* 23:169-196.

- Johnson, D.W. and S.E. Lindberg (eds). (1991) *Atmospheric Deposition and Nutrient Cycling in Forest Ecosystems*. Springer-Verlag, New York.
- Johnson, D.W., H. Van Miegroet, S.E. Lindberg, R.B. Harrison, and D.E. Todd. 1991. Nutrient Cycling in Red Spruce Forests of the Great Smoky Mountains. *Can. J. For. Res.* 21: 769-787
- Klemmedson, J.O. 1975. Nitrogen and Carbon Regimes in an Ecosystem of Young Dense Ponderosa Pine in Arizona. *Forest Sci.* 21: 163-168.
- Lindberg, S.E., G.M. Lovett, D.D. Richter, and D.W. Johnson. 1986. Atmospheric Deposition and Canopy Interactions of Major Ions in a Forest. *Science* 231:141-145
- Liu, S., R. Munson, D.W. Johnson, S. Gherini, K. Summers, R. Hudson, K. Wilkinson, and L.F. Pitelka. 1991. The Nutrient Cycling Model (NuCM): Overview and Application. pp. 583-609. Chapter 14, In: Johnson, D.W. and S.E. Lindberg (eds)., *Atmospheric Deposition and Forest Nutrient* Ecological Series 91, Springer-Verlag, New York. 707 pages
- Lovett, G.M. 1991. Atmospheric Deposition and Canopy Interactions of Nitrogen. pp. 152-165 IN: Johnson, D.W., and S.E. Lindberg (eds)., *Atmospheric Deposition and Forest Nutrient* Ecological Series 91, Springer-Verlag, New York. 707 pages
- Nilsson, J., and P. Grennfelt (eds). 1988. Critical Loads for Sulphur and Nitrogen. Report from a Workshop Held at Skolster, Sweden 19-24 March, 1988. Nordic Council of Ministers, Copenhagen.
- Peake, E., and A.H. Legge. 1987. Evaluation of Methods Used to Collect Air Quality Data at Remote and Rural Sites in Alberta, Canada. EPA/APCA Symposium "Measurements of Toxic and Related Air Pollutants", Research Triangle Park, NC 3-6 May, 1987.
- Possanzini, M., A. Febo, and A. Liberti. 1983. New Design of a High[®]Performance Denuder for the Sampling of Atmospheric Pollutants. *Atmos. Environ.*, 17, 2605-2612.
- Prenzel, J. 1994. Sulfate Sorption in Soils under Acidic Deposition: Comparison of Two Modeling Approaches. *J. Environ.Qual.* 23:188-194.
- Reuss, J.O. and D.W. Johnson. 1986. *Acid Deposition and the Acidification of Soil and Water*. Springer-Verlag, New York.
- Richter, D.D., D.W. Johnson, and K.H. Dai 1991. Cation Exchange Reactions in Acid Forested Soils: Effects of Atmospheric Pollutant Deposition. In: Johnson, D.W., and S.E. Lindberg, (eds) *Atmospheric Deposition and Forest Nutrient Cycling: A Synthesis of the Integrated Forest Study*. (pp 341-357) Ecological Series 91, Springer Verlag, New York. 707 pages.
- Robarge, W.P., and I. Fernandez. 1986. *Quality Assurance Methods Manual for Laboratory Analytical Techniques*. USEPA, Corvallis Environmental Research Laboratory, Forest Response Program. 204 pages.
- Roelofs, J.G.M., A.W. Boxman, and H.F.G. van Dijk. 1987. Effects of Airborne Ammonium on Natural Vegetation and Forests. pp 266-276 In: W.A. Asman and S.M.A. Diederer (eds). *Ammonia and*

Acidification. Proceedings, Symposium of the European Association for the Science of Air Pollution (EURASAP) held at the National Institute of Public Health and Environmental Hygiene, Bilthoven, The Netherlands, 13-15 April 1987. Netherlands Organization for Applied Scientific Research, Division of Technology for Society, Delft.

- Schulze, E.D., W. De Vries, M. Hauhs, K. Rosen, L. Rasmussen, C.O. Tamm, and J. Nilsson. 1989. Critical Loads for Nitrogen Deposition on Forest Ecosystems. *Water, Air, and Soil Pollut.* 48: 451-456.
- Van Breemen, N., P.A. Burrough, E.J. Velthorst, H.F. van Dobben, T. de Witt, T.B. Ridder, and H.F.R. Reijnders. 1982. Soil Acidification from Atmospheric Ammonium Sulphate in Forest Canopy Throughfall. *Nature* 299:548-550.
- Van Breemen, N., J. Mulder, and J.J.M. Van Grinsven. 1987. Impacts of Atmospheric Deposition on Woodland Soils in the Netherlands: II. Nitrogen Transformations. *Soil Sci. Soc. Amer. J.* 51:1634-1640.
- Van Miegroet, H. and D.W. Cole. 1984. The Impact of Nitrification on Soil Acidification and Cation Leaching in Red Alder Ecosystem. *J. Environ. Qual.* 13:586-590
- Van Miegroet, H., D.W. Cole, and N.W. Foster. 1991. Nitrogen Distribution and Cycling. pp. 178-195 IN: Johnson, D.W. and S.E. Lindberg (eds.), *Atmospheric Deposition and Forest Nutrient* Ecological Series 91, Springer-Verlag, New York. 707 p.

Table 2-1. Simulated net ecosystem balances of N, P, Ca, K, Mg, and S under varying N deposition scenarios (kmol ha⁻¹ 40 yrs⁻¹). % retention = % of deposition not lost to leaching, or balance/deposition.

Scenario	0.1 x N	0.5 x N	1 x N	2 x N	5 x N
Nitrogen					
Deposition	5.46	27.31	54.60	109.25	273.10
<u>Leaching</u>	<u>2.02</u>	<u>3.47</u>	<u>5.65</u>	<u>49.11</u>	<u>203.44</u>
Balance	3.44	23.84	48.95	59.62	69.65
% Retention	63%	87%	89%	55%	25%
Phosphorus					
Deposition	0.000	0.000	0.000	0.000	0.000
<u>Leaching</u>	<u>0.040</u>	<u>0.029</u>	<u>0.027</u>	<u>0.014</u>	<u>0.008</u>
Balance	-0.040	-0.029	-0.027	-0.014	-0.008
% Retention	-	-	-	-	-
Calcium					
Deposition	0.47	0.47	0.47	0.47	0.47
<u>Leaching</u>	<u>5.20</u>	<u>3.67</u>	<u>4.07</u>	<u>8.46</u>	<u>30.15</u>
Balance	-4.74	-3.20	-3.60	-7.99	-29.68
% Retention	-	-	-	-	-
Potassium					
Deposition	0.06	0.06	0.06	0.06	0.06
<u>Leaching</u>	<u>7.19</u>	<u>5.54</u>	<u>5.86</u>	<u>6.61</u>	<u>10.61</u>
Balance	-7.13	-5.48	-5.80	-6.54	-10.55
% Retention	-	-	-	-	-
Magnesium					
Deposition	0.09	0.09	0.09	0.09	0.09
<u>Leaching</u>	<u>3.57</u>	<u>2.53</u>	<u>2.84</u>	<u>5.75</u>	<u>16.92</u>
Balance	-3.48	-2.44	-2.75	-5.66	-16.83
% Retention	-	-	-	-	-
Sulfur					
Deposition	7.39	7.39	7.39	7.39	7.39
<u>Leaching</u>	<u>5.93</u>	<u>5.17</u>	<u>5.12</u>	<u>4.25</u>	<u>4.24</u>
Balance	1.46	2.22	2.28	3.14	3.15
% Retention	20%	30%	31%	42%	43%

Table 2-2. Simulated nutrient distribution after 40 years under varying N deposition scenarios (kmol ha^{-1} and $\text{kmol ha}^{-1} \text{ yr}^{-1}$).

Scenario	<u>0.1 x N</u>	<u>0.5 x N</u>	<u>1 x N</u>	<u>2 x N</u>	<u>5 x N</u>
<u>N Deposition</u>	<u>0.14</u>	<u>0.68</u>	<u>1.37</u>	<u>2.73</u>	<u>6.83</u>
Nitrogen					
Vegetation	39.97	53.96	74.56	83.14	83.14
Forest Floor	29.62	33.57	36.16	37.68	37.68
<u>Soil, Exchangeable</u>	<u><0.01</u>	<u><0.01</u>	<u><0.01</u>	<u>0.05</u>	<u>8.19</u>
Total	69.59	87.53	110.72	120.87	129.01
Phosphorus					
Vegetation	2.93	3.93	4.43	5.68	5.68
Forest Floor	0.72	0.96	0.84	1.08	1.08
<u>Soil, Exchangeable</u>	<u>111.10</u>	<u>109.80</u>	<u>109.60</u>	<u>108.10</u>	<u>108.40</u>
Total	114.75	114.69	114.87	114.86	115.16
Calcium					
Vegetation	17.93	21.68	23.96	30.68	31.82
Forest Floor	3.82	4.29	4.08	4.75	4.87
<u>Soil, Exchangeable</u>	<u>191.30</u>	<u>188.70</u>	<u>186.40</u>	<u>174.90</u>	<u>152.80</u>
Total	213.05	214.67	214.44	210.33	189.49
Potassium					
Vegetation	10.97	13.52	14.93	18.91	19.46
Forest Floor	7.46	8.70	8.13	9.97	10.39
<u>Soil, Exchangeable</u>	<u>19.41</u>	<u>16.68</u>	<u>15.98</u>	<u>8.54</u>	<u>3.69</u>
Total	37.84	38.90	39.04	37.42	33.54
Magnesium					
Vegetation	5.90	7.39	8.11	10.68	10.68
Forest Floor	2.36	2.67	2.52	2.96	2.96
<u>Soil, Exchangeable</u>	<u>43.94</u>	<u>43.57</u>	<u>42.95</u>	<u>38.16</u>	<u>28.79</u>
Total	52.20	53.63	53.58	51.80	42.43
Sulfur					
Vegetation	1.69	2.19	2.36	2.94	2.93
Forest Floor	9.88	10.03	9.96	10.11	10.10
<u>Soil, Exchangeable</u>	<u>0.87</u>	<u>0.94</u>	<u>0.93</u>	<u>1.01</u>	<u>1.05</u>
Total	12.44	13.16	13.25	14.06	14.08

Figure 2-1. Simulated nitrogen leaching at Barton Flats under various N deposition scenarios: 0.1 x = 0.14, 0.5 x = 0.68, 1 x = 1.37, 2 x = 2.73, and 5 x = 6.83 kmol ha⁻¹ yr⁻¹ (1.9, 9.5, 28.7, 38.2, and 95.6 kg ha⁻¹ yr⁻¹).

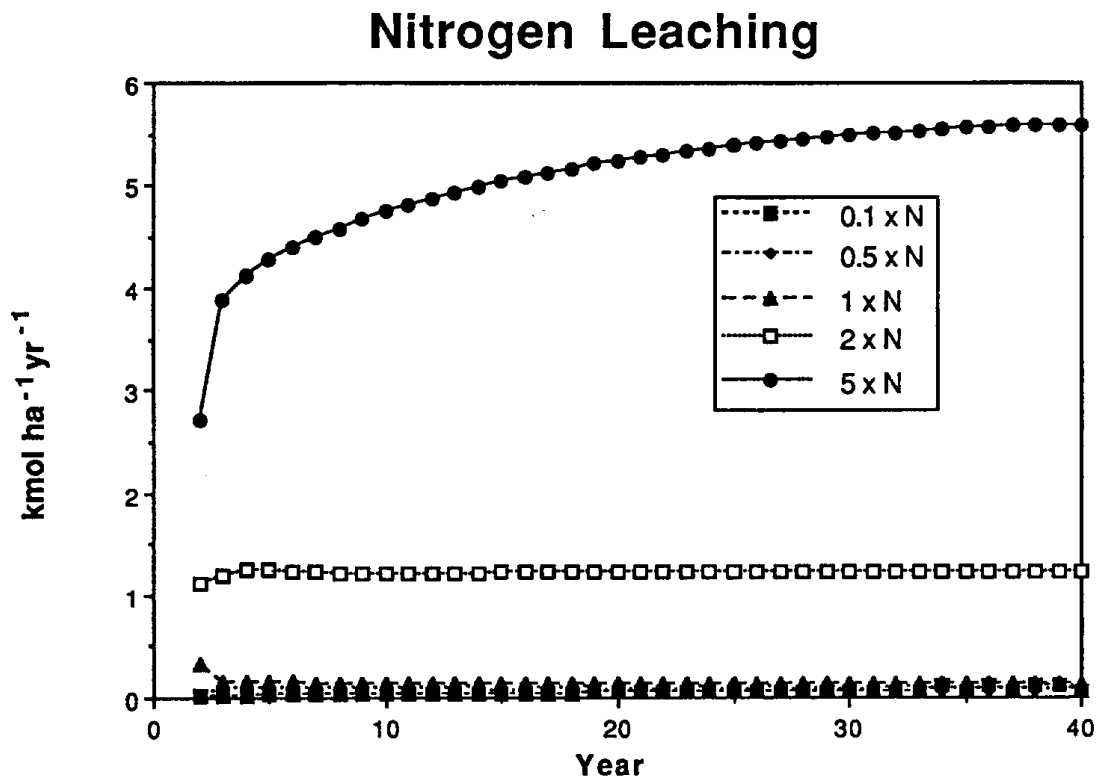


Figure 2-2. Simulated biomass at Barton Flats under various N deposition scenarios: 0.1 x = 0.14, 0.5 x = 0.68, 1 x = 1.37, 2 x = 2.73, and 5 x = 6.83 kmol ha⁻¹ yr⁻¹ (1.9, 9.5, 28.7, 38.2, and 95.6 kg ha⁻¹ yr⁻¹).

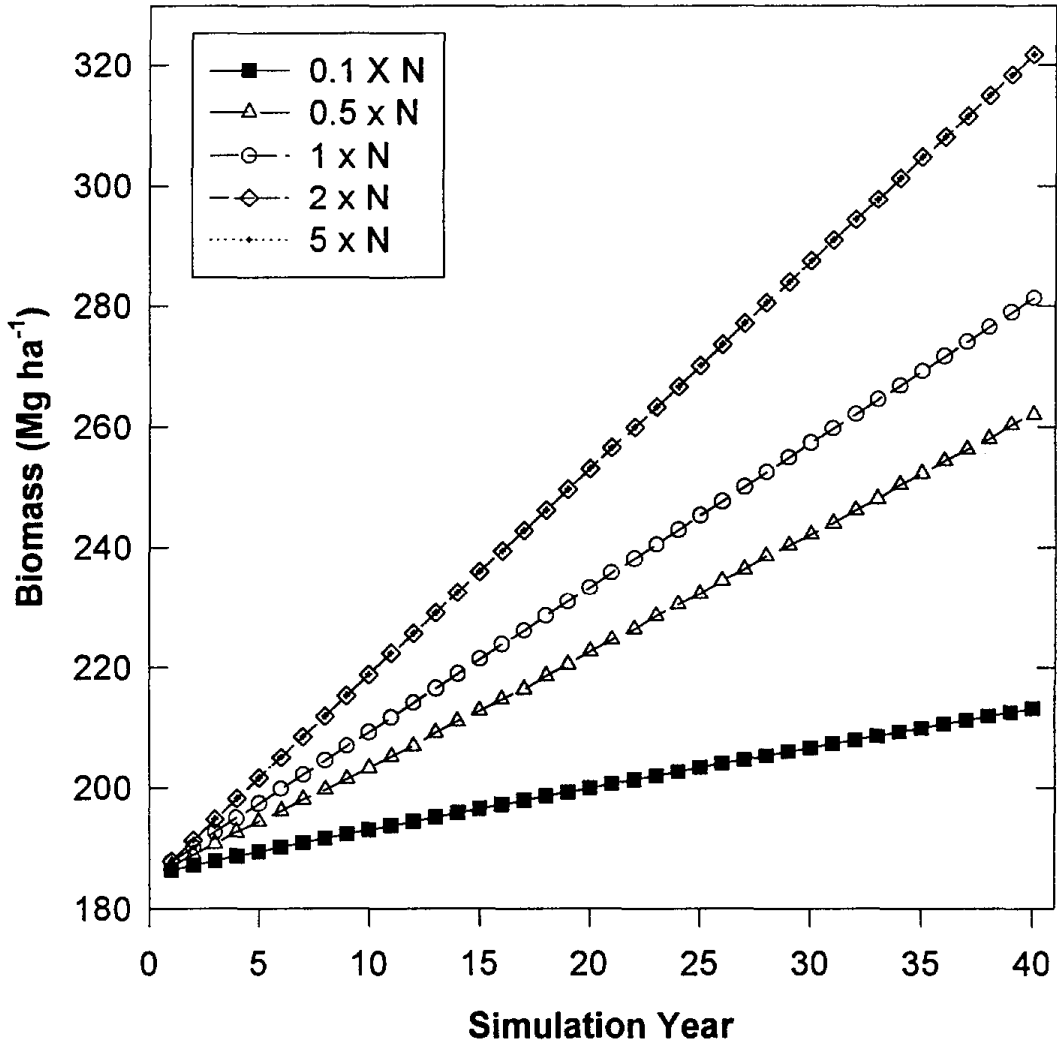


Figure 2-3. Simulated phosphorus leaching at Barton Flats under various N deposition scenarios: 0.1 x = 0.14, 0.5 x = 0.68, 1 x = 1.37, 2 x = 2.73, and 5 x = 6.83 kmol ha⁻¹ yr⁻¹ (1.9, 9.5, 28.7, 38.2, and 95.6 kg ha⁻¹ yr⁻¹).

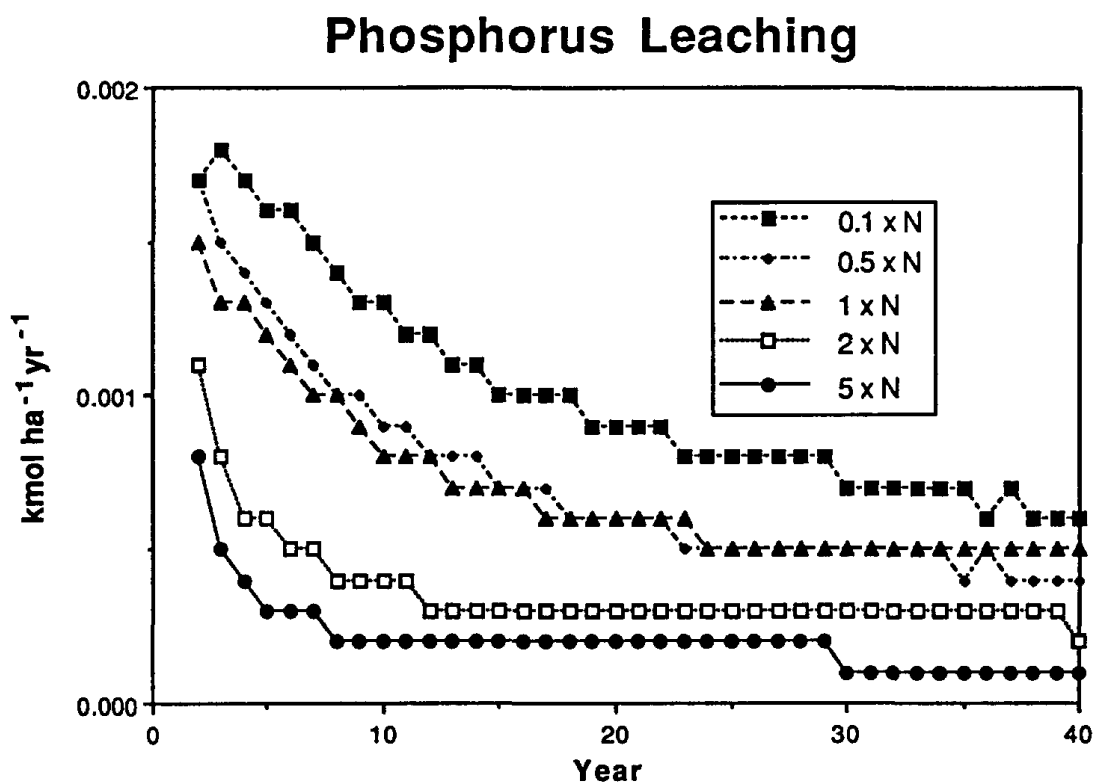


Figure 2-4. Simulated potassium leaching at Barton Flats under various N deposition scenarios: 0.1 x = 0.14, 0.5 x = 0.68, 1 x = 1.37, 2 x = 2.73, and 5 x = 6.83 kmol ha⁻¹ yr⁻¹ (1.9, 9.5, 28.7, 38.2, and 95.6 kg ha⁻¹ yr⁻¹).

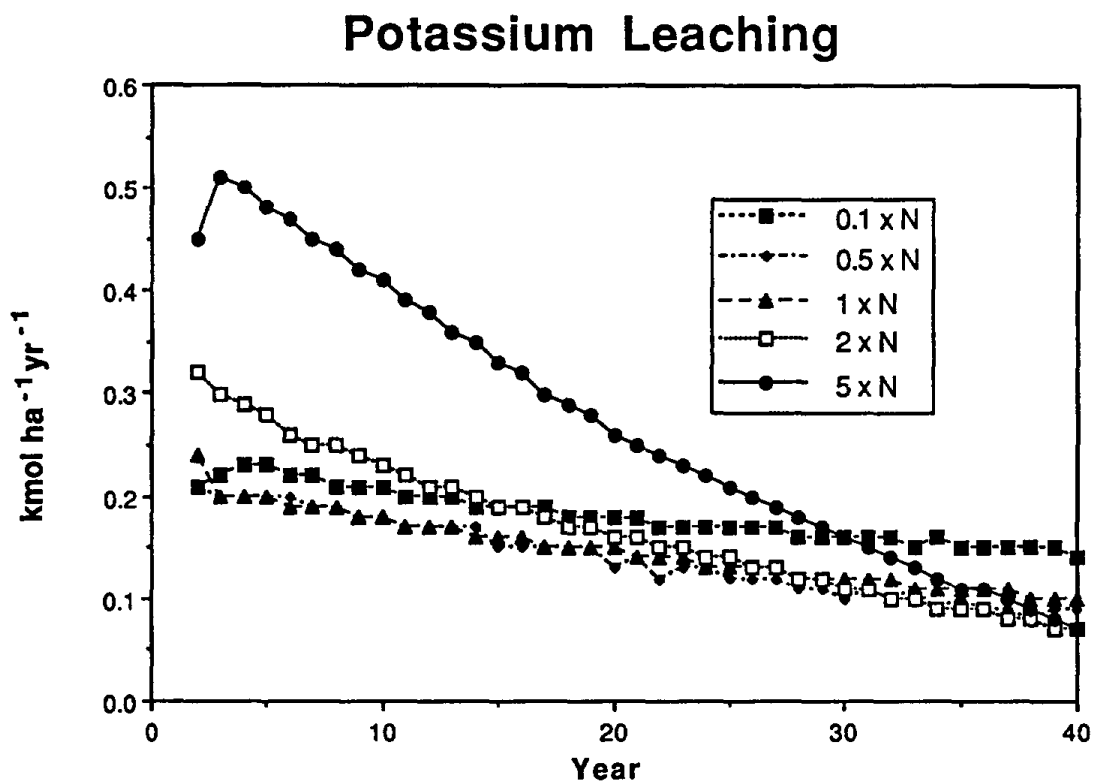


Figure 2-5. Simulated calcium leaching at Barton Flats under various N deposition scenarios: 0.1 x = 0.14, 0.5 x = 0.68, 1 x = 1.37, 2 x = 2.73, and 5 x = 6.83 kmol ha⁻¹ yr⁻¹ (1.9, 9.5, 28.7, 38.2, and 95.6 kg ha⁻¹ yr⁻¹).

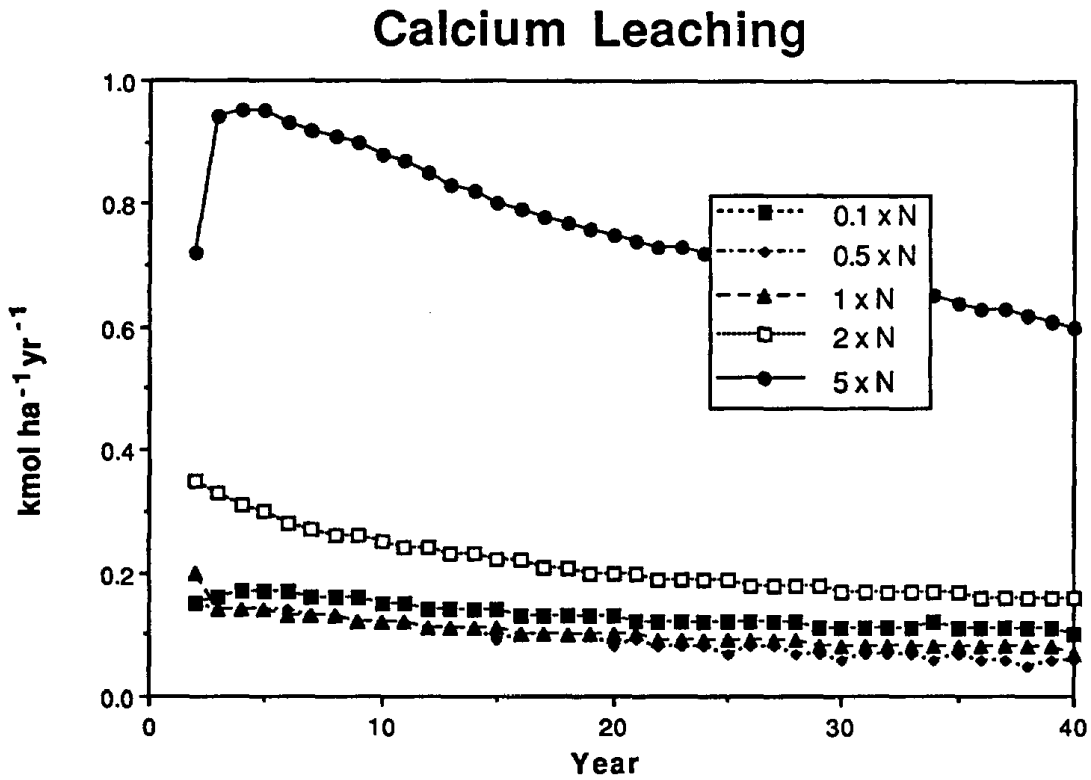


Figure 2-6. Simulated magnesium leaching at Barton Flats under various N deposition scenarios: 0.1 x = 0.14, 0.5 x = 0.68, 1 x = 1.37, 2 x = 2.73, and 5 x = 6.83 kmol ha⁻¹ yr⁻¹ (1.9, 9.5, 28.7, 38.2, and 95.6 kg ha⁻¹ yr⁻¹).

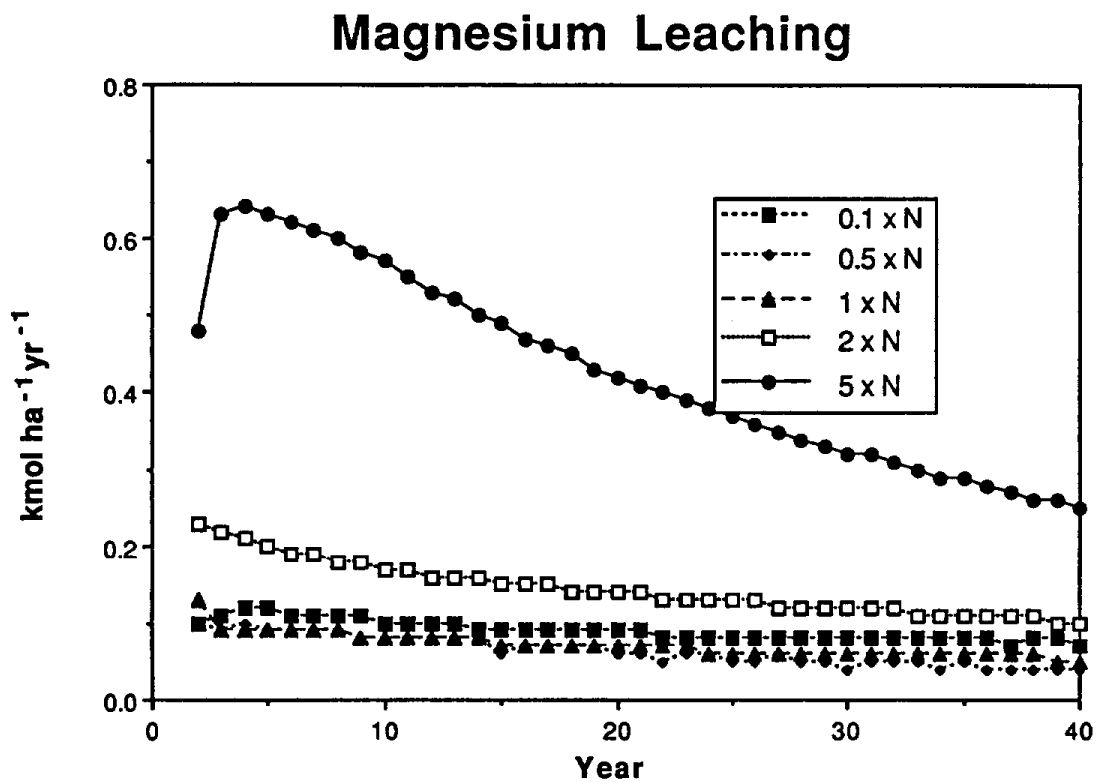


Figure 2-7. Simulated base cation leaching at Barton Flats under various N deposition scenarios: 0.1 x = 0.14, 0.5 x = 0.68, 1 x = 1.37, 2 x = 2.73, and 5 x = 6.83 kmol ha⁻¹ yr⁻¹ (1.9, 9.5, 28.7, 38.2, and 95.6 kg ha⁻¹ yr⁻¹).

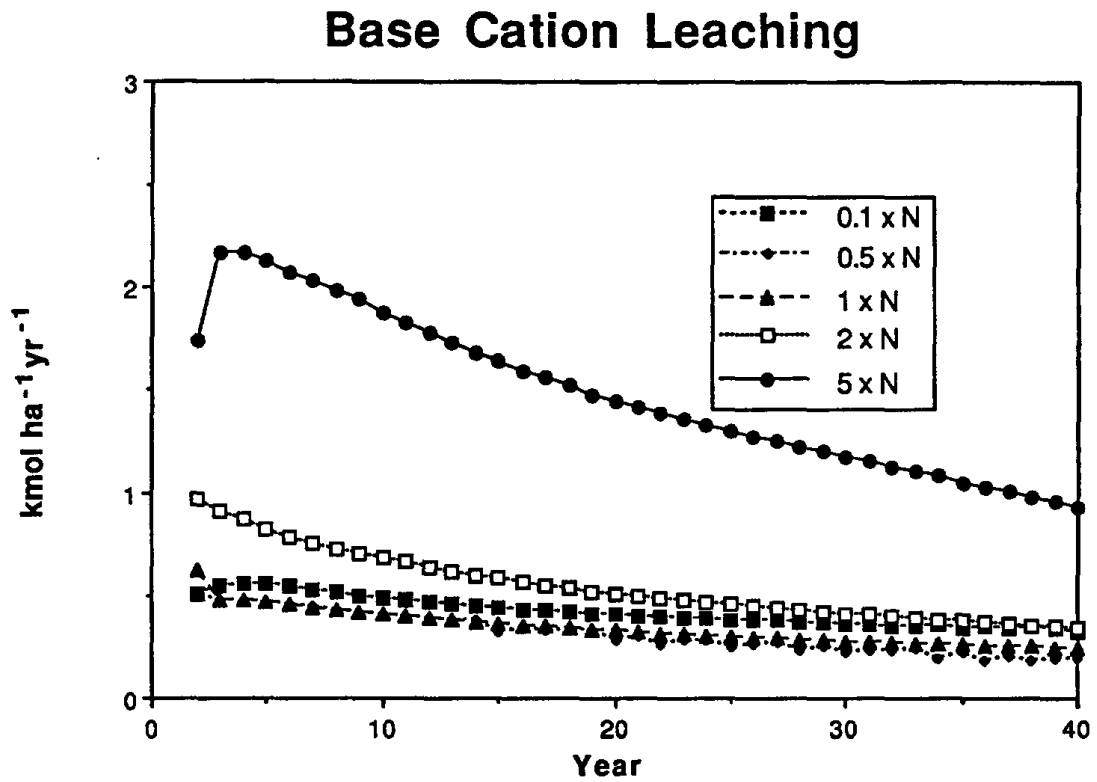


Figure 2-8. Simulated acid neutralizing capacity (ANC) leaching at Barton Flats under various N deposition scenarios: $0.1 \times = 0.14$, $0.5 \times = 0.68$, $1 \times = 1.37$, $2 \times = 2.73$, and $5 \times = 6.83 \text{ kmol ha}^{-1} \text{ yr}^{-1}$ (1.9 , 9.5 , 28.7 , 38.2 , and $95.6 \text{ kg ha}^{-1} \text{ yr}^{-1}$).

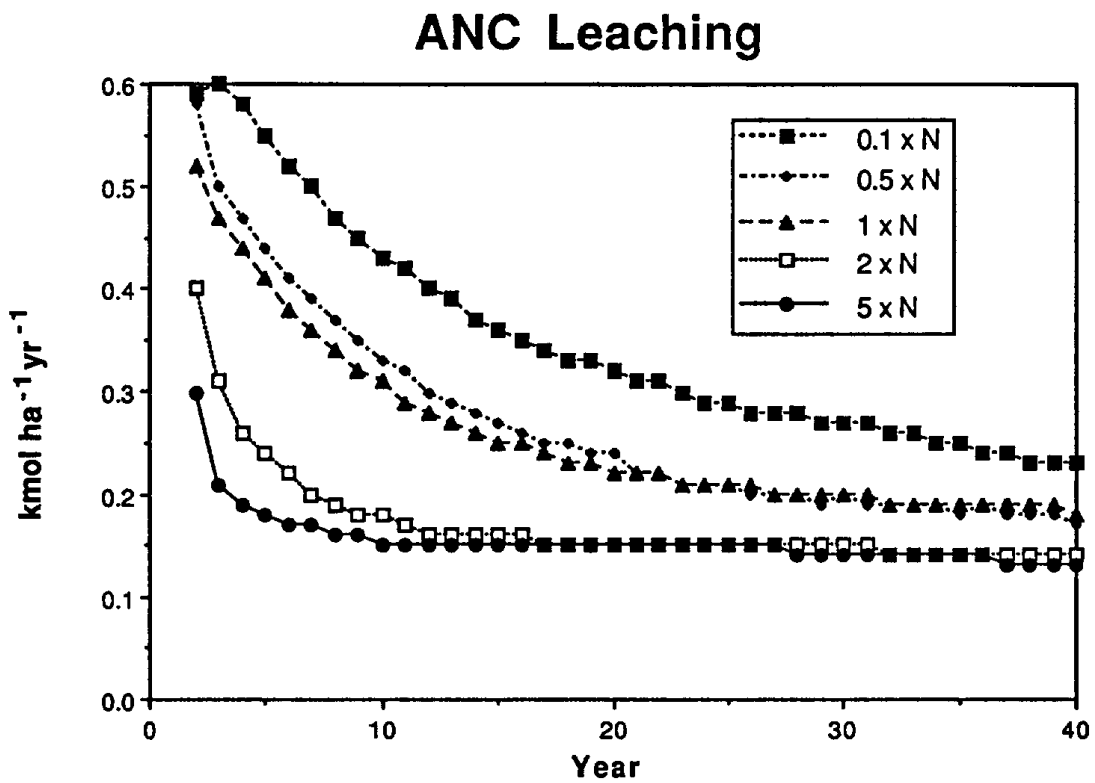


Figure 2-9. Simulated soil solution nitrate concentrations in years 2 and 40 at Barton Flats under various N deposition scenarios: 0.1 x = 0.14, 0.5 x = 0.68, 1 x = 1.37, 2 x = 2.73, and 5 x = 6.83 kmol ha⁻¹ yr⁻¹ (1.9, 9.5, 28.7, 38.2, and 95.6 kg ha⁻¹ yr⁻¹).

B Horizon NO₃⁻

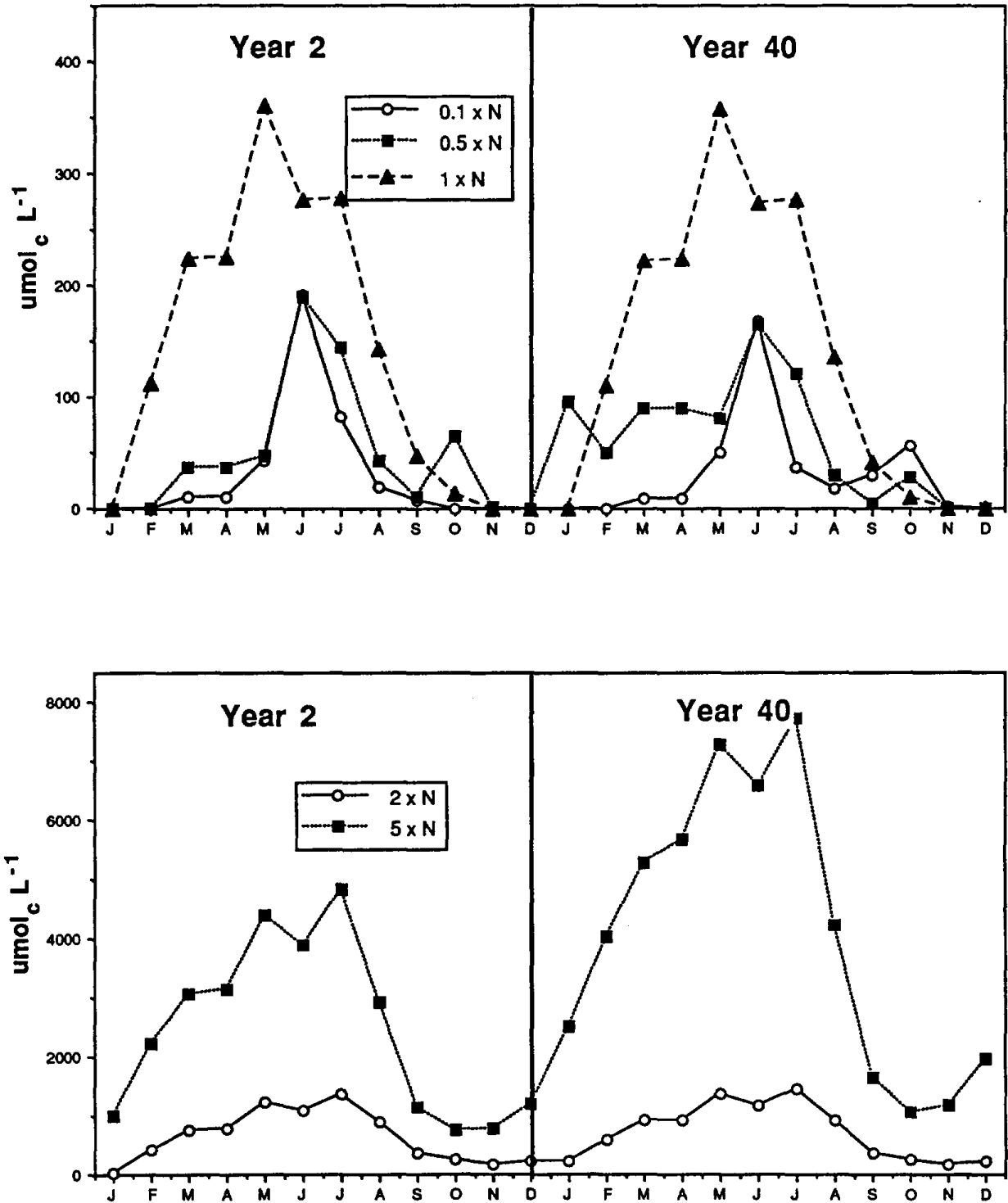


Figure 2-10. Simulated soil solution pH in years 2 and 40 at Barton Flats under various N deposition scenarios: 0.1 x = 0.14, 0.5 x = 0.68, 1 x = 1.37, 2 x = 2.73, and 5 x = 6.83 kmol ha⁻¹ yr⁻¹ (1.9, 9.5, 28.7, 38.2, and 95.6 kg ha⁻¹ yr⁻¹).

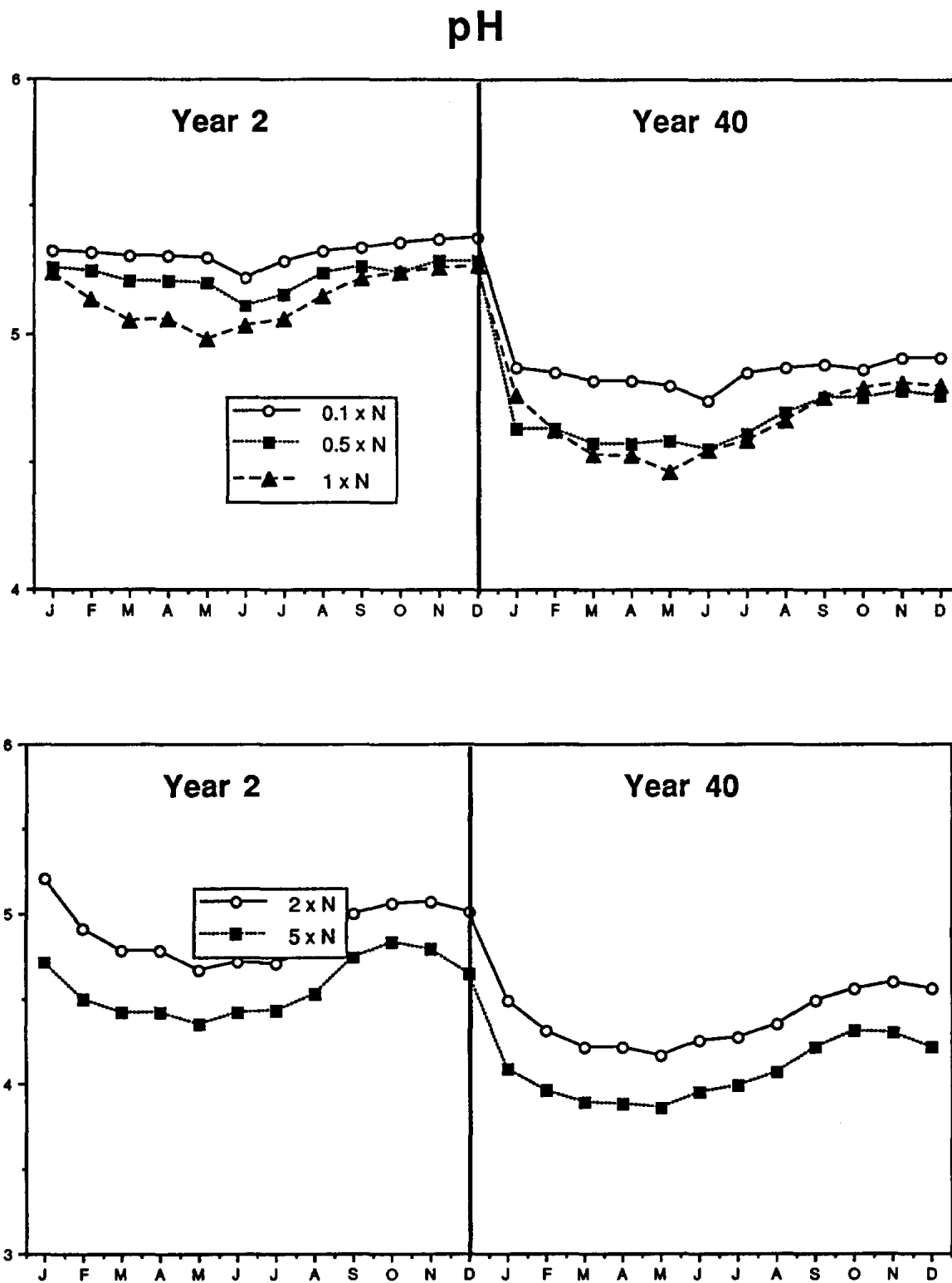


Figure 2-11. Simulated soil base saturation at Barton Flats under various N deposition scenarios: $0.1 \times = 0.14$, $0.5 \times = 0.68$, $1 \times = 1.37$, $2 \times = 2.73$, and $5 \times = 6.83 \text{ kmol ha}^{-1} \text{ yr}^{-1}$ (1.9, 9.5, 28.7, 38.2, and $95.6 \text{ kg ha}^{-1} \text{ yr}^{-1}$).

Base Saturation

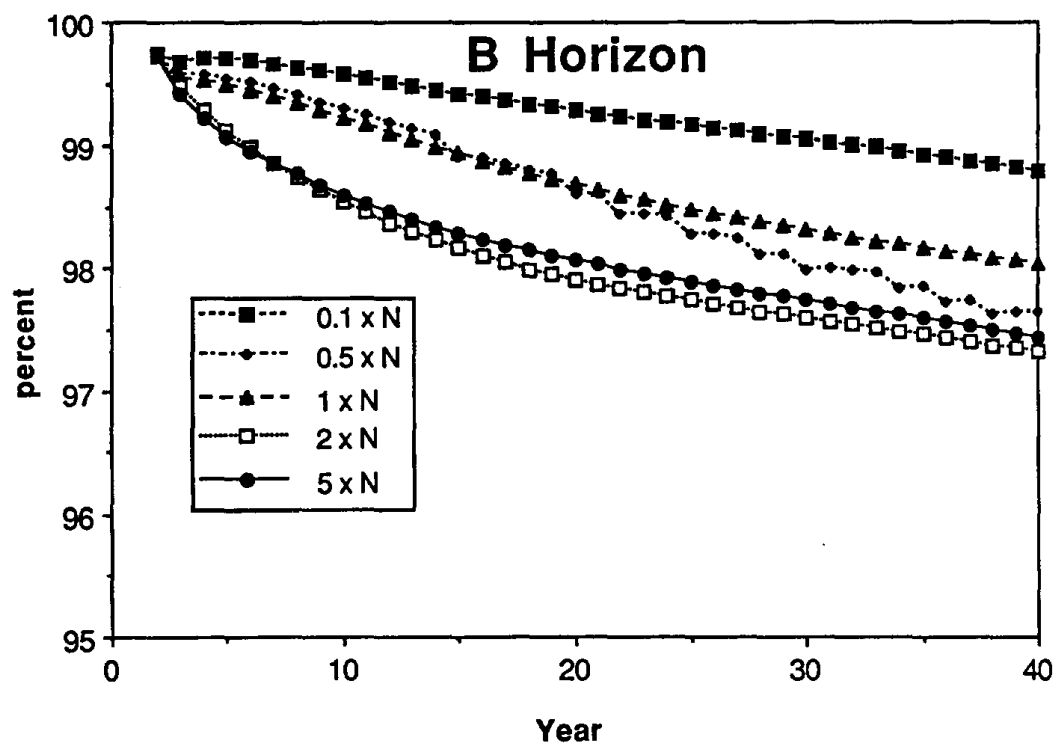
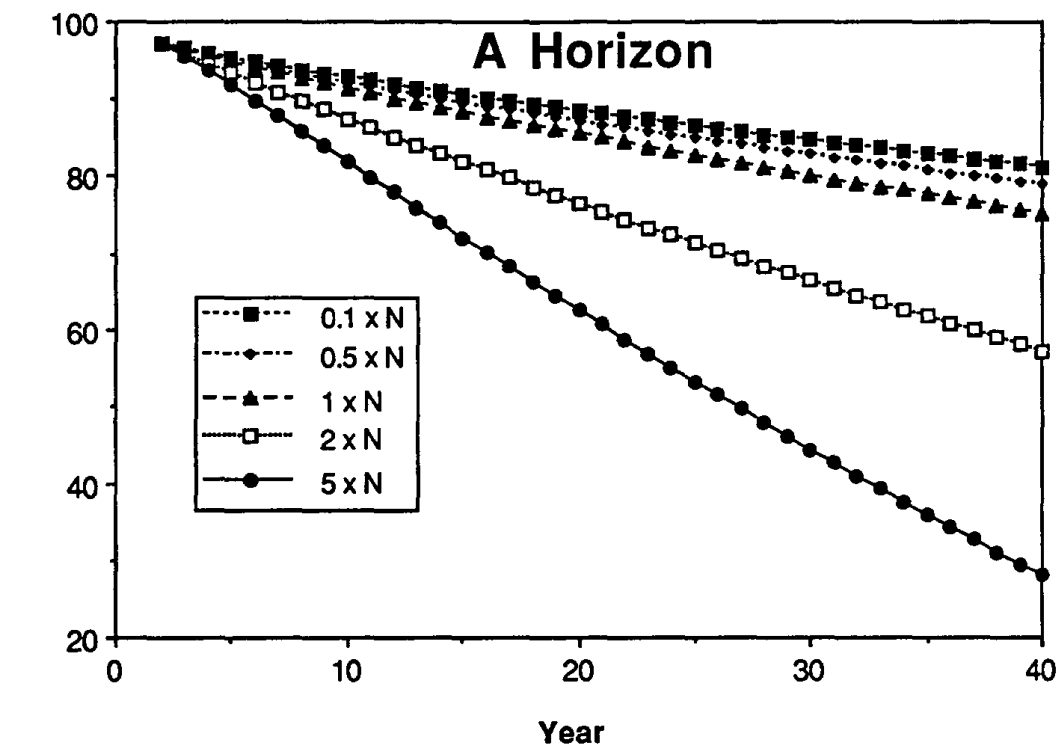


Figure 2-12. Simulated soil solution acid neutralizing capacity (ANC) concentrations in years 2 and 40 at Barton Flats under various N deposition scenarios: $0.1 \times = 0.14$, $0.5 \times = 0.68$, $1 \times = 1.37$, $2 \times = 2.73$, and $5 \times = 6.83 \text{ kmol ha}^{-1} \text{ yr}^{-1}$ (1.9, 9.5, 28.7, 38.2, and $95.6 \text{ kg ha}^{-1} \text{ yr}^{-1}$).

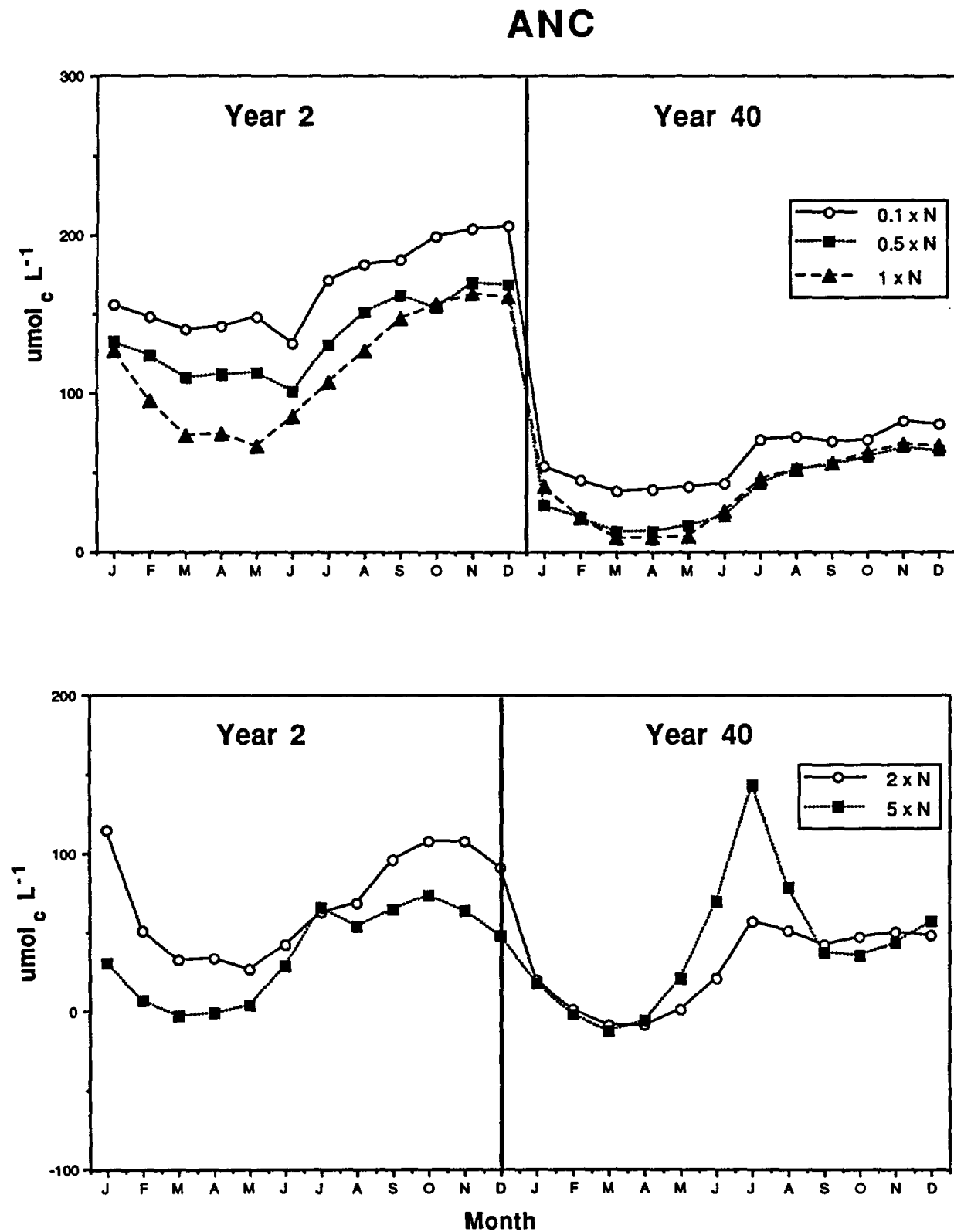


Figure 2-13. Simulated soil solution sulfate concentrations in years 2 and 40 at Barton Flats under various N deposition scenarios: 0.1 x = 0.14, 0.5 x = 0.68, 1 x = 1.37, 2 x = 2.73, and 5 x = 6.83 kmol ha⁻¹ yr⁻¹ (1.9, 9.5, 28.7, 38.2, and 95.6 kg ha⁻¹ yr⁻¹).

B Horizon SO₄²⁻

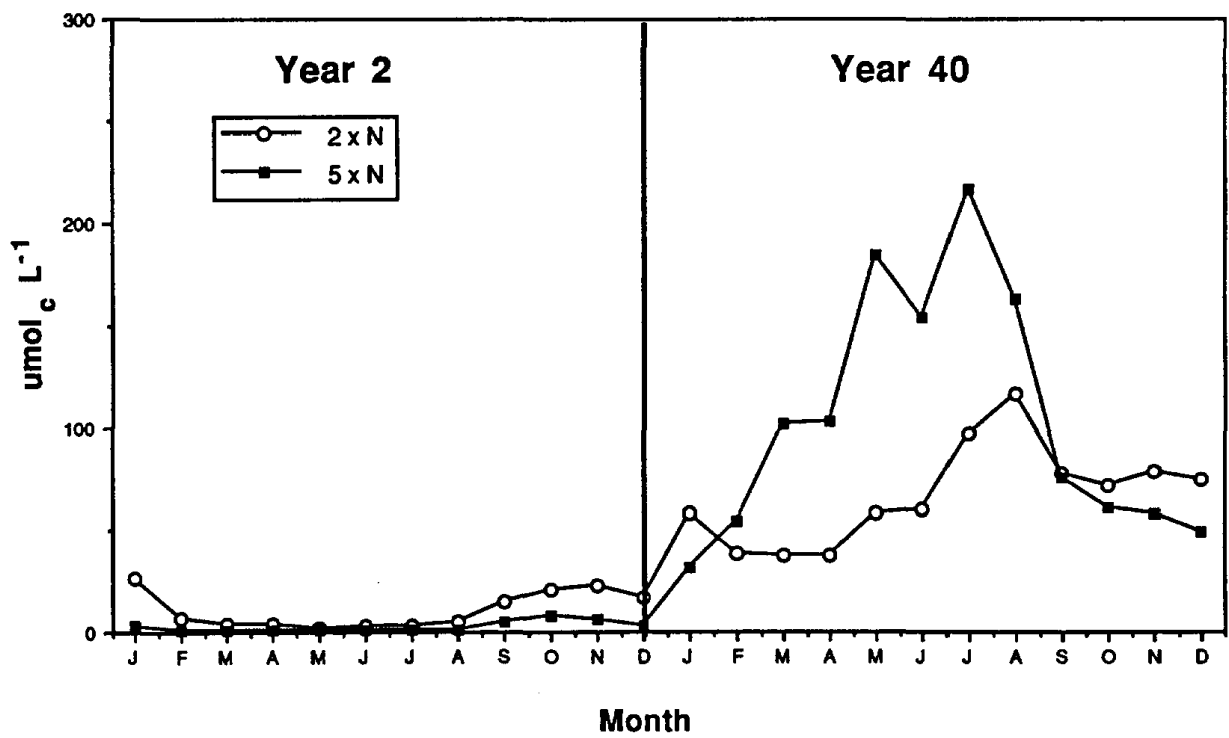
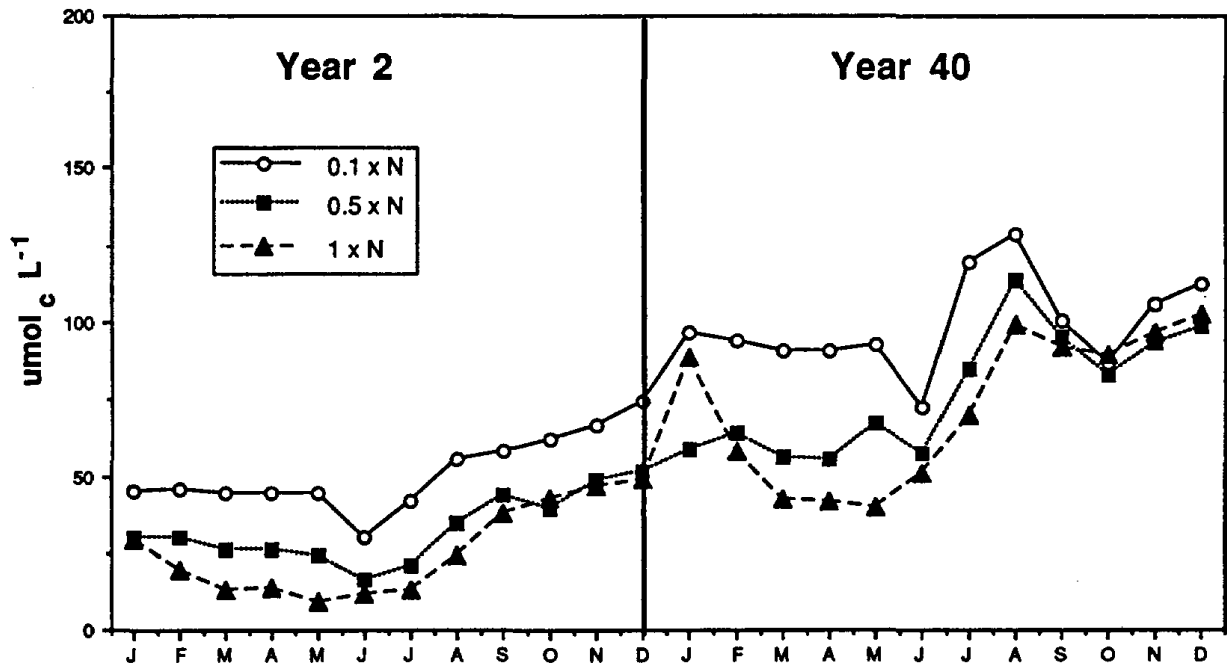


Figure 2-14. Simulated soil solution total anion concentrations in years 2 and 40 at Barton Flats under various N deposition scenarios: 0.1 x = 0.14, 0.5 x = 0.68, 1 x = 1.37, 2 x = 2.73, and 5 x = 6.83 kmol ha⁻¹ yr⁻¹ (1.9, 9.5, 28.7, 38.2, and 95.6 kg ha⁻¹ yr⁻¹).

Total Anions

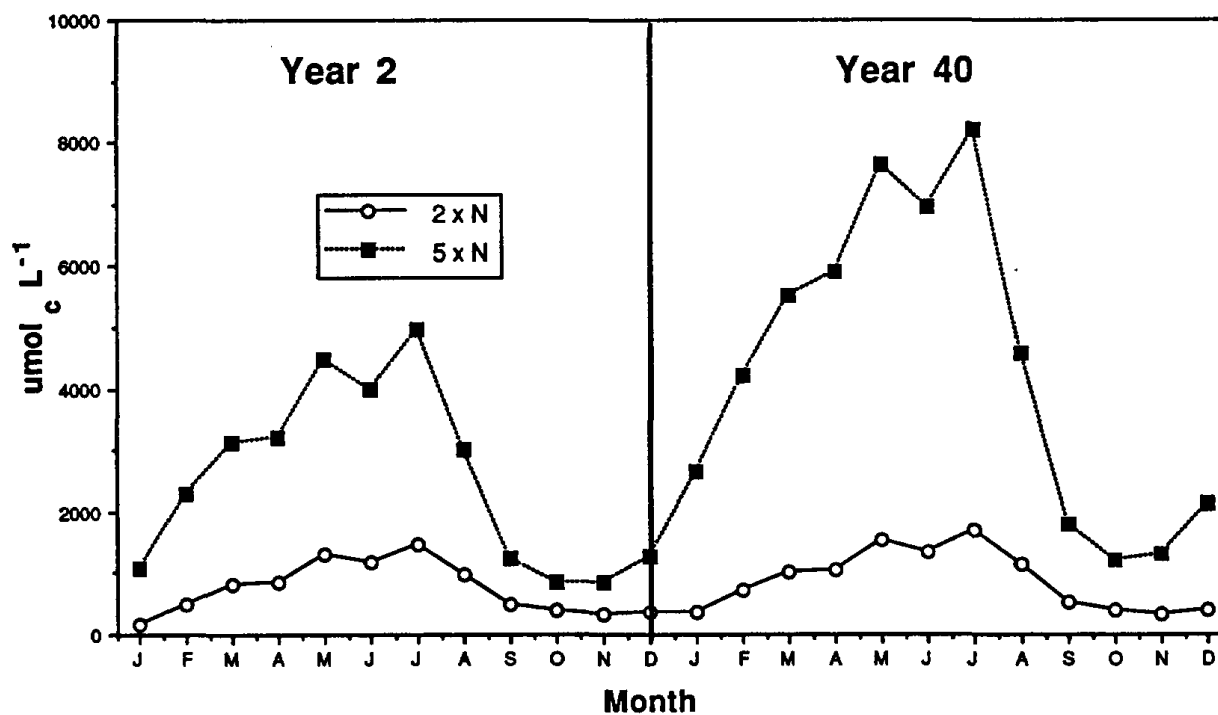
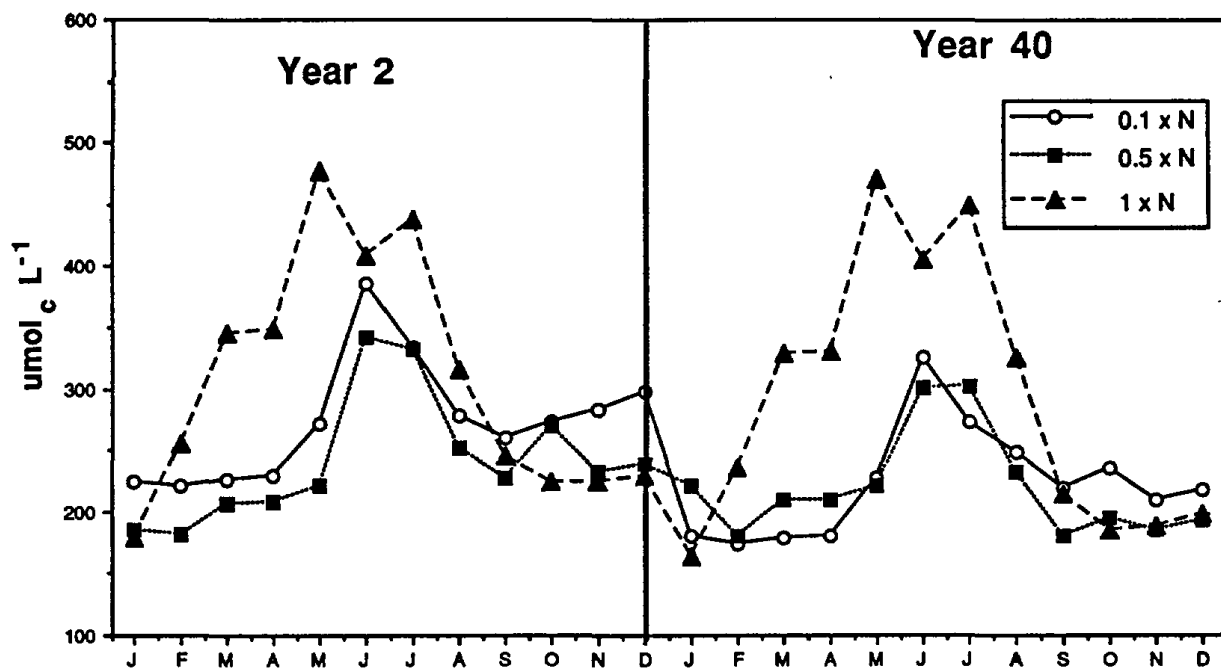
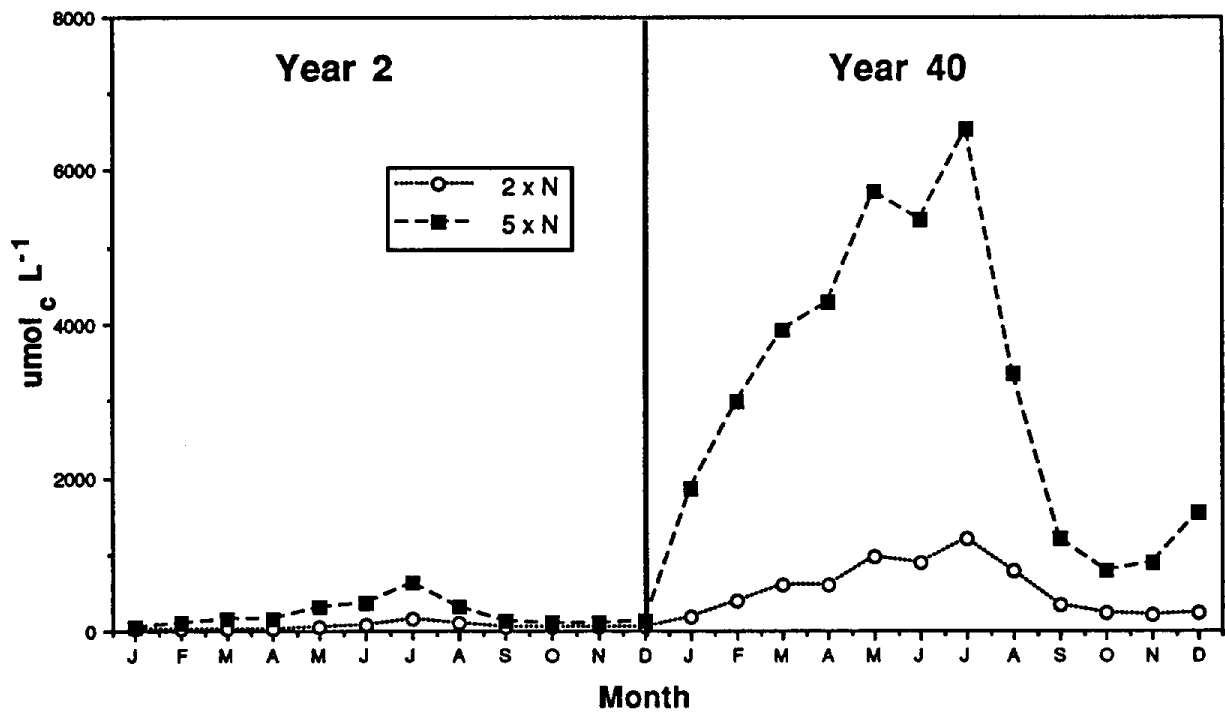
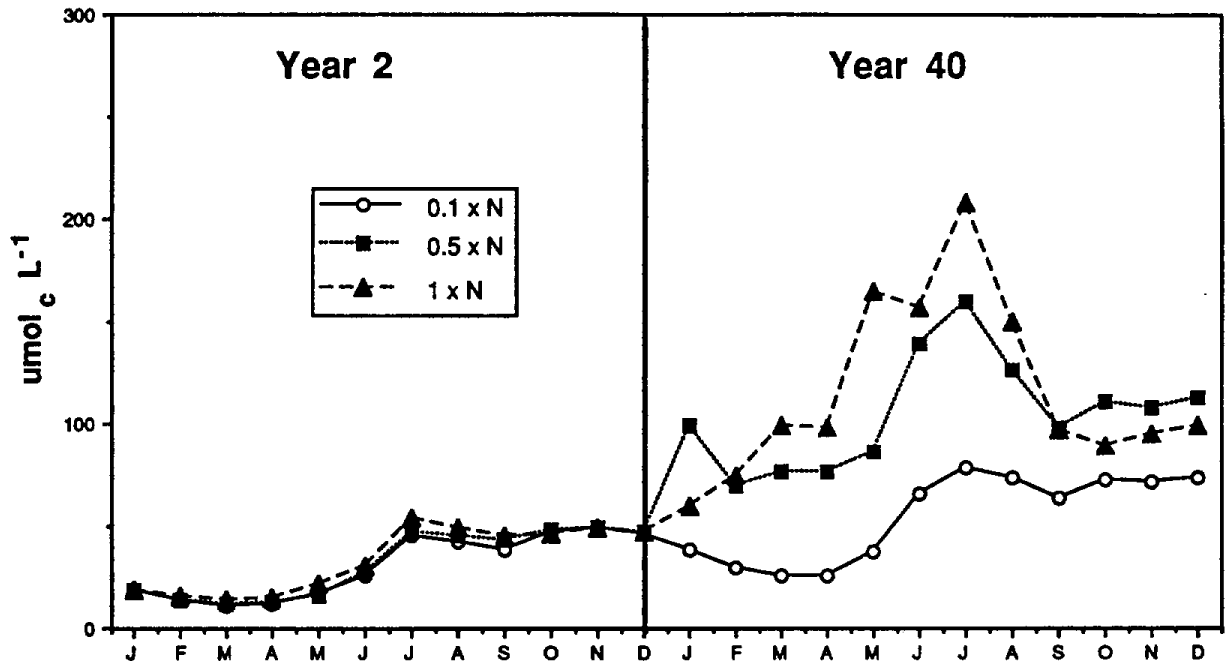


Figure 2-15. Simulated soil solution aluminum concentrations in years 2 and 40 at Barton Flats under various N deposition scenarios: 0.1 x = 0.14, 0.5 x = 0.68, 1 x = 1.37, 2 x = 2.73, and 5 x = 6.83 kmol ha⁻¹ yr⁻¹ (1.9, 9.5, 28.7, 38.2, and 95.6 kg ha⁻¹ yr⁻¹).

B Horizon Alⁿ⁺



3.0 PATTERNS OF GAS EXCHANGE AND OZONE UPTAKE IN PINES AT BARTON FLATS

Patrick J. Temple

3.1 Introduction

The photochemical air pollutant ozone (O_3) is responsible for significant adverse effects on foliar injury and growth of forest trees, particularly ponderosa and Jeffrey pines, in the mountains of southern and central California (Miller, 1992). Efforts to establish ambient air quality standards for O_3 that will protect trees from injury have been hampered by uncertainties in establishing clear dose-response relationships between atmospheric concentrations of O_3 and foliar injury and growth responses of trees. A major component of these uncertainties is the observation that the adverse effects of O_3 are determined not by atmospheric concentrations but by the biologically-effective dose of O_3 absorbed by the tree (Runeckles, 1991). Uptake of ambient O_3 by plant foliage is determined by the gas exchange characteristics of the tree, which are controlled primarily by rates of stomatal conductance. Factors that determine the rate of stomatal conductance will also determine the rate of absorption of the biologically effective dose of O_3 derived from atmospheric concentrations (Fowler *et al.*, 1989). Thus, in order to link ambient air monitoring of O_3 with predicted or observed effects on foliar injury or tree growth, it is necessary to determine the amount of O_3 absorbed by the tree over the monitoring period (Taylor and Hanson, 1992).

Stomatal conductance is a highly complex physiological parameter, under the control of a suite of exogenous and endogenous factors. Current attempts to model stomatal conductance and pollutant deposition, such as the Big Leaf model, have emphasized exogenous or environmental control variables, particularly light, relative humidity, soil water, and temperature (Baldocchi *et al.*, 1987, 1991). However, endogenous factors, such as species-specific rates of conductance, or difference in rates of conductance between seedlings and mature trees, may play an even greater role in determining O_3 uptake. Relatively few studies of rates of stomatal conductance have been conducted in the field, and even fewer have measured conductance in the canopies of mature trees for extended periods of time.

3.2 Objective

The objective of this research was to provide specific information on rates of stomatal conductance of different age classes of ponderosa and Jeffrey pines in relation to seasonal changes in environmental conditions, particularly soil water, and to endogenous factors, particularly tree age and developmental stage of the foliage. These data were then used to derive monthly and annual budgets for absorbed O_3 dose, which will be used to link ambient O_3 concentrations with measurements of foliar O_3 injury in the field.

3.3 Methodology

The research was conducted at the Barton Flats tower site, at 2150 m in elevation in the San Bernardino mountains. Systematic measurements of leaf stomatal conductance were taken on a population of Jeffrey pines, consisting of seedlings < 0.5 m in height, saplings 2 to 3 m in height, and mature trees accessed from the tower to a height of approximately 30 m. Intensive measurements were taken on an individual seedling underneath the mature tree canopy and on an individual sapling growing in the clearing 10 m from the base of the tower. Comparative measurements with other seedlings and saplings indicated that rates of stomatal conductance in the seedling and sapling were representative of their age classes of pines. Measurements of stomatal conductance at the tops of mature trees could only be taken from the tower, so the representativeness

of these measurements could not be determined. However, foliage from the three trees accessible from the tower usually had rates of stomatal conductance that were in agreement to within +/- 10 percent, suggesting of these measurements that they were representative of the population of mature pines at that site.

Beginning in May 1992, rates of stomatal conductance were measured on seedlings, saplings, and mature trees using a steady-state porometer (Model LI-1600, Licor Corp., Lincoln, NE) equipped with a cuvette head especially designed for conifer foliage. Measurements were conducted weekly or biweekly from May to October of 1992, 1993, and 1994, and monthly during the winters of 1992-3 and 1993-4, except when the site was inaccessible. Rates of conductance were measured on three needle fascicles of each age class of foliage, between 0900 and 1200, when rates of conductance were usually at their maximum. Hourly measurements of conductance and transpiration were made on the three age classes of trees from 0600 to 2000 during a period of intensive study in the third week of July 1993, to determine complete diurnal profiles of gas exchange for the trees during the course of the day.

The diameter of each needle fascicle in the cuvette was measured with a digital electronic microcaliper (Mitutoyo Corp., Japan) and the leaf area of the needles was calculated using the formula:

$$\text{Area (cm}^2\text{)} = 2 R L (n + \pi),$$

where R = fascicle radius (cm), L = needle length (cm), and n = number of needles per fascicle, 3 for both ponderosa and Jeffrey pine. These data on leaf area were used to calculate leaf gas exchange on a leaf area basis. Simultaneous measurements of light intensity, relative humidity, and ambient and leaf temperatures were taken with sensors attached to the porometer cuvette.

Concurrent measurements of volumetric soil water contents in the clearing and under the mature tree canopy at the tower site were obtained using an instrument that employed the principle of time-domain reflectometry (TRASE Soil Moisture Meter, SoilMoisture Corp., Santa Barbara, CA). Because of the rocky nature of the soil at the tower site, measurements of soil water were confined to the upper 15 cm of the soil profile. Records of annual and monthly precipitation in the area were obtained from a weather station in Big Bear, 10 km north.

Data on ambient O₃ concentrations in the area were obtained from a monitoring station located at Barton Flats. Average monthly O₃ for daylight hours was calculated for each of the three years of the study. Rates of stomatal conductance as measured for water vapor were converted to rates of conductance for O₃ and the average daily rate of conductance was calculated for each month. Flux of O₃ to foliage was calculated as average daily O₃ concentration (μmol mol⁻¹) times daily conductance rate (mol O₃ m⁻² day⁻¹) = O₃ flux, in μmol m⁻² day⁻¹ for each month of the year.

3.4 Results and Discussion

3.4.1 Patterns of Precipitation and Conductance

Stomatal conductance in the seedlings, saplings, and mature ponderosa and Jeffrey pines at the Barton Flats tower site were strongly influenced by annual and seasonal patterns of precipitation both before and during the three years of the study. Annual precipitation in the area in the previous seven years (1984 to 1990) had averaged 30 percent below normal. This prolonged drought affected the foliar characteristics of the needles, which were significantly shorter than normal. The trees also retained greater numbers of annual whorls of foliage, so that the Jeffrey pines in 1992 retained 7 or more years of foliage, rather than the typical 4 to 5

years of needle retention. The 1990 needle cohort was very small, and in some cases was missing, in response to the extremely dry year of 1989, which was 70 percent below the long-term average precipitation. In 1991, nearly 20 cm of rain fell in March and the trees began to recover from the drought, although annual precipitation totals were below long-term means.

In contrast, precipitation in 1992 was 10 percent above the long-term average of 22.65 cm. Summer rains during July-August increased soil water contents that had been depleted earlier in the summer (Figure 3-1). Maximum rates of stomatal conductance for the seedling and sapling trees of $0.08 \text{ mol m}^{-2} \text{ s}^{-1}$ occurred in early July but by early August conductance had decreased significantly, and then rates gradually declined during the rest of the year to values of $0.01 \text{ mol m}^{-2} \text{ s}^{-1}$ (Figure 3-1). The peak rates of conductance for the young trees measured in 1992 were the highest observed during the three years of the study, which may have reflected recovery from low conductance during the drought years. Peak stomatal conductance for the foliage of mature trees was less than half that of the younger trees, but by mid-August there were no differences in rates of stomatal conductance among the three age classes of trees (Figure 3-1). The relationship between rates of stomatal conductance in the trees and amount of water in the surface soil was not clear, because peak stomatal conductance had occurred before the onset of the summer rainy period, and conductance rates declined at the time that soil water contents remained high (Figure 3-1).

Annual precipitation in 1993 was greater than that of 1992, averaging 42 percent higher than the long-term mean. A late seasonal storm in early June increased the water content of the soil to levels higher than those at the beginning of the year, and soil water remained relatively constant from July to October (Figure 3-2). Patterns of stomatal conductance in the trees were significantly different than those observed in 1992 (Figure 3-2). Stomata were effectively closed during mid-winter months for all age classes of trees. Conductance in seedlings increased gradually in April and remained relatively constant at $0.03 \text{ mol m}^{-2} \text{ s}^{-1}$ until late August, then declined throughout the remainder of the year. Stomatal conductance in the sapling showed a similar pattern, except that the decrease in rates of conductance began earlier in August (Figure 3-2). Conductance in foliage of the mature trees fluctuated throughout the summer, but the decline in conductance rates began in July (Figure 3-2). Rates of conductance in mature tree foliage averaged 30 percent lower than those of the seedling and sapling trees for the entire growing season.

In contrast to the previous two years, winter precipitation in 1994 was below the long-term average and little rain fell from April to August. Soil water reserves became depleted early in the summer (Figure 3-3), and this lack of available soil water impacted rates of gas exchange in the trees. Rates of conductance in the seedling rose from mid-winter levels beginning in March and conductance peaked in May at $0.055 \text{ mol m}^{-2} \text{ s}^{-1}$. Conductance in the sapling peaked in early May at $0.035 \text{ mol m}^{-2} \text{ s}^{-1}$ and in mature trees maximum conductances of $0.03 \text{ mol m}^{-2} \text{ s}^{-1}$ occurred in early May. Conductances began to decline in mid-June and rates of gas exchange were equally low for the remainder of the year for each age class of pines (Figure 3-3). Seedlings had the highest rate of conductance during the active period from April to June, but after June the three age classes of pines had similar rates of conductance (Figure 3-3). During the period in which the trees were active (early April to mid-June) rates of conductance in the mature trees averaged 35 percent lower than in seedlings, but 22 percent higher than in the sapling.

Rates of stomatal conductance and seasonal patterns of conductance for Jeffrey pines in the Sierra Nevada were similar to those observed at Barton Flats in the San Bernardino Mountains. Patterson (1993) reported that maximum rates of stomatal conductance for a stand of Jeffrey pines growing at 2000 m in the Sierras in

1989 occurred in April, with peak conductances of 0.08 to 0.10 mol m⁻² s⁻¹. Conductances remained relatively high until July, then declined through September to less than 0.01 mol m⁻² s⁻¹. However, Patterson observed an increase in conductances in October to levels of 0.04 mol m⁻² s⁻¹, a pattern that did not occur in the San Bernardino Mountains. Gas exchange characteristics of seedling vs. mature foliage of ponderosa pines were compared in a study by Helms *et al.* (1994), conducted in 1992 using grafted clonal material. At their low elevation site in Chico, stomatal conductance of the seedlings peaked in April at 0.11 mol m⁻² s⁻¹, then declined in June to 0.06 mol m⁻² s⁻¹ and remained relatively constant until the end of the measurement period in November. Rates of conductance in mature foliage were lower, with peak conductances in March and July of 0.08 mol m⁻² s⁻¹, but with relatively little variation throughout the season. Conductance values for one year old seedling needles ranged from 8 to 45 percent greater than conductances in similar aged needles from mature trees. Rates of conductance reported in this study (Helms *et al.*, 1994) of ponderosa pine were generally higher than those observed at Barton Flats; however, the ponderosa pines were irrigated throughout the summer, so the data may not reflect conductance rates of trees exposed to drought stress in the field. Coyne and Bingham (1982) in a study of seasonal patterns of stomatal conductance in ponderosa pine conducted in the San Bernardino Mountains at 1600 m, reported that rates of conductance peaked in May, then gradually declined throughout the summer. This pattern was similar to that observed in the present study, except that in the dry year of 1994 rates of conductance declined rapidly after May and remained low throughout the year.

3.4.2 Diurnal Curves of Stomatal Conductance

Hourly measurements of stomatal conductance for the three age classes of pines, averaged over a two-day period of intensive study in July 1993, are shown in Figure 3-4. Conductance in the seedling peaked at 0900, then remained relatively constant until 1500, when stomates began to close. Stomatal conductance in the sapling remained relatively constant throughout the day and declined only as light began to fade after 1800. The mature trees showed a similar pattern, with a rapid decline in conductance only after 1700, in response to fading light.

These diurnal patterns of stomatal conductance for the three age classes of pines suggested that conductance rates were relatively constant throughout the day. Thus, a daily mean rate of conductance, calculated using conductance measurements taken from 0900 to 1200 and the number of hours of daylight, was used to determine ozone flux rates to the pines.

3.4.3 Ozone Flux to Pine Foliage

Ambient ozone concentrations at the field site varied relatively little during the three years of the study (Figure 3-5). Highest daylight ozone concentrations averaged 83 ppb in June and 79 ppb in July. Ozone levels were slightly lower than average in July 1992 because of the prevalent cloudy and rainy conditions during that time. Ozone concentrations during the winter months, November to March, averaged 47 ppb. Although ambient ozone concentrations were relatively uniform from 1992 to 1994, ozone flux to pine foliage varied widely over the three year period, because of the highly variable patterns of stomatal conductance described above. The mean daily ozone flux from 1992 to 1994, averaged on a monthly basis, to one-year-old needles of a seedling Jeffrey pine growing in partly shaded conditions under the canopy of the mature pine trees is shown in Figure 3-6. Flux rates were highest in 1992, with a peak flux rate of 141 μmol O₃ m⁻² day⁻¹ for the month of June. The high flux rate for June was a response not only to the ambient ozone concentrations, which also peaked in June (Figure 3-5), but also to the number of hours of daylight which were also greatest

in June. In 1993, ozone flux averaged 37 percent lower than 1992 over the year. Ozone flux was also more uniformly distributed over the growing season. Flux of ozone in 1994 peaked in June, as in 1992, but peak flux rates were 32 percent lower in 1994 than in 1992. Flux of ozone declined rapidly in July 1994, and continued to decline throughout the summer, reflecting the drought-stressed conditions in 1994. On a yearly basis, average monthly ozone flux in 1994 was similar to 1993, although seasonal patterns of ozone uptake differed significantly between the two years.

Ozone flux rates to the sapling were similar to those measured to the seedling. Flux rates in 1992 averaged twice those of 1993 and 1994, with highest flux rates during the months of May, June, and July (Figure 3-7). These three months accounted for 70 percent of all ozone uptake for the year. In 1994, the drought conditions reduced ozone flux rates in July, August, and September and relatively little ozone uptake occurred during those late summer months. On an annual basis, ozone uptake in the sapling in 1994 was similar to that of 1993, and flux rates in the sapling were similar to those of the seedling over the three years of the study (Table 3-1).

The seasonal patterns of ozone uptake in the mature trees differed significantly among the three years of the study (Figure 3-8). In 1992, ozone uptake was maximum in June, and this one month accounted for 30 percent of total annual ozone flux. Peak ozone uptake in the mature trees was 32 percent lower than that of seedling and sapling trees, and on an annual basis, ozone flux to the mature trees was 30 percent lower than to seedlings and saplings in 1992. Ozone flux to mature trees was lower in 1993, particularly early in the year, and mean annual ozone uptake averaged 44 percent lower than in 1992. However, in the dry year of 1994, ozone flux rates were higher early in the year, and on an annual basis ozone flux to mature foliage averaged only 10 percent lower than fluxes to seedlings and saplings.

3.5 Conclusions

1. Ozone flux to pine foliage was highly variable, both from year-to-year and within the year.
2. Ozone flux to foliage was highest in June, and declined rapidly after June particularly in a dry year such as 1994. From 60 percent to 70 percent of total annual ozone uptake occurred in the months of May, June, and July.
3. Flux of ozone to foliage of mature pine trees averaged 30 percent lower than flux to seedlings and saplings during peak periods in early summer. Later in the summer and in dry years, ozone flux to mature trees was equal to or only slightly lower than flux to foliage of other age classes of trees.
4. Total amount of precipitation the previous winter was associated with total ozone uptake in 1992 (high precipitation) and 1994 (low precipitation), but not in 1993, a year of high precipitation but low ozone uptake.

3.6 References

- Baldocchi, D.D., Hicks, B.B., and Camara, P. (1987). A canopy stomatal resistance model for gaseous deposition to vegetated surfaces. *Atmos. Environ.* 21: 91-101.
- Baldocchi, D.D., Luxmoore, R.J., and Hatfield, J.L. (1991). Discerning the forest from the trees: an essay on scaling canopy conductance. *Agric. Forest Meteorol.* 54: 197-226.
- Coyne, P.I. and Bingham, G.E. (1982). Variation in photosynthesis and stomatal conductance in an ozone-stressed ponderosa pine stand: light response. *Forest Sci.* 28: 257-273.
- Fowler, D., Cape, J.N., and Unsworth, M.H. (1989). Deposition of atmospheric pollutants on forests. *Phil. Trans. R. Soc. London, Ser. B* 324: 247-265.
- Helms, J.A., Anderson, P.D. and Houppis, J.L.J. (1994). Gas exchange by *Pinus ponderosa* in relation to atmospheric pollutants. Final Report, Contract No. A132-101, California Air Resources Board, Sacramento, CA.
- Miller, P.R. (1992). Mixed conifer forests of the San Bernardino Mountains, California. pp. 461-500. In: R.K. Olson, D. Binckley, and M. Bohm, eds. *The Response of Western Forests to Air Pollution*. Ecological Studies, vol. 97. Springer-Verlag, NY.
- Patterson, M.T. (1993). The ecophysiology of ozone-stressed Jeffrey pine. Ph.D. dissertation, Department of Biology, UCLA.
- Runeckles, V.C. (1991). Uptake of ozone by vegetation. pp. 157-188. In: A.S. Lefohn, ed. *Surface level ozone exposures and their effects on vegetation*. Lewis Publ., Inc. Chelsea, MI.
- Taylor, G.E. and Hanson, P.J. 1992. Forest trees and tropospheric ozone - role of canopy deposition and leaf uptake in developing exposure response relationships. *Agric. Ecosys. Environ.* 42: 255-273.

Figure 3-1. Maximum rates of stomatal conductance in one-year-old needles of three age classes of Jeffrey pines, and soil water content (0 to 15 cm) at the Barton Flats tower site in 1992.

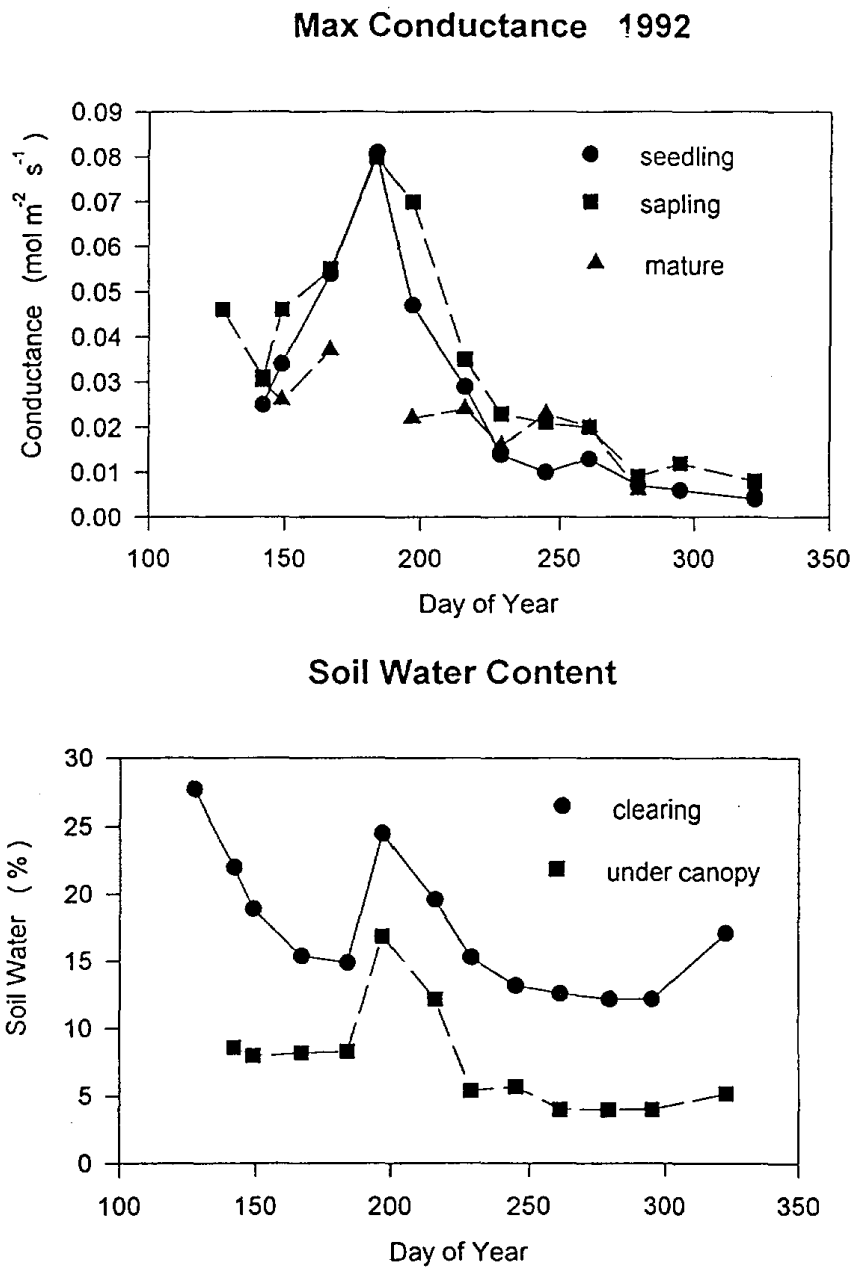


Figure 3-2. Maximum rates of stomatal conductance in one-year-old needles of three age classes of Jeffrey pines, and soil water content (0 to 15 cm) at the Barton Flats tower site in 1993.

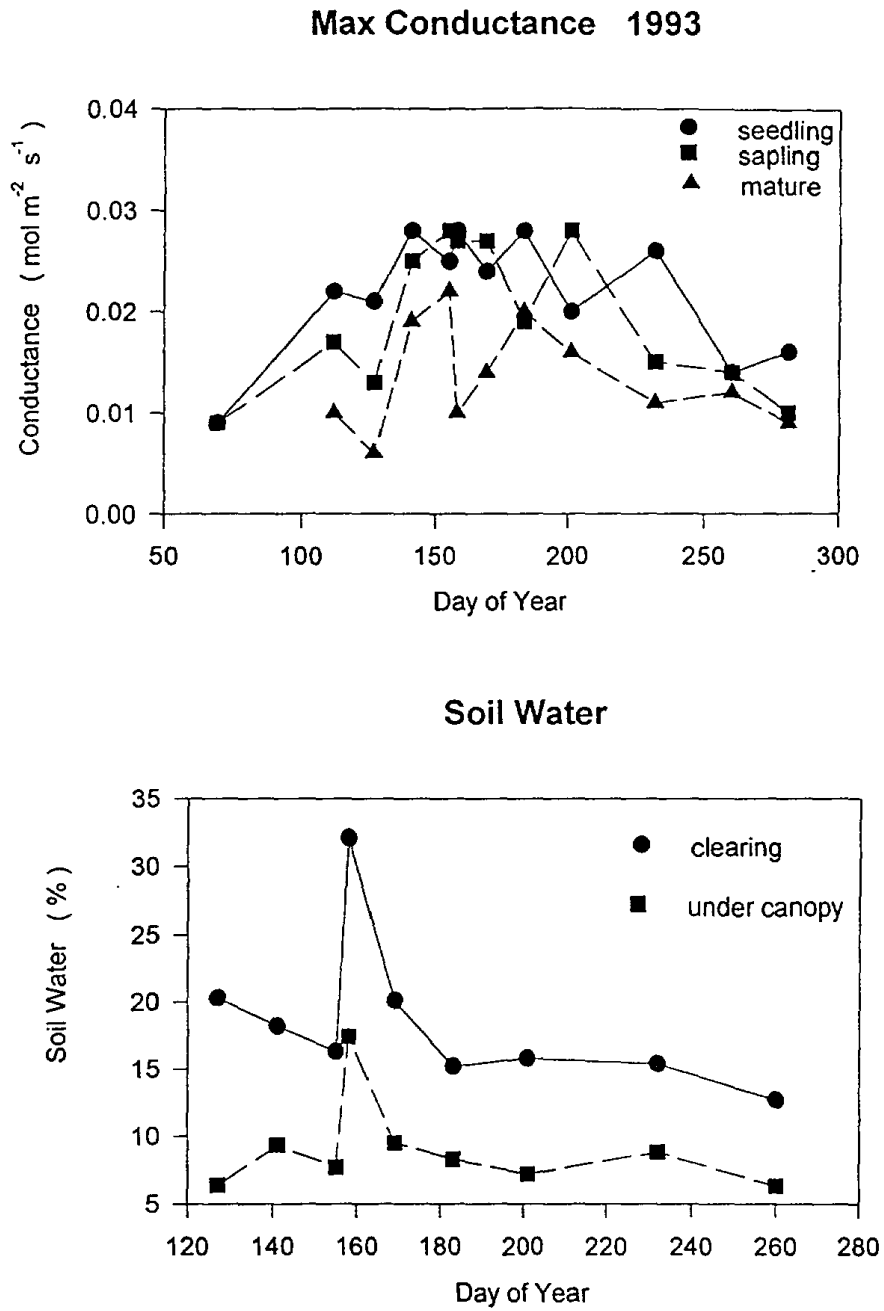


Figure 3-3. Maximum rates of stomatal conductance in one-year-old needles of three age classes of Jeffrey pines, and soil water content (0 to 15 cm) at the Barton Flats tower site in 1994.

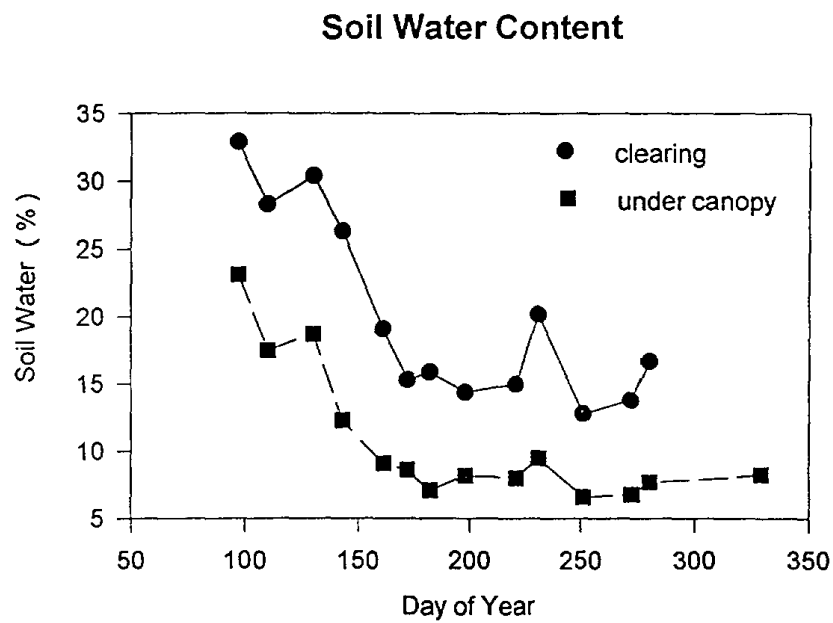
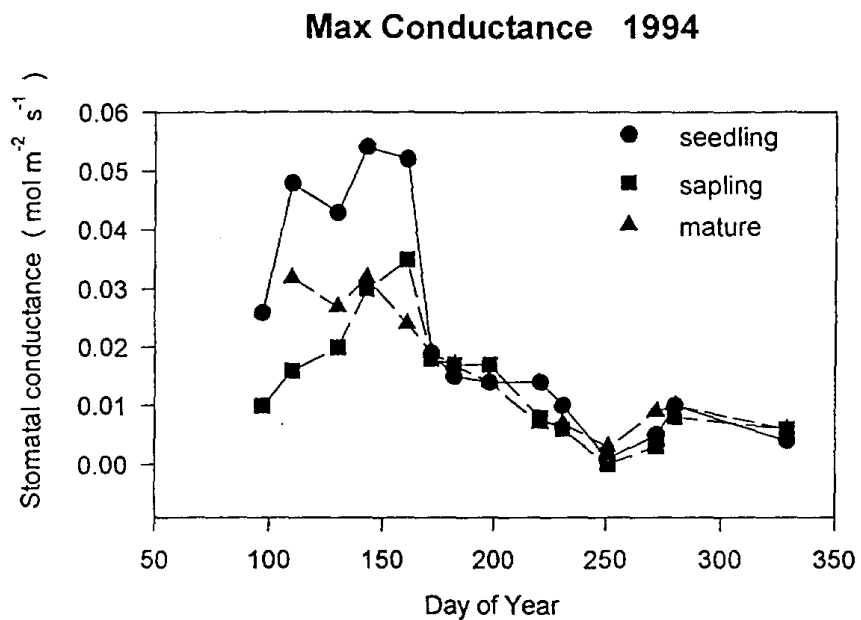


Figure 3-4. Diurnal patterns of stomatal conductance in seedling, sapling, and mature Jeffrey pines at Barton Flats, based upon hourly measurements taken over 21-22 July 1993.

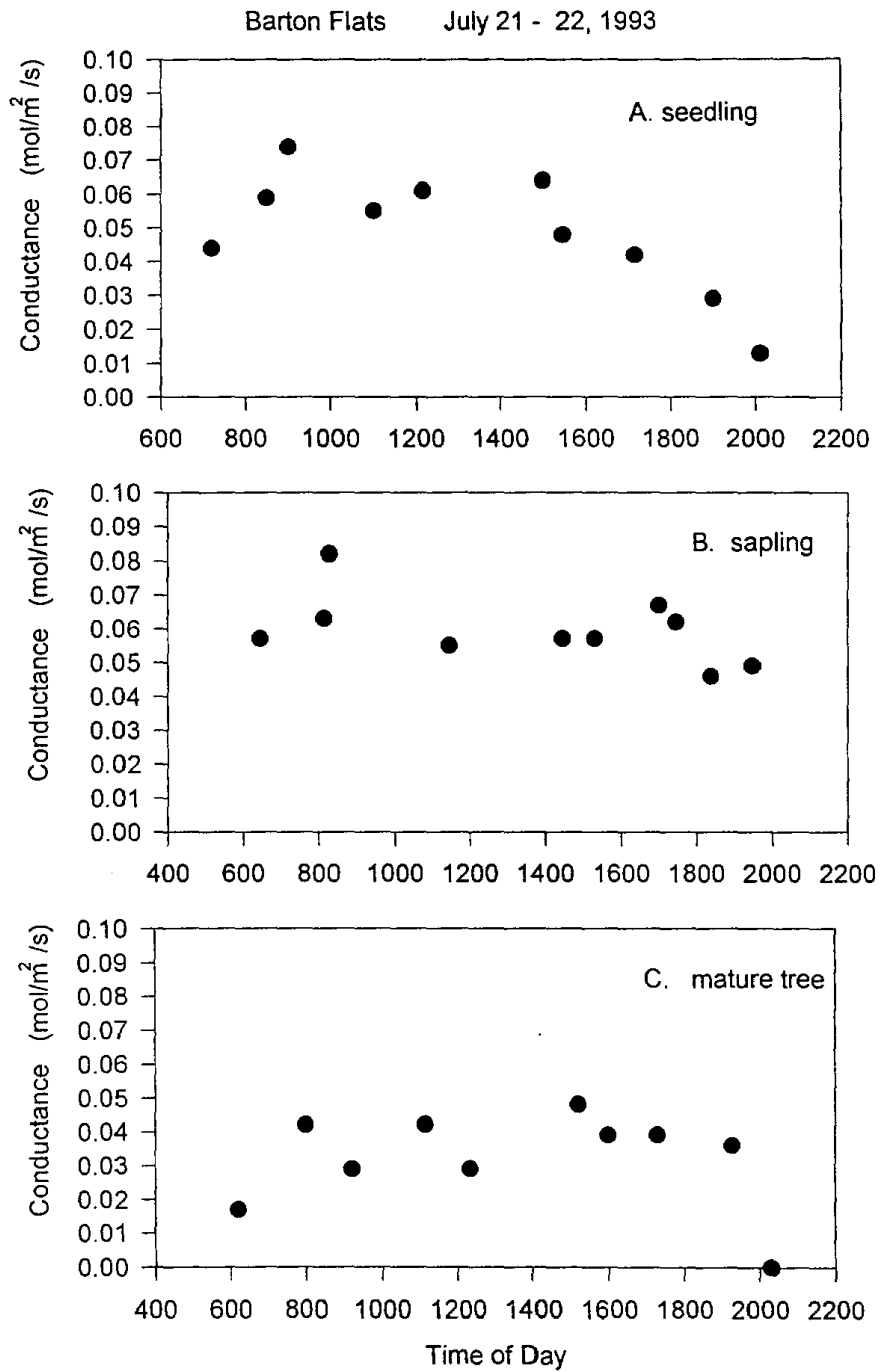


Figure 3-5. Mean monthly ambient ozone concentrations at Barton Flats, 1992 to 1994.

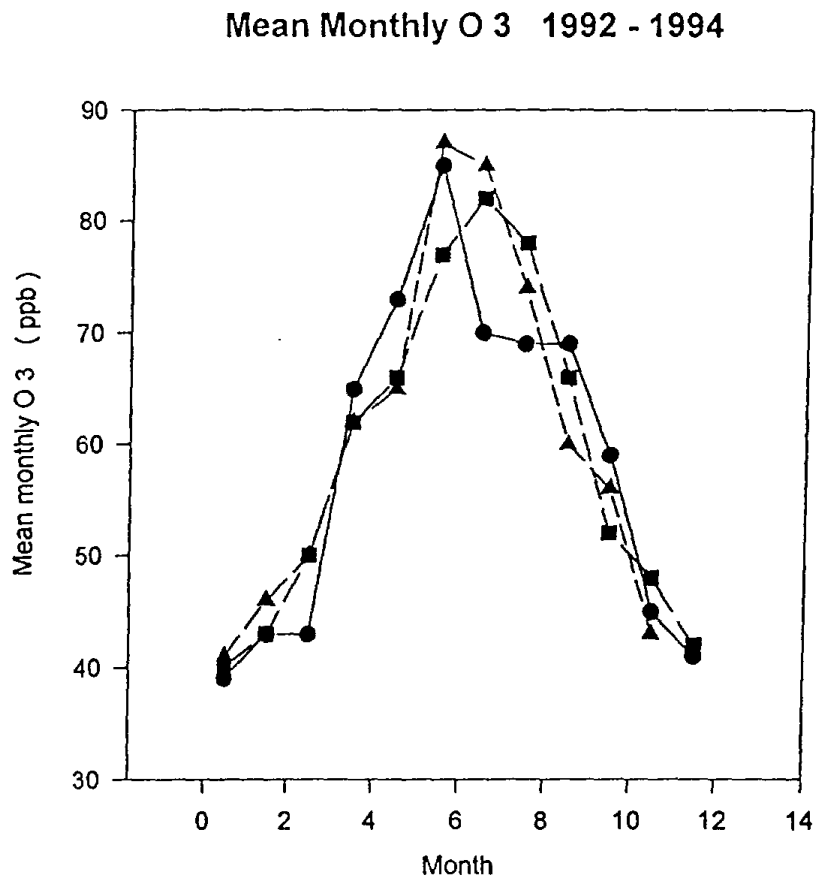


Figure 3-6. Monthly mean daily ozone flux to one-year-old foliage of seedling Jeffrey pine at Barton Flats, 1992 to 1994.

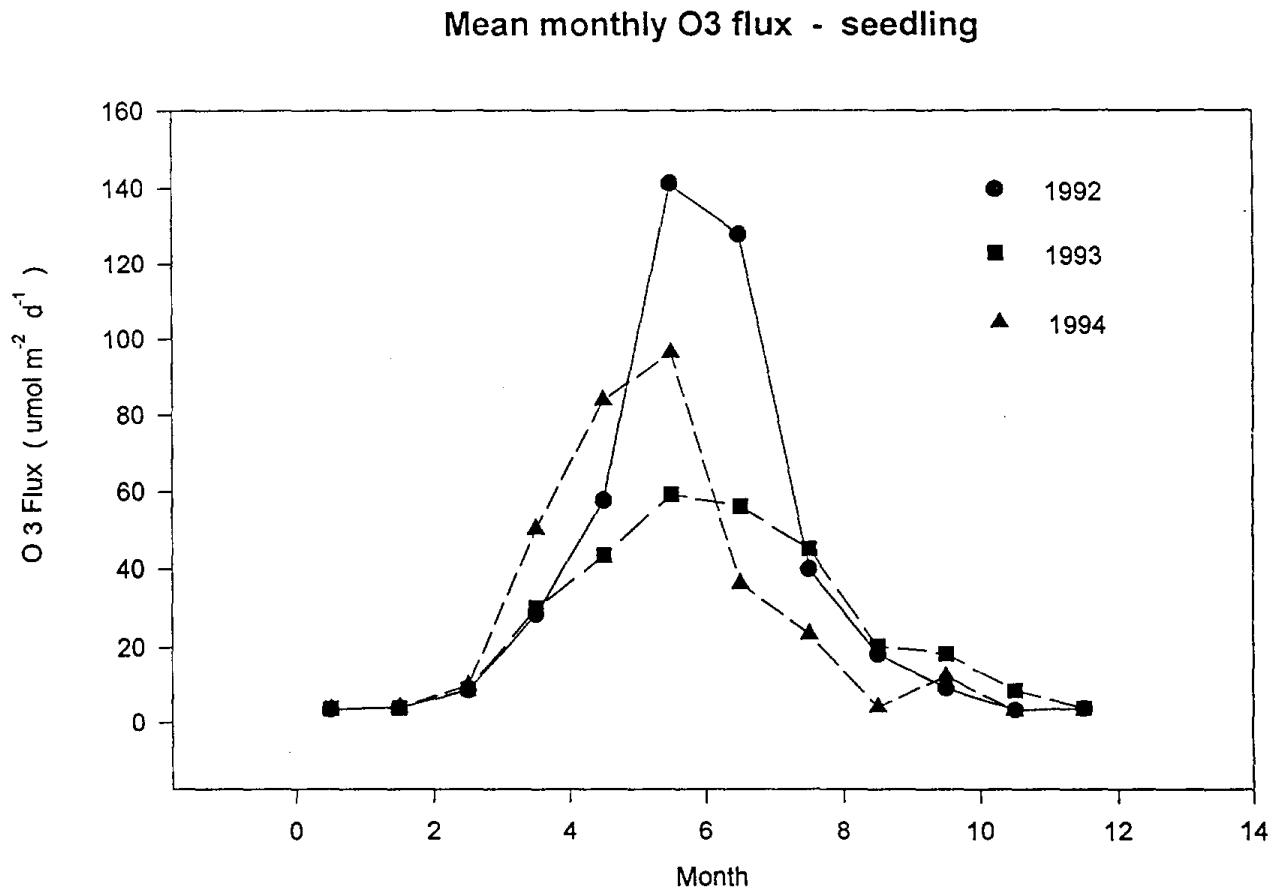


Figure 3-7. Monthly mean daily ozone flux to one-year-old foliage of sapling Jeffrey pine at Barton Flats, 1992 to 1994.

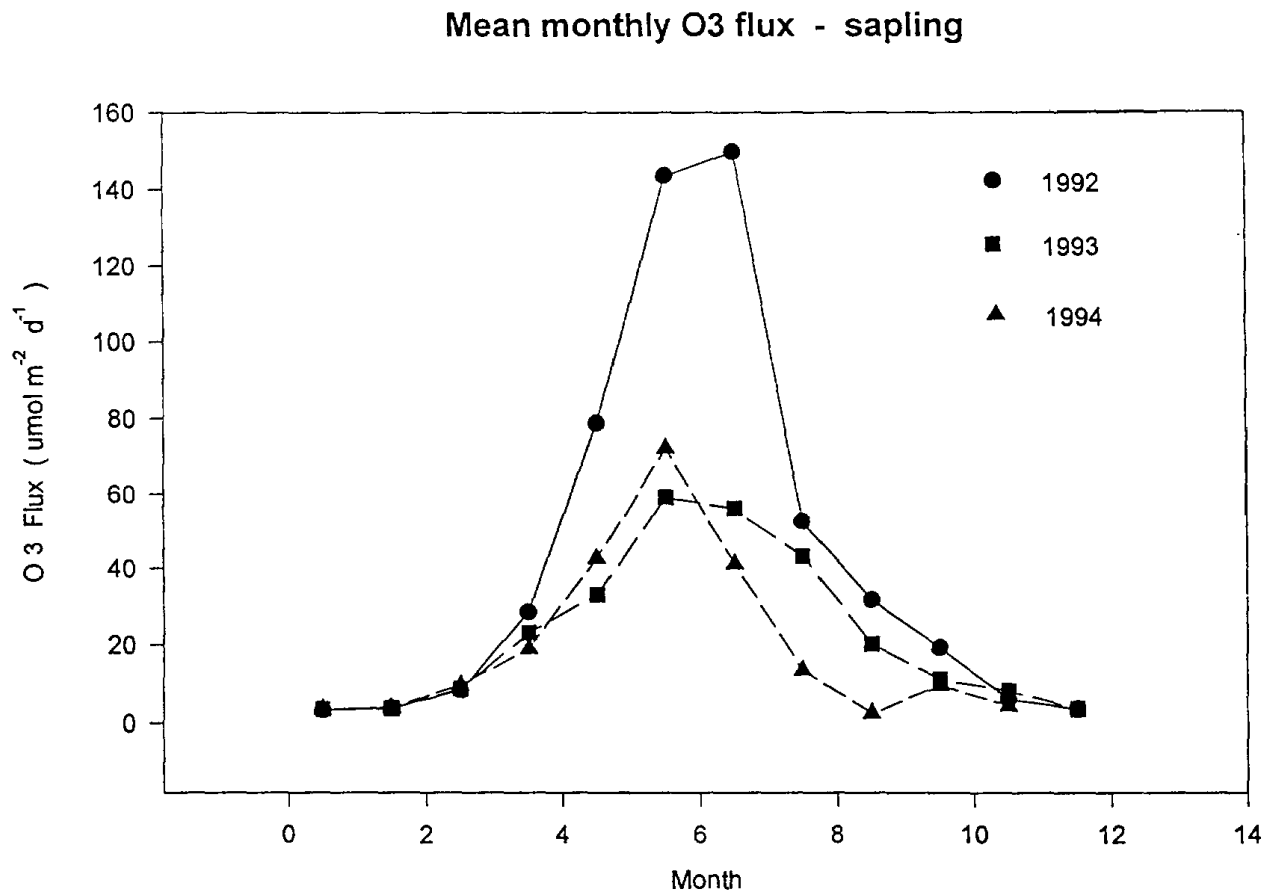
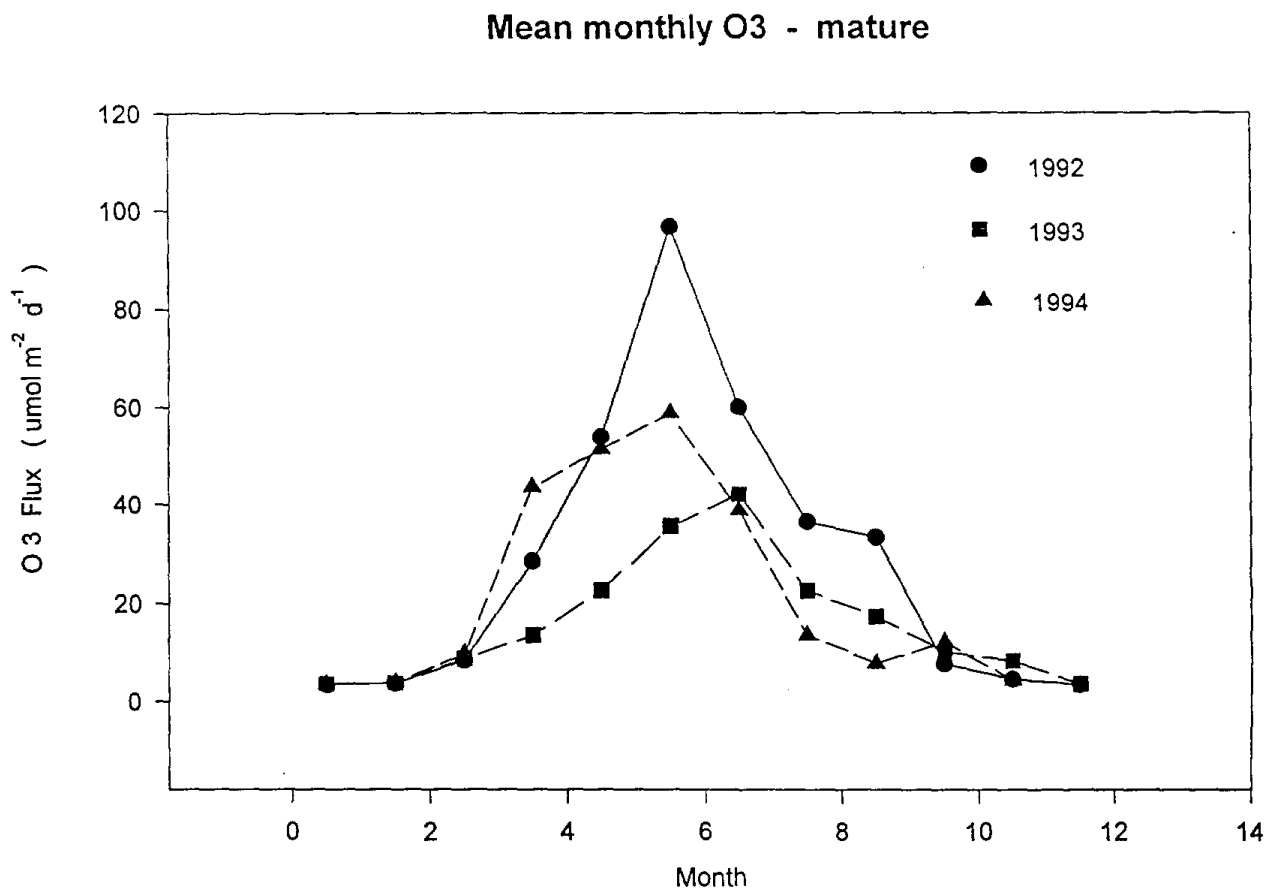


Figure 3-8. Monthly mean daily ozone flux to one-year-old foliage of mature Jeffrey pine at Barton Flats, 1992 to 1994.



Appendix A

Appendix A ENVIRONMENTAL EVALUATION OF FOLIAR INJURY OBSERVATION PLOTS IN FOREST OZONE RESPONSE PROJECT

Patrick J. Temple

A1. Introduction

Six Forest Ozone Response Project plot locations were visited between 24 August and 3 September 1993. The names and locations of the sites are given in Table A3-1. The objectives of these site visits were to measure stomatal conductance on the trees used in foliar injury evaluations and to record physical characteristics of the plots, in particular soil water availability, that could influence stomatal conductance of the trees. The overall objective was to relate the severity of ozone foliar injury symptoms in the pine plots to measurements of ambient ozone concentrations in the area through estimations of ozone flux to pine foliage. These estimates of ozone flux based upon actual measurements of stomatal conductance in the field can be used to validate models of ozone uptake by pine foliage.

A2. Methods

Stomatal conductance of pine foliage was measured with a null-balance steady-state porometer equipped with a cuvette specifically designed for conifer foliage (Model LI-1600, Licor Corp., Lincoln, NE). Wherever possible, tagged trees used in the injury evaluations were measured but in several cases these trees lacked branches low to the ground that could be reached with the porometer. In these cases, smaller pines within the plot were substituted. Stomatal conductance and transpiration were measured on three fascicles from current and one year old needles on tree branches. Concurrent measurements of relative humidity, photosynthetically-active light intensity (PAR), leaf and ambient temperature were made with sensors on the porometer. The volumetric water contents of surface (0 to 15 cm) soil was measured in the plots using time-domain reflectometry (TRASE Model 6050 XI, SoilMoisture Corp., Santa Barbara, CA).

A3. Plot Descriptions

A3.1 White Cloud - Tahoe N.F.

- Plot 1. Fairly dense ponderosa pine dominated mixed conifer stand on S-facing 25 slope with open exposure to the west. Tall ponderosa pines mixed with sugar pine, incense cedar, California black oak, white fir; understory of sapling ponderosa pine, *Ceanothus*, *Arctostaphylos*; ground cover of *Chamaebatia*.
- Plot 2. Fairly open ponderosa pine dominated mixed conifer stand on flat terrain with good exposure to the W. Pines generally younger than those in Plot 1.
- Plot 3. No access to Plot 3.

A3.2 Sly Park - Eldorado N.F.

- Plot 1. Tall ponderosa pine mixed with incense cedar, white fir, occasional sugar pine, black oak; understory of seedling and sapling ponderosa pine. Plot is on shallow S-facing slope, high ridge to SW.
- Plots 2,3. No access.

A3.3 Five-Mile - Stanislaus N.F.

- Plots 1,2,3. Very open ponderosa pine stands on gentle S-facing slopes; clear exposure to W. Trees are mostly young, with dense clumps of seedlings near isolated tall ponderosa pines. Many young pines appeared stressed, possibly because of drought but also heavy infestation of mistletoe in the area. Soil is fine-textured, light reddish-yellow, rocky under thin litter layer.

A3.4 Jerseydale - Sierra N.F.

- Plot 1. Scattered large ponderosa pines on gentle W-facing slope; exposure to W may be limited by intervening ridge to W. Trees are clumped and separated by grassy clearings; occasional large incense cedars and sugar pines; occasional canyon oak (*Q. chrysolepis*).
- Plot 2. Fairly dense ponderosa pine stand on gentle slope; poor exposure to W.
- Plot 3. No access.

A3.5 Shaver Lake - Sierra N.F.

- Plot 1. Very open Jeffrey pine stand on ridge-top; large areas of exposed granite with trees growing in pockets of rocky soil. Sparse understory. Some trees appeared stressed, others had begun senescence of older needles.
- Plot 2. Mixed ponderosa and Jeffrey pine stand on gentle SE-facing slope, interspersed with incense cedar and black oak. Understory is *Rosa* and *Arctostaphylos*. Good soil water availability. Trees appeared healthy and less stressed than at Plot 1.
- Plot 3. Very open mixed ponderosa and Jeffrey pine stand. Trees are scattered in a clearing near meadows; good soil water availability. Oldest age class of needles, usually fourth year but occasionally third year, beginning to senesce.

A3.6 Mountain Home - Sequoia N.F.

- Plot 1. Fairly dense mixed conifer plot on steep (45) E-facing slope, with some exposure to SW. Young ponderosa pines mixed with large black oaks, young incense cedar and white fir. Ground cover is dense *Chamaebatia*.
- Plot 2. Open ponderosa pine stand on ridge-top with good exposure to W. Many dead pines, interspersed with black oak and incense cedar, occasional sugar pine. Ground cover is dense *Chamaebatia*.
- Plot 3. Dense stand of mixed conifers in SE-facing ravine. Trees are on steep slopes on either side of ravine. Oaks dominate near bottom of slope, pines near top. Understory of dense incense cedar saplings and seedlings. Ground cover of dense *Chamaebatia*.

A4. Stomatal Conductance and Soil Water Contents

Age class	Conductance (mol m ⁻² s ⁻²)	Transpiration (mmol m ⁻² s ⁻¹)	Fascicle diam.(mm)	Needle length (mm)
-----------	---	--	--------------------	-----------------------

White Cloud

Plot 1.

Tree No. 76: Time 1250, RH 23.2%, PAR 430, Temp. 31.2°

1993	0.044	2.36	1.4	183
1992	0.031	1.78	1.4	156

Tree No. 75: Time 1315, RH 18.0%, PAR 1510, Temp. 33.0°

1993	0.037	1.81	1.6	166
1992	0.022	1.08	1.5	160

Soil water content 12.0%

Plot 2.

Tree No. 51: Time 1515, RH 24.8%, PAR 1270, Temp. 33.8°

1993	0.043	2.25	2.25	183
1992	0.043	2.21	1.4	188

Soil water content 21.8%

Sly Park

Plot 1.

P. pine sapling (ca. 15 yrs old): Time 0945, RH 31.6%, PAR 1060, Temp. 24.4°

1993	0.070	1.83	1.5	235
1992	0.070	1.64	1.3	185

Soil water content 9.2%

Five Mile

Plot 1.

P. pine sapling (ca. 25 yrs old): Time 1530, RH 18.8%, PAR 610, Temp. 28.6°

1993	0.026	0.96	1.3	153
1992	0.042	1.55	1.3	152

Jerseydale

Plot 1.

Tree No. 21: Time 0930, RH 42.4%, PAR 47, Temp. 17.6°

1993	0.026	0.36	1.6	209
1992	0.026	0.35	1.6	194

Tree No. 49: Time 1000, RH 42.0%, PAR 450, Temp. 18.0°

1993	0.042	0.61	1.3	187
1992	0.036	0.56	1.4	197

Soil water 13.1%

Plot 2.

P. pine sapling: Time 1030, RH 25.2%, PAR 490, Temp. 24.3°

1993	0.076	2.05	1.8	203
1992	0.067	1.81	1.7	247

Shaver Lake

Plot 1.

Tree No. 14 (J. pine): Time 1015, RH 24.4%, PAR 650, Temp. 27.2°

1993	0.025	0.97	1.5	170
1992	0.025	0.85	1.6	151

Tree No. 13 (J. pine): Time 1030, RH 24.0%, PAR 1520, Temp. 29.6°

1993	0.016	0.68	1.5	166
1992	0.016	0.77	1.5	139

Soil water 6.6%

Plot 2.

J. pine near tree No. 51: Time 1130, RH 21.2%, PAR 1730, Temp. 30.6°

1993	0.025	1.01	1.31	157
1992	0.031	1.27	1.2	163

Plot 3.

J. pine sapling near tree no. 43 (tree has only current and previous year's needles, green older needles senescent): Time 1230, RH 22.4%, PAR 164, Temp. 29.2°

1993	0.053	1.93	1.4	138
1992	0.047	1.80	1.4	150

J. pine sapling near tree no. 42 (tree has 5-6 yrs of healthy green needles): Time 1245, RH 22.4%, PAR 126, Temp. 29.2°

1993	0.019	0.74	1.3	142
------	-------	------	-----	-----

1992	0.019	0.73	1.7	175
Soil water 8.8%				

Mountain Home

Plot 1.

P. pine sapling: Time 0900, RH 39.6%, PAR 1170, Temp. 26.2°

1993	0.054	1.67	1.7	199
1992	0.026	0.81	1.6	148

Soil water (thick litter layer) 6.3%

Plot 2.

Tree no. 8 (four years of needles): Time 110, RH 28.4%, PAR 1450, Temp. 28.0°

1993	0.028	0.98	1.5	190
1992	0.044	1.39	1.5	150

Soil water 8.3%

Plot 3.

Stressed P. pine sapling (3 years needle retention): Time 1130, RH 24.8%, PAR 1820, Temp. 29.8°

1993	0.007	0.28	1.5	169
1992	0.003	0.23	1.4	145

Healthy P. pine sapling (5 years needle retention): Time 1145, RH 29.6%, PAR 240, Temp. 30.2°

1993	0.003	0.16	1.4	142
1992	0.003	0.18	1.2	106

A5. Trends in Stomatal Conductance

A5.1 Comparisons Among Sites

The average stomatal conductance for all measured trees at each site is shown in Figure A3-1. The sites are arranged in sequence from White Cloud in the North to Mountain Home in the South. The plots at Sly Park had the highest conductances and the Shaver Lake plots had the lowest. No geographical trends were observed either for 1993 or 1992 needles. Conductances for 1993 needles averaged $0.039 \text{ mol m}^{-2} \text{ s}^{-1}$, slightly greater than 1992 needles, which averaged 0.036 , but these differences were not statistically significant.

A5.2 Comparisons Among Plots

The average stomatal conductance for each plot is shown for 1993 foliage in Figure A3-2 and for 1992 foliage in Figure A3-3. The plots at Mountain Home had the greatest variation in conductance for a particular site. Plot 2 at Jerseydale had the highest conductance for 1993 needles, but plot 1 at Sly Park had a higher

conductance for 1992 needles. Although the plots at Shaver Lake had the lowest average conductance, plot 3 at Mountain Home had the lowest absolute conductance. Stomates were almost completely closed at this plot, despite apparently favorable environmental conditions. This plot was not included in the average stomatal conductance measurements used in section A5.1.

A5.3 Environmental Controls of Conductance

Multivariate regression analysis was used to determine the important environmental variables driving stomatal conductance and transpiration of the trees in these plots. Data on stomatal conductance and transpiration were the dependent variables and time of day, ambient temperature, PAR, RH, soil water, and elevations were the independent variables used in the regressions. For stomatal conductance, elevation and PAR were the only significant environmental variables in the regression equation:

$$\text{Conductance} = 0.12 - 0.22 \times 10^{-4} (\text{elev}) + 0.14 \times 10^{-4} (\text{PAR})$$

$$F = 8.00, r = 0.74, r^2 = 0.48, p < 0.01.$$

Elevation appeared to be a significant negative factor because the plots at Shaver Lake, which at 5400 ft were the highest plots, also had the lowest average conductance. The multivariate regression for transpiration was different in that soil water content was a significant factor, as was PAR:

$$\text{Transpiration} = 0.16 + 0.06 (\text{soil water}) + 0.59 \times 10^{-3} (\text{PAR})$$

$$F = 6.03, r = 0.69, r^2 = 0.40, p < 0.01.$$

The one factor that best predicted stomatal conductance was needle length (Figure A3-4). The regression equation between needle length and conductance had an r^2 of 0.56, $p < 0.01$. This suggests that needle length may be a good surrogate indicator for favorable growing conditions, which would also be correlated with more rapid rates of stomatal conductance. Number of years of needle retention, which is another indicator of favorable growing conditions in pines, may be inversely related to stomatal conductance, but in this study, years of needle retention was not significantly correlated with conductance.

A6. Conclusions

This survey of environmental factors controlling stomatal conductance in pine injury evaluation plots found significant variation in rates of conductance among sites, among plots, and among trees within plots. The trees at the Shaver Lake plots had the lowest average conductances, although plot 3 at Mountain Home had the lowest conductance of any plot. Plot 1 at Sly Park had the highest rate of conductance. No geographical trends were observed in these data. Although rates of stomatal conductance were inversely correlated with elevation, this appeared to be due to the low conductances of trees in the high elevation plots at Shaver Lake. Multiple regression analysis indicated a statistically significant but weak correlation between rates of stomatal conductance and transpiration and PAR. The best predictor of rates of conductance was needle length, which may be a good surrogate indicator of favorable growing conditions for the tree.

Table A3-1. Location of sites in the Forest Ozone Response Study.

Location	Latitude	Longitude	Elevation (m)
White Cloud (WC)	39 18	120 50	1270
Sly Park (SP)	38 44	120 33	1150
Five-Mile (FM)	38 03	120 18	1240
Jerseydale (JD)	37 32	119 50	1120
Shaver Lake (SL)	37 08	119 16	1636
Mountain Home MH	36 13	118 41	1364

Figure A3-1. Average stomatal conductance for 1993 and 1992 foliage for each site of the Forest Ozone Response Study. Sites are arranged geographically from north to south. 1 = White Cloud, 2 = Sly Park, 3 = Five Mile, 4 = Jerseydale, 5 = Shaver Lake, 6 = Mountain Home.

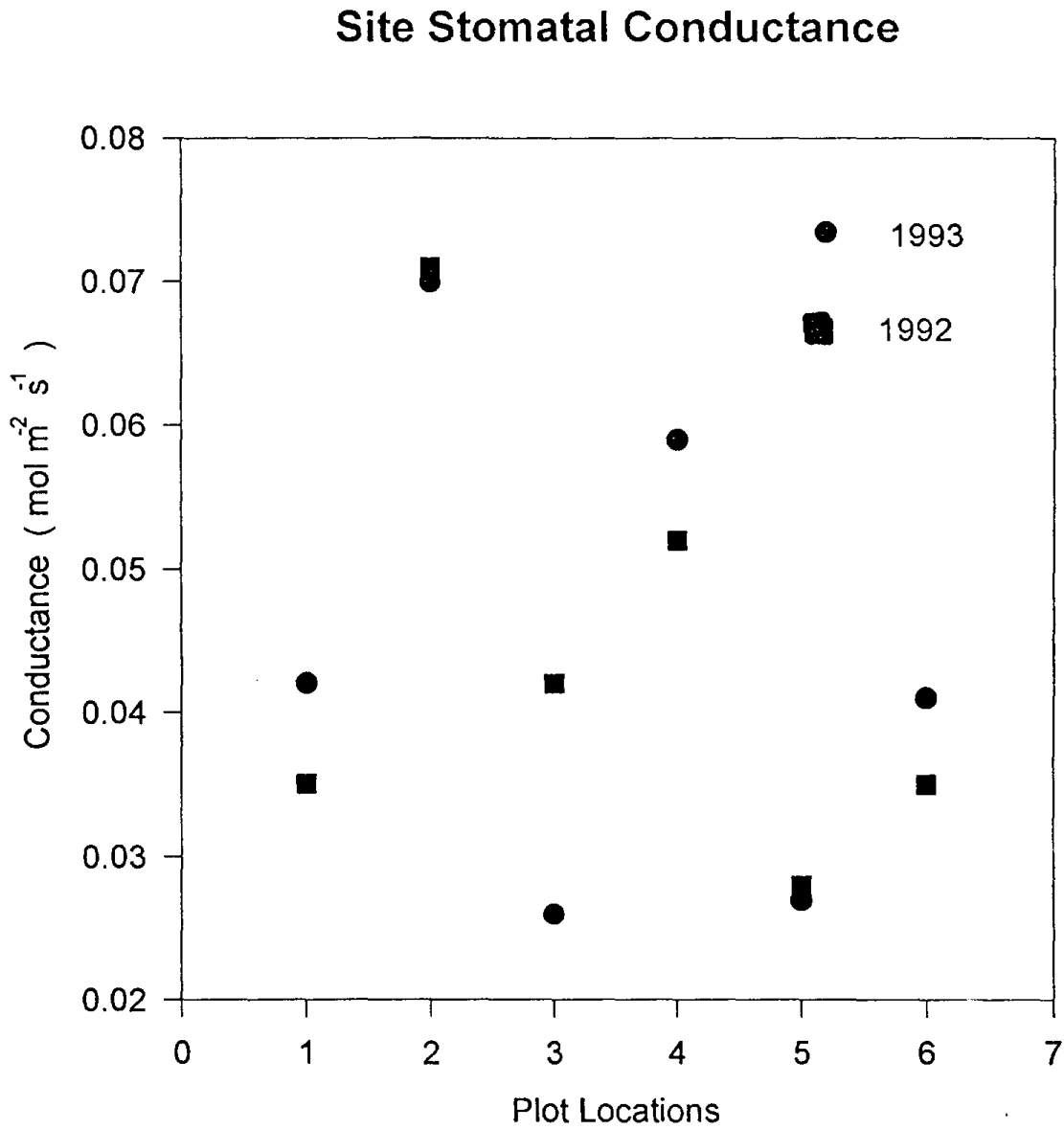


Figure A3-2. Average stomatal conductance for 1993 foliage from each plot at each FOREST site, arranged as in Figure A3-1.

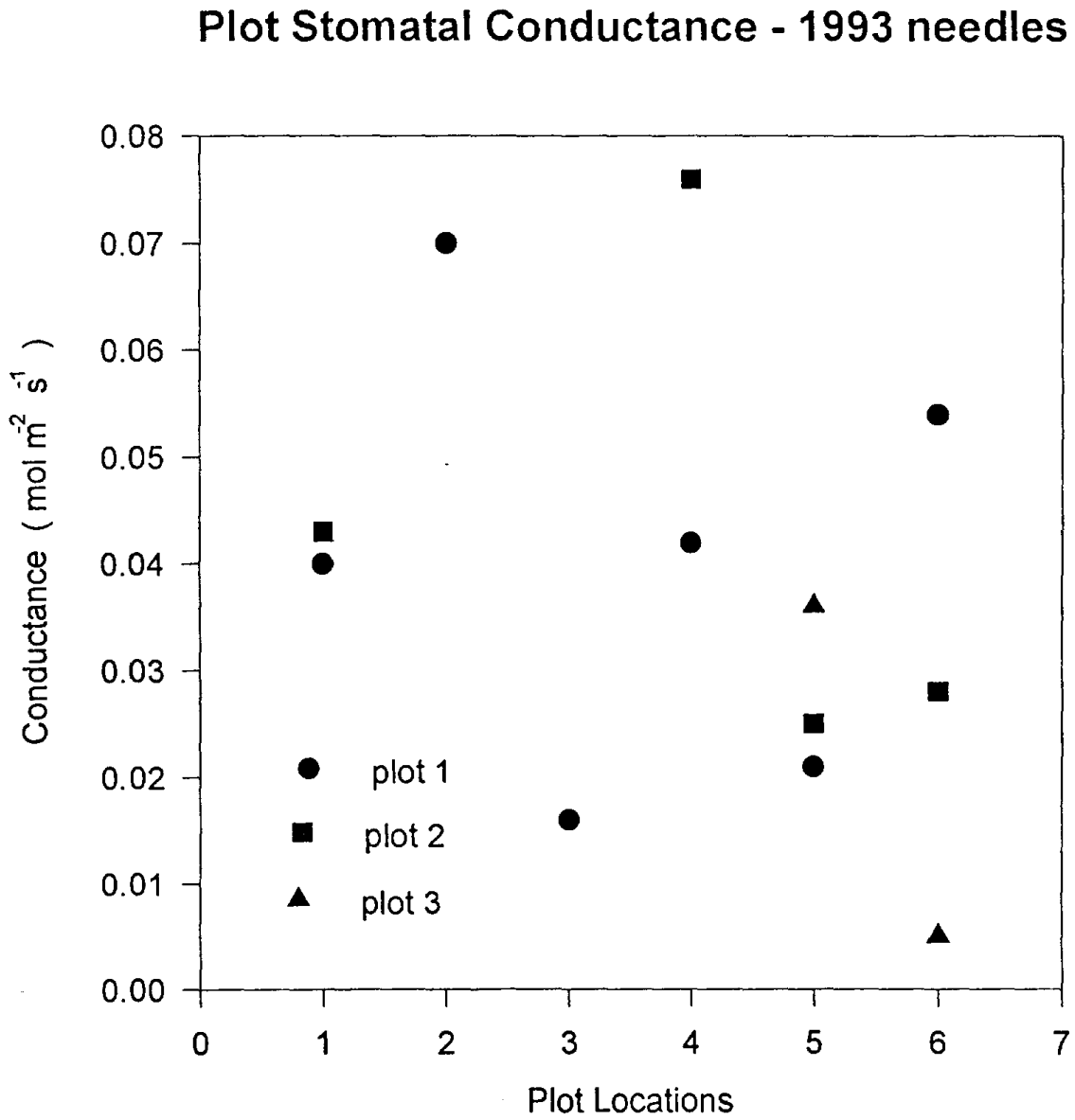


Figure A3-3. Average stomatal conductance for 1992 foliage from each plot at each FOREST site, arranged as in Figure A3-1.

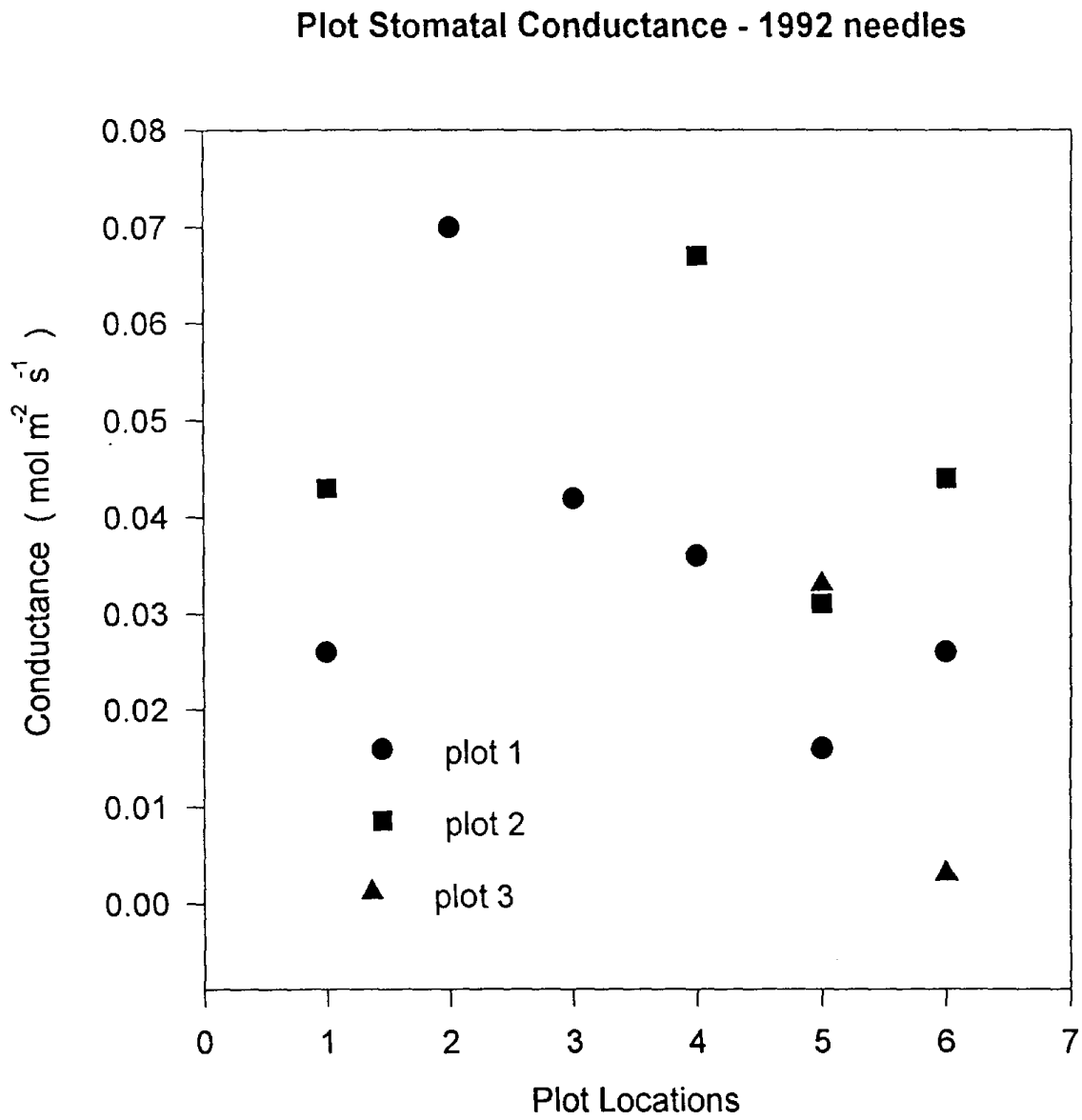
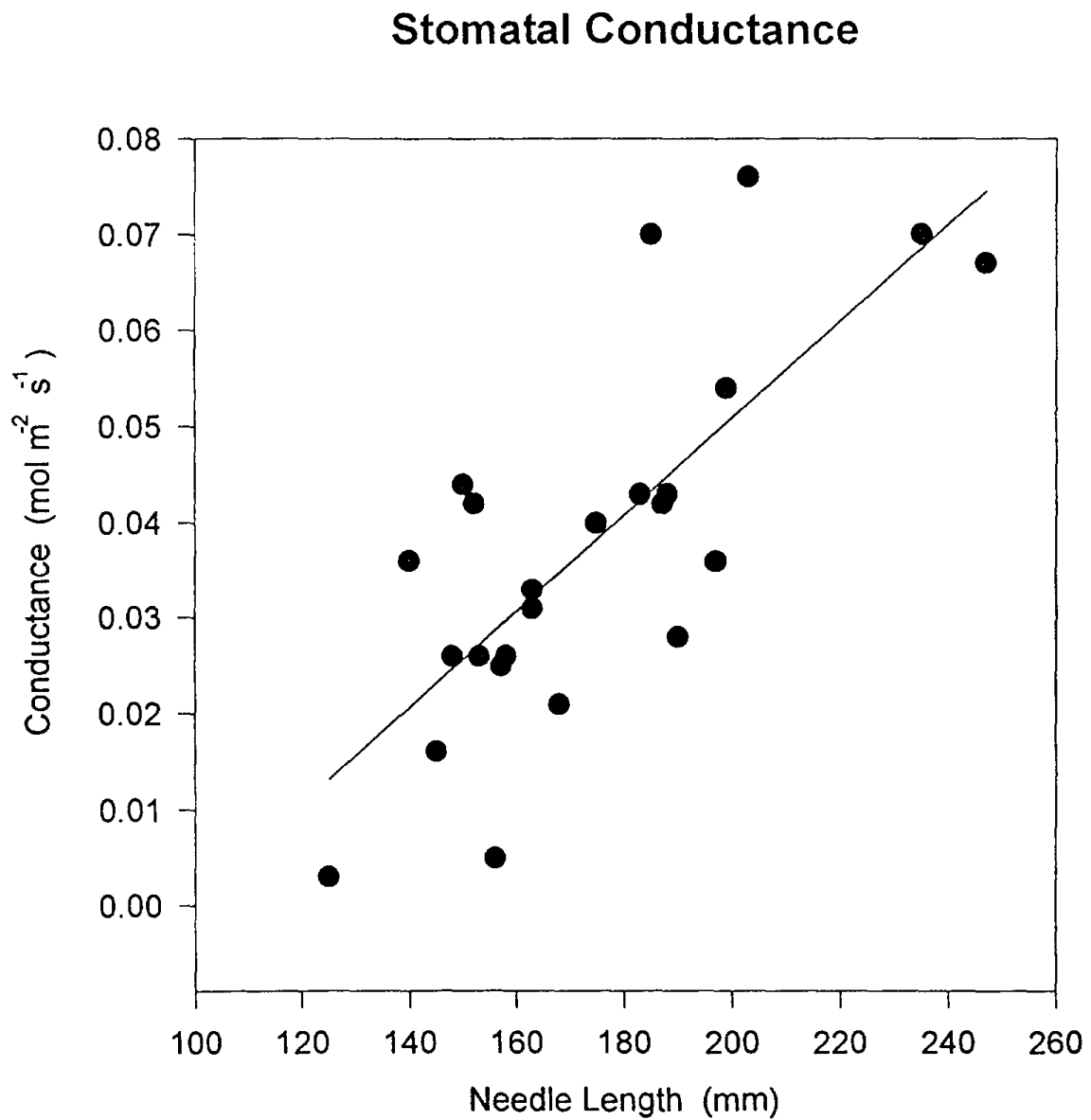


Figure A3-4. Relationship between stomatal conductance and needle length, across plots and sites for 1993 and 1992 foliage; $r^2 = 0.58$, $p = 0.01$.



4.0 INTENSIVE STUDY: DAY-TO-DAY DESCRIPTION OF METEOROLOGY, POLLUTANT CONCENTRATIONS, POLLUTANT DEPOSITION AND TREE RESPONSES FROM JULY 18 TO 31, 1993.

J. Chow, J. Watson, C. Frazier, G. Taylor, A. Bytnerowicz,
M. Poth, P. Temple, R. Glaubig, S. Schilling, D. Jones and P. Miller

4.1 Introduction

The purpose of this task was to examine selected variables measured at the Barton Flats monitoring station, the 29 m scaffold at plot 2, and the other vegetation plots on a day-to-day basis. This schedule was designed to reveal fine structure in events that may have been overlooked by the routine monitoring schedule carried out from 1991 to 1994. Figure 4-1 lists the variables to be measured and the frequency of measurement. The measurement of some variables, particularly throughfall and wet deposition and dry deposition/leaf washing depended on the occurrence of rain.

4.2 Methods

Most of the methods employed for this phase of the study, except for gas fluxes from soils, have already been documented in the final report of the companion ARB-sponsored Contract No. A032-180, and Volumes 1 and 2 of the associated Standard Operating Procedure manuals.

Soil Greenhouse Chamber System

Fluxes of NO and CO₂ were measured using a closed box flux technique (Anderson and Levine, 1987; Anderson and Poth, 1989). One day prior to making flux measurements six stainless steel frames, covering an area of 0.581 m² were driven 2.5 cm into the soil. In order to measure fluxes of either CO₂ or NO, a Teflon lined, expanded-cell polycarbonate box, fitted with a fan, and with a total volume of 150.5 liters (including the frame volume) was placed over the frame. The base of the flux box sealed to the frame via a Teflon covered foam lining. Two openings (0.64 cm) in the top of the flux box prevented pressure changes from developing during sampling. Since measurements were made during the summer, soils were relatively dry. After measuring trace gas flux rates of dry soils, distilled water equivalent to a 1 cm rainfall was added. After 1 hour, gas flux measurements were repeated and measured again the following day (24 hours after the water addition).

Analysis of Carbon Dioxide

Immediately upon setting the flux chamber on its frame, CO₂ was analyzed in sample air over a 3 min period using a LiCor 6200 photosynthesis system with integrated infrared gas analyzer and data system. The instrument was modified by removing the cuvette and substituting the flux box cover system described above as the input source. Standard errors for CO₂ fluxes using this system were < 1 percent of the rates measured.

Analysis of Nitric Oxide

Immediately following the 3 minute sampling period for CO₂ the sample stream was switched to a system for analysis of NO, which was detected over an 8 minute period using a Luminol, nitrogen dioxide (NO₂) detector (Model LMA-3, Scintrex-Unisearch, Toronto, Canada) as described in Anderson and Poth (1989). Sample air from the flux box, pumped at approximately 2.8 l min⁻¹ by a Teflon bellows, battery operated

pump was dried by passage through nafion tubing (Type 815, Dupont perfluorinated polymer, Perma Pure, Inc., Toms River, NJ) packed in indicating silica gel. NO in the dried sample gas was converted to NO₂ by passage through a tube (7.6 cm) containing 10 percent chromium trioxide on firebrick (30/60 mesh, Chromosorb P, Altech) before being pumped to a tee inlet on the LMA-3 NO₂ detector, which then sampled the gas stream at the rate of 1.5 l min⁻¹. A three-way valve which switched flow of sample air from the converter tube to a blank tube allowed measurement of either background NO₂ in sample air (following passage through the blank tube) or NO + NO₂ (following passage through the converter tube). The chromium trioxide/firebrick was replaced whenever a decrease in converter efficiency was observed during calibration. Calibrations and measurements of flow rates through the pumping system and the LMA-3 were performed at the beginning and at the end of each day of data collection. During calibration the LMA-3 was zeroed with room air which was first passed through a column containing pellets of alumina coated with KMnO₄ (Purafil, Southeastern Engineering Co., Midlothian, VA). This column reduces the background NO in room air to approximately 2 - 4 ppbv and obviates the need for transporting cylinders of zero air to field sites. For calibration NO (approximately 9 ppmv, Scott Environmental Technology, Plumsteadville, PA) was mixed with room air (after passage through KMnO₄ coated alumina) providing known concentrations of NO ranging from 20 - 50 ppbv. Gas flows were controlled with mass flow controllers (Tylan, model FC 280). Fluxes of NO were calculated from the slope of the regression line of NO vs. time (4 - 8 min) after correction of the NO concentration for dilution during sampling. The minimum flux of NO that could be measured with this detection and sampling system over an 8 min time span at 298K was 3.7 pg-N m⁻² s⁻¹.

4.3 Results

4.3.1 Description of Weather and Ozone during the Intensive Study.

4.3.1.1 Comparison of Meteorological Variables and Ozone for the July 18-31 Periods of 1992, 1993 and 1994 at the Barton Flats Monitoring Station

The intensive sampling period was characterized by comparing it with the same time interval in 1992 and 1994 using daylight (0600 to 1800 PST) means for temperature, relative humidity, solar radiation and ozone (Table 4-1). During the 1993 intensive study the 14 day temperature mean was 19.8° C compared to 21.4° C in 1992 and 22.7° C in 1994. The daylight relative humidity average was 33 percent in 1992 and 27 percent in 1993; the record was incomplete in 1994. The daylight ozone mean for the 14 day period was 68, 69, and 78 ppb for 1992, 1993, and 1994. Figure 4-2 shows the daily course of temperature and ozone for the July 18-31 periods of 1992, 1993, and 1994. In 1992 the temperature was rising gradually from the beginning to the end of the period. The ozone trace was relatively flat (range 51 to 82 ppb) for the same period compared to 1994 when daylight averages exceeded 100 ppb on two occasions. The mean daily solar radiation (w/m²) was 656, 711 and 597 for 1992, 1993, and 1994, respectively. There was a trace of rain on one day in each 1992 and 1994 but 1993 was dry. Wind speed and wind direction at 1600 did not vary much among the 3 years (Table 4-1). The 14 day average for wind speed at 1600 was 3.1 m/sec in 1993, generally from the west-northwest (263-332°). In conclusion, the 1993 intensive sampling period was a little cooler but otherwise not very different from 1992 and 1994.

4.3.1.2 Meteorological and Ozone Measurements in the Forest Canopy at Plot # 2 During July 18-31, 1993.

The day-to-day conditions at Barton Flats vegetation plot #2 are described by the hourly values for

temperature, relative humidity, and average wind speed, measured at 29 m and 2 m on the scaffold; ozone was measured nearby at 2 m using the solar powered trailer. There was very little variation in the daily temperature, wind speed and ozone measurements except for slight increase in all variables during Julian days 211 and 212 (Figure 4-3). The major feature on the weather map was a 500 millibar (mb) high pressure system that developed over the area. The ozone peak was highest on Julian day 212. Relative humidity shows a different pattern with the highest values on Julian days 205 to 207. The weather map showed a southward extension of a 500 mb low pressure system on these days. There was no rain. In conclusion, the weather during this period was very representative of the preceding and the following summers.

4.3.2 Dry Deposition Measurements at the Monitoring Station.

Intensive monitoring was conducted daily between 07/18/93 and 07/31/93 at three times per day to assess the diurnal variations of particulate matter and reactive gaseous species. Table 4-2 summarizes the averages; standard deviations; maximum and minimum concentrations for the morning (0600 to 1200 PST), afternoon (1200 to 1800 PST) and nighttime (1800 to next day 0600 PST) periods; and time weighted average of morning and afternoon samples.

The breakdown of daytime sampling intervals into the morning and afternoon periods provided more insight into the concentration variations. Table 4-2 shows that maximum mass, ions, and reactive species concentrations all occurred during the afternoon periods. In contrast, the lowest concentrations for the intensive monitoring period all occurred during the morning period, with the exception of $PM_{2.5}$ chloride and gaseous ammonia, sulfur dioxide, and nitric acid concentrations. It implies that $PM_{2.5}$ mass and ions varies significantly during the daytime and much of the information was not attainable by acquiring an integrated 12-hour sample.

Average daytime (0600-1800 PST) and nighttime (1800 to the next day 0600 PST) concentrations during the intensive sampling period (from 07/18/93 to 07/31/93 (14 samples), as originally presented in Table 2-9 of the Final Report of the companion project, ARB Contract No. A032-180, and 15 to 17 daytime and nighttime samples acquired from the same site during 06/01/94 and 08/31/94 (originally Table 2-10 in the Final Report of Contract No. A032-180) are presented together in Table 4-3 in order to compare the same number of samples taken in differing time periods. The difference among species were variable between 1993 and 1994.

4.3.3 Diurnal Variations of Particulate Nitrate, Nitric Acid, Particulate Ammonium, and Ammonia

Variations of gaseous and particulate phases of nitrate and ammonium compounds were examined for the morning, afternoon, and nighttime samples. Figure 4-4 shows that nitrate and ammonium compounds were a factor of two or more higher during the afternoon periods as compared to the other sampling periods. The most distinguishing features were found for $PM_{2.5}$ volatilized nitrate and ammonium concentrations which were a factor of two to ten times higher during the afternoon periods. Nitric acid concentrations were similar between the morning and afternoon samples, and a factor of seven to ten higher than the nighttime samples. Similar phenomena were found for ammonia with more pronounced concentrations during the afternoon periods.

07/27/93 - This day had a high concentration of nitric acid in the afternoon and higher than usual ratio of nitric acid to volatilized particulate nitrate. A trough of low surface pressure was present over the western United States. A trace of precipitation was recorded at San Diego. There appeared to be a deep

marine layer, resulting in greater than usual inland penetration of low clouds. This moisture would enhance formation of nitric acid, while the lower temperatures would minimize the volatilization of particulate nitrate.

4.3.4 Measurement of Greenhouse Gas Efflux from Soils at Plot 2

CO₂ and NO fluxes for the soils at Barton Flats are summarized in Figure 4-5. Because these measurements were made in August when water is limiting, the rates dramatically increased with the addition of water. Rates remained elevated for 24 hours. This experiment simulates the potential for gaseous emissions from these soils following summer rains.

4.3.5 Dry Deposition to Foliage at Plots 1, 2 and 3.

Deposition fluxes of nitrate and ammonium to branches of ponderosa pine seedlings placed at the forest floor were similar at all the study sites. Deposition fluxes to the pine seedlings at the top of the canopy (tower top) were higher than at the forest floor (Figures 4-6 and 4-7). Similar trends were seen for sulfate during the second period of the intensive study (Figure 4-8) (during the first period sulfate deposition fluxes were very variable and inconsistent). Deposition fluxes of nitrate, ammonium and sulfate to the branches of mature ponderosa pine, white fir and California black oak trees were also similar among different study sites. The highest deposition fluxes of nitrate and sulfate were recorded for California black oak. Deposition fluxes of ammonium to pine and oak were similar and higher than the deposition to white fir (Tables 4-4 and 4-5). In addition measurements of deposition to branches of seedlings and mature ponderosa pine trees at different levels of the forest canopy were also continued during the intensive study.

Information on deposition of nitrate, ammonium and sulfate to seedlings and mature trees, different tree species, and distribution of fluxes within forest canopy allowed for calculation of deposition of nitrogen and sulfur at the forest stand level.

In addition to the measurements of deposition of nitrate, ammonium and sulfate, determinations of deposition fluxes of potassium, sodium, calcium, and magnesium were also conducted. This information permitted the calculation of metal deposition to a forest stand during the "polluted" part of the year (see Section 5.0 of the Report for Contract No. A032-180).

The simulation of deposition to pine, white fir, and black oak with the Big Leaf model was available only for the entire month of July and not on a day-by-day basis.

4.3.6 Diurnal Variation of Stomatal Conductance During July 20-22, 1993

Hourly measurements of stomatal conductance for the three age classes of pines, averaged over a two-day period of intensive study in July 1993, are shown in Section 3 of this report in Figure 3-4. Conductance in the seedlings peaked at 0900, then remained relatively constant until 1500, when stomates began to close. Stomatal conductance in the saplings remained relatively constant throughout the day and declined only as light began to fade after 1800. The mature trees showed a similar pattern, with a rapid decline in conductance only after 1700, in response to fading light. These diurnal patterns of stomatal conductance for the three age classes of pines suggested that conductance rates were relatively constant throughout the day. Thus, a daily mean rate of conductance, calculated using conductance measurements taken from 0900 to 1200 and the number of hours of daylight, was an appropriate assumption for the calculation of ozone flux rates to the pines.

4.4 Discussion

The meteorological conditions and air chemistry measured during the intensive sampling period were very similar to the same period in 1992 and 1994. The morning (0600-1200) and afternoon (1200-1800) sample periods were a departure from the routine of daylight (0600-1800) sample period for the entire project and presented the opportunity to show clearly that most chemical species were at their lowest concentration in the morning, and highest in the afternoon. Nitric acid was an exception because highest concentrations could occur either in morning or afternoon. The 14 samples taken as daytime (0600 to 1800 PST) and nighttime (1800 to 0600 the following day) during the intensive study compared with 15-17 daytime and nighttime samples taken during a longer time span (06/01/94 to 08/31/94) suggested that results during these two spans were generally higher in the 1993 intensive period, except for SO₂ and NO₂.

The intensive study was the only time that nitrate and ammonium fluxes to ponderosa pine seedlings were measured simultaneously at all plots. There was no difference in flux rates at the three plots for pine seedlings. Similarly, a plot to plot comparison of flux rates of ammonium, nitrate and sulfate to mature branches of ponderosa pine, white fir and black oak did not show differences. California black oak received the highest amounts of nitrate and sulfate.

During this time of summer when soil moisture availability is declining it is expected that the amplitude of stomatal conductance would not be very large. Indeed, the daily curves were relatively flat and there was not much difference among conductances of the seedling, sapling and mature trees. The diurnal curves confirmed that 0900 to 1200 conductances were suitable for calculating ozone flux for the entire day.

CO₂ fluxes from soils were comparable to rates observed in Florida pine plantations (Castro *et al.*, 1994) and California chaparral (Anderson and Poth, 1989). The results can be considered typical and provide a reference point for making future comparisons.

The production of NO by soils is typically facilitated by nitrifying soil bacteria. The ratio of NO to N₂O emissions from soils is controlled by the water filled pore space. Given the relatively coarse nature of the soil at Barton Flats water filled pore space is typically low. Hence NO emissions dominate. Given that the processes that produce NO and N₂O are closely linked their emission are comparable on the basis of N content. The highest emissions of N trace gases are from soils in fertilized agricultural fields. These measurements are of the same order of magnitude as those seen in fertilized agriculture (Eichner, 1990). N fluxes from Barton Flats exceed the N flux from eastern forests (0.11 to 0.58 ng-N m⁻² s⁻¹) by an order of magnitude (Castro *et al.*, 1994).

Trace gas fluxes from soil can be a useful diagnostic tool when trying to determine forest condition. In dryer forests, like those in most of California, soil NO flux may be an important indicator of disturbance and N status. This is analogous to measurements of N₂O flux at more mesic sites (Sitaula *et al.*, 1996). N saturated sites in the San Bernardino Mountains of southern California have elevated NO soil fluxes (Fenn *et al.* in press). Soil CO₂ fluxes do increase in response to management disturbances (Dulohery *et al.*, 1996) and fire in California chaparral (Anderson and Poth, 1989). The results presented here for CO₂ provide a baseline for future comparisons in relation to acidic deposition or other changes and disturbances.

4.5 Summary

The separation of daytime sampling intervals into the morning and afternoon periods during the intensive

monitoring program between 07/18/93 and 07/31/93 provided insight into the diurnal variations of particle and gaseous concentrations. In most cases, gas and particle concentrations were lowest during the morning (i.e., 0600 to 1200 PST) and highest during the afternoon (i.e., 1200 to 1800 PST). Distribution and concentration levels found during the intensive period were mostly similar to routine monitoring data acquired during the summers of 1992 and 1994.

Dry deposition amounts to ponderosa pine, white fir, and black oak were similar for each species at plots 1,2 and 3. Of the three species black oak, showed the most deposition.

The measurement of stomatal conductances of seedling, sapling and mature Jeffrey pines over a diurnal period showed that 0900 to 1200 conductances were appropriate for estimating ozone flux for the entire daylight period.

CO₂ fluxes from soils were comparable to rates observed in other forest and chaparral soils. NO fluxes exceed those of eastern forests (0.11 to 0.58 ng-N m⁻² s⁻¹) by an order of magnitude.

In general, the conditions during the intensive study sampling period were very representative of typical mid-summer meteorology, air chemistry and tree physiology.

4.6 References

- Anderson, I. C., and J. S. Levine. 1987. Simultaneous field measurements of biogenic emissions of nitric oxide and nitrous oxide. *J. Geophys. Res.* 92:965-976.
- Anderson, I. C., and M. A. Poth. 1989. Semiannual losses of nitrogen as NO and N₂O from unburned and burned chaparral. *Global Biogeochem. Cycles* 3 (2):121-135.
- Castro, M. S., W.T. Peterjohn, J. M. Melillo, P. A. Steudler, H. L. Gholz, and D. Lewis. 1994. Effects of nitrogen fertilization on the fluxes of N₂O, CH₄, and CO₂ from soils in Florida slash pine plantations. *Canadian Journal of Forest Research* 24:9-13.
- Dulohery, C. J., L. A. Morris, and R. Lowrance. 1996. Assessing forest disturbance through biogenic gas fluxes. *Soil Science Society of America* 60:291-298.
- Eichner, M. J. 1990. Nitrous oxide emissions from fertilized soils: Summary of available data. *Journal of Environmental Quality* 19:272-280.
- Fenn, M. E., M. A. Poth, and D. J. Johnson. 1996. Evidence for nitrogen saturation in the San Bernardino Mountains in southern California. *Forest Ecology and Management* 81:in press.
- Sitaula, B. K., L. R. Bakken, and G. Abrahamsen. 1996. N-fertilization and soil acidification effects on N₂O and CO₂ emissions temperate pine forest soil. *Soil Biology and Biochemistry* 27:1401-14-08.

Table 4-1. Contrast of 0600 to 1800 (PST) averages for temperature, relative humidity, solar radiation and ozone; total daily precipitation, and winds at 1600 (the approximate time of the daily ozone peak) for the 07/18 to 07/31 periods of 1992, 1993 and 1994.

Date	July (Station)													
	18	19	20	21	22	23	24	25	26	27	28	29	30	31
1992														
¹ Temp. C°	24.7	25.2	21.2	19.8	18.4	19.1	18.8	19.7	21.2	22.8	24.0	23.6	20.1	20.8
¹ RH percent	18.6	16.4	30.9	28.0	35.9	31.7	46.1	39.0	32.8	29.2	27.2	17.5	48.1	55.1
¹ Solar Rad.	730	738	736	691	745	736	714	716	652	717	704	705	211	389
² Wind Speed	4.1	4.3	3.8	3.2	2.6	3.7	3.3	4.0	3.5	4.3	4.2	4.0	2.1	1.9
³ Wind Dir.	290	261	267	266	275	273	272	253	275	268	281	271	255	168
⁴ Precip (in.)	0	0	0	0	0	0	0	0	0	0	0	0	0	.24
¹ Ozone (ppb)	68	69	89	88	74	85	95	80	64	67	72	66	42	51
1993														
¹ Temp. C°	19.0	19.0	17.9	16.8	19.1	18.4	19.1	18.2	20.0	21.5	21.5	20.8	22.6	24.8
¹ RH percent	18.4	20.7	23.5	40.2	31.8	28.2	43.7	48.0	30.3	22.9	22.7	18.0	18.4	15.2
¹ Solar Rad.	748	724	752	695	693	718	723	723	736	735	730	654	714	615
² Wind Speed	3.6	3.3	4.1	2.1	2.8	3.3	3.1	2.6	2.6	2.7	2.6	4.1	3.7	4.0
³ Wind Dir.	270	274	263	332	279	268	290	295	314	278	284	267	273	272
⁴ Precip (in.)	0	0	0	0	0	0	0	0	0	0	0	0	0	0
¹ Ozone (ppb)	78	78	77	68	82	82	69	67	51	66	65	58	64	68
1994														
¹ Temp. C°	19.4	19.5	20.8	21.0	23.1	23.4	23.6	24.7	25.3	26.6	25.8	21.9	21.6	22.4
¹ RH percent	-	-	-	-	-	-	-	-	-	22.7	49.5	41.1	28.6	-
¹ Solar Rad.	425	568	403	415	648	698	733	721	655	694	689	290	707	713
² Wind Speed	2.6	3.4	2.4	3.7	4.0	4.5	3.8	5.1	4.0	3.8	4.1	1.3	5.0	4.0
³ Wind Dir.	283	274	268	278	263	259	263	313	302	292	259	313	261	267
⁴ Precip (in.)	0	0	0	0	0	0	0	0	0	0	0	.05	0	0
¹ Ozone (ppb)	70	79	79	103	76	65	66	67	64	83	107	87	85	66

¹ 6am - 6pm average

² meters/sec. @ 4pm

³ degrees @ 4pm

⁴ 24 hour total

Table 4-2. Statistical summary of gas/particle ambient concentrations acquired at the Barton Flats Station, CA, during the summer intensive period between 07/18/93 and 07/31/93

	Concentrations in $\mu\text{g}/\text{m}^3$					Concentrations in $\mu\text{g}/\text{m}^3$				
	Morning (0600 to 1200 PST)					Afternoon (1200 to 1800 PST)				
	Average	Std. Dev.	Maximum	Minimum	No. in Avg.	Average	Std. Dev.	Maximum	Minimum	No. in Avg.
PM _{2.5} Mass	4.	2.	8.	0.	13	15.	4.	22.	7.	14
Chloride (Cl ⁻)	0.02	0.02	0.07	0.00	14	0.03	0.03	0.11	0.00	14
Non-volatilized Nitrate (NO ₃ ⁻)	0.30	0.03	0.35	0.24	14	0.58	0.32	1.55	0.30	14
Sulfate (SO ₄ ⁼)	0.91	0.40	1.51	0.31	14	3.31	1.07	5.1	1.20	14
Ammonium (NH ₄ ⁺)	0.38	0.14	0.60	0.16	14	1.46	0.44	2.1	0.59	14
Ammonia (NH ₃)	1.79	0.68	3.6	0.90	14	5.4	1.7	9.0	2.2	14
Sulfur Dioxide (SO ₂)	0.4	0.2	0.7	0.0	14	0.9	0.4	1.6	0.1	14
Nitrogen Dioxide (NO ₂)	1.	1.	3.	0.	13	3.	2.	6.	2.	14
Total Particulate Nitrate (NO ₃ ⁻)	0.61	0.35	1.28	0.21	14	6.8	2.5	10.7	2.2	14
Nitric Acid (HNO ₃)	3.4	0.8	4.4	2.3	14	4.9	0.9	6.7	3.5	14
Sum of Ionic Species	1.62	0.55	2.5	0.78	14	5.4	1.6	7.5	2.3	14

	Concentrations in $\mu\text{g}/\text{m}^3$					Concentrations in $\mu\text{g}/\text{m}^3$				
	Daytime (0600 to 1800 PST) ^a					Nighttime (1800 to next day 0600 PST)				
	Average	Std. Dev.	Maximum	Minimum	No. in Avg.	Average	Std. Dev.	Maximum	Minimum	No. in Avg.
PM _{2.5} Mass	9.	2.	13.	6.	13	7.8	3.2	16.0	4.1	13
Chloride (Cl ⁻)	0.03	0.02	0.06	0.00	14	0.01	0.01	0.03	0.00	14
Non-volatilized Nitrate (NO ₃ ⁻)	0.44	0.16	0.90	0.32	14	0.40	0.39	1.53	0.08	14
Sulfate (SO ₄ ⁼)	2.11	0.69	3.1	0.89	14	1.42	0.40	2.3	0.89	14
Ammonium (NH ₄ ⁺)	0.92	0.27	1.3	0.42	14	0.69	0.23	1.11	0.39	14
Ammonia (NH ₃)	3.60	0.87	5.1	1.72	14	1.25	0.73	3.2	0.62	14
Sulfur Dioxide (SO ₂)	0.6	0.3	1.0	0.1	14	0.29	0.14	0.61	0.11	14
Nitrogen Dioxide (NO ₂)	2.	1.	4.	1.	13	2.1	1.1	4.5	0.8	14
Total Particulate Nitrate (NO ₃ ⁻)	3.7	1.4	5.8	1.2	14	1.64	1.09	3.2	0.24	14
Nitric Acid (HNO ₃)	4.2	0.8	5.5	3.1	14	0.5	0.2	0.9	0.2	14
Sum of Ionic Species	3.5	1.0	4.9	1.7	14	2.52	0.87	3.9	1.36	14

^a Calculated from daily averages of Morning and Afternoon concentrations.

Table 4-3. Comparison of the averages of 15-17 gas/particle ambient daytime and nighttime concentrations acquired at Barton Flats between 06/01/94 and 08/31/94 with 13-14 daytime and nighttime samples obtained during the intensive sampling period between 7/18/93 and 7/31/93.

Species	Concentrations $\mu\text{g}/\text{m}^3$			
	Daytime 1993	Daytime 1994	Nighttime 1993	Nighttime 1994
PM _{2.5} Mass	9.0	7.4	7.8	6.8
Chloride	0.03	0.04	0.01	0.04
Non-Volatilized Nitrate	0.44	0.40	0.40	0.31
Sulfate	2.11	1.50	1.42	1.39
Ammonium	0.92	0.62	0.69	0.64
Ammonia	3.60	3.80	1.25	1.30
Sulfur Dioxide	0.60	1.18	0.29	0.71
Nitrogen Dioxide	2.0	3.0	2.1	2.4
Total Particulate Nitrate	3.70	2.96	1.64	1.29
Nitric Acid	4.2	4.5	0.5	0.99
Sum of Ionic Species	3.5	2.4	2.5	2.2

Table 4-4. Deposition of nitrate and ammonium ($\mu\text{g m}^{-2} \text{h}^{-1}$) to branches of mature trees at the forest floor level during the intensive study.

Plot Number	Pine		Oak		Fir	
	NO_3^-	NH_4^+	NO_3^-	NH_4^+	NO_3^-	NH_4^+
July 19-23, 1993						
1	12.88 (4.68)	4.10 (1.38)	32.80 (5.67)	5.80 (1.59)	13.45 (1.11)	2.92 (0.75)
2	12.65 (3.99)	4.14 (1.13)	35.30 (11.32)	5.74 (1.61)	9.32 (6.45)	1.78 (1.55)
3	18.33 (9.95)	4.96 (2.37)	22.23 (8.94)	4.75 (2.44)	7.80 (4.80)	1.64 (1.54)
July 23-30, 1993						
1	13.21 (3.26)	3.80 (0.92)	29.70 (5.70)	5.53 (1.56)	15.06 (1.29)	2.90 (0.76)
2	16.10 (1.45)	4.84 (0.55)	30.37 (6.80)	5.08 (0.50)	8.18 (1.36)	1.21 (0.34)
3	19.58 (6.98)	4.71 (1.72)	24.89 (8.74)	4.16 (1.42)	10.08 (3.34)	2.14 (0.52)

Table 4-5. Deposition of sulfate to branches of mature trees at the forest floor level during the intensive study ($\mu\text{g m}^{-2} \text{h}^{-1}$).

Plot Number	Pine	Oak	Fir
July 19-23, 1993			
1	2.31 (1.17)	5.90 (2.26)	3.79 (4.10)
2	2.15 (0.30)	5.68 (2.12)	5.23 (0.23)
3	2.08 (0.62)	4.78 (3.22)	1.88 (0.20)
July 23-30, 1993			
1	2.02 (2.25)	3.13 (1.28)	0.68 (0.39)
2	1.70 (1.22)	4.00 (0.48)	1.35 (0.88)
3	2.48 (0.59)	8.67 (4.22)	1.25 (1.09)

Figure 4-2. Daily course of temperature and ozone for the 07/18 to 07/31 periods of 1992, 1993 and 1994.

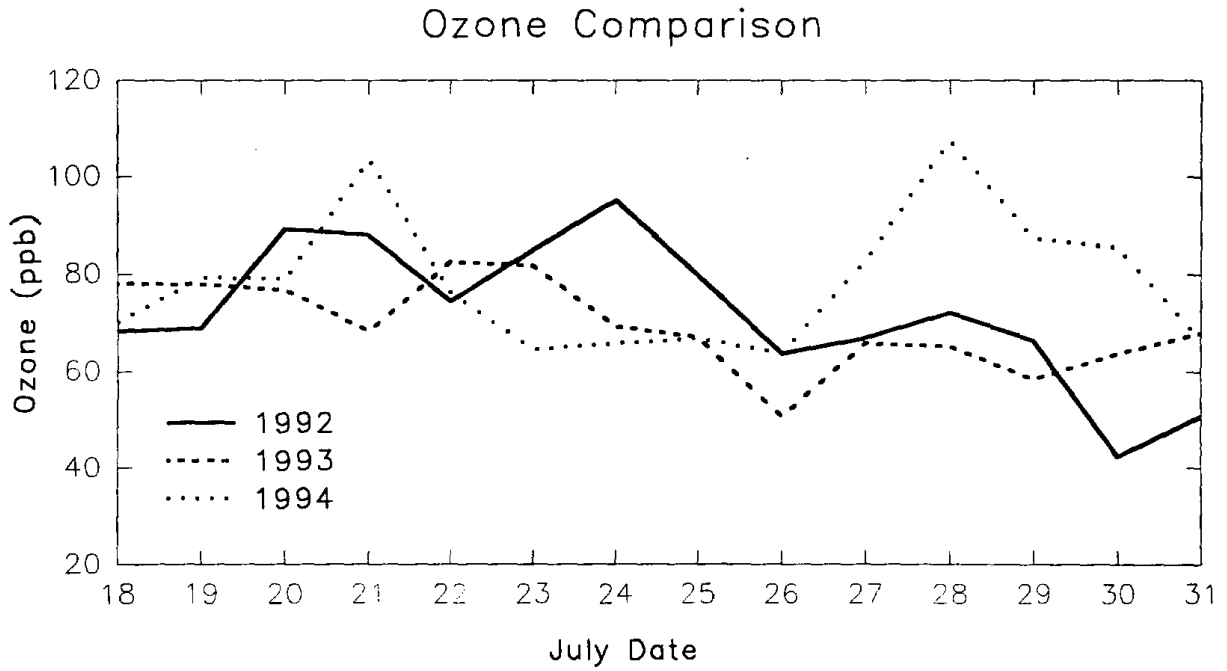
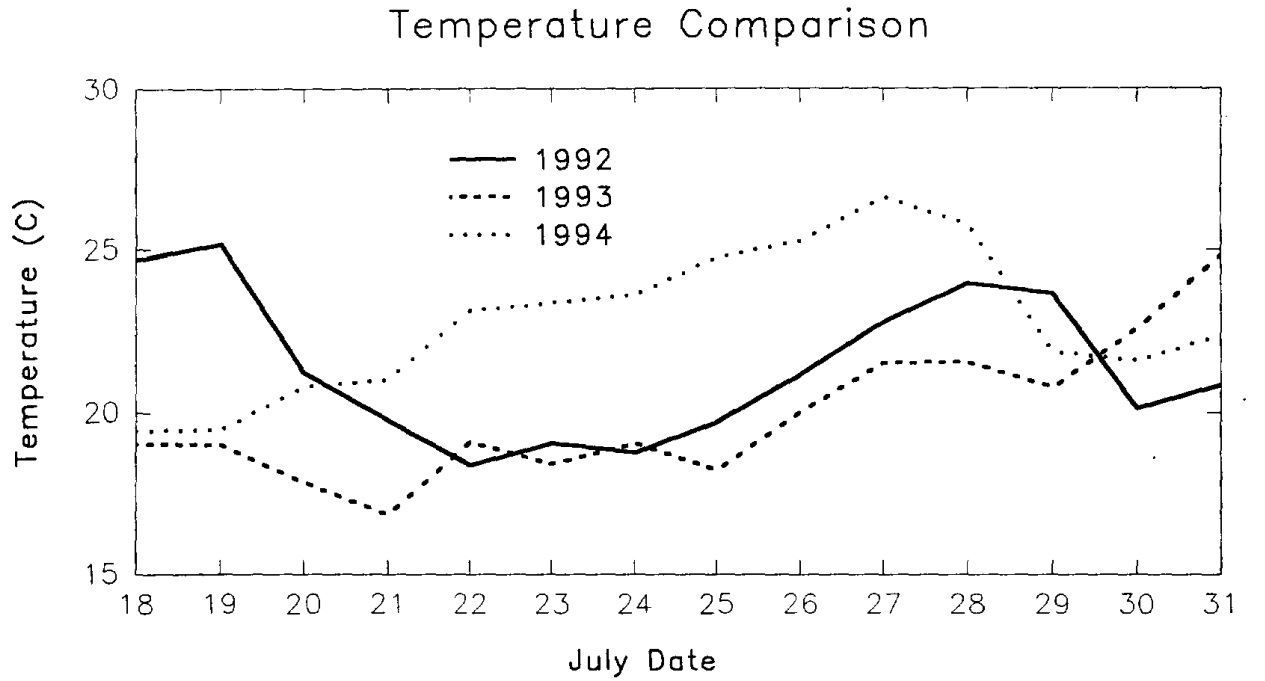


Figure 4-3. Average ozone, relative humidity, wind speed and temperature at the Plot 2 scaffolding during the intensive study, July 18-31, 1993.

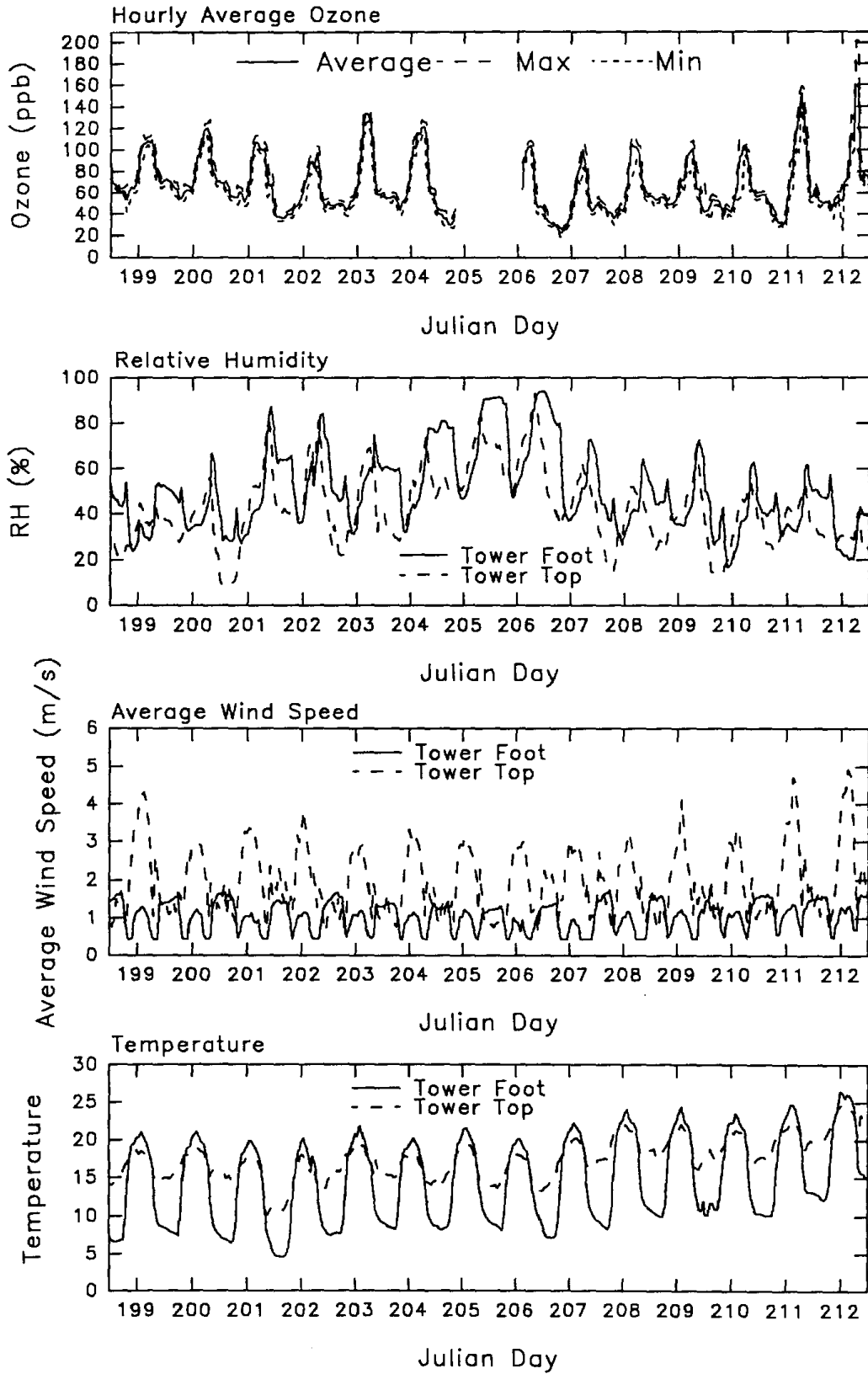


Figure 4-4. Diurnal variations of a) PM_{2.5} non-volatilized particulate nitrate, PM_{2.5} volatilized particulate nitrate and nitric acid, and b) PM_{2.5} non-volatilized particulate ammonium, PM_{2.5} volatilized particulate ammonium and gaseous ammonia at the Barton Flats Station, CA, during the 1993 summer intensive study (M=06:00-12:00, A=12:00-18:00, N=18:00-06:00 the next day)

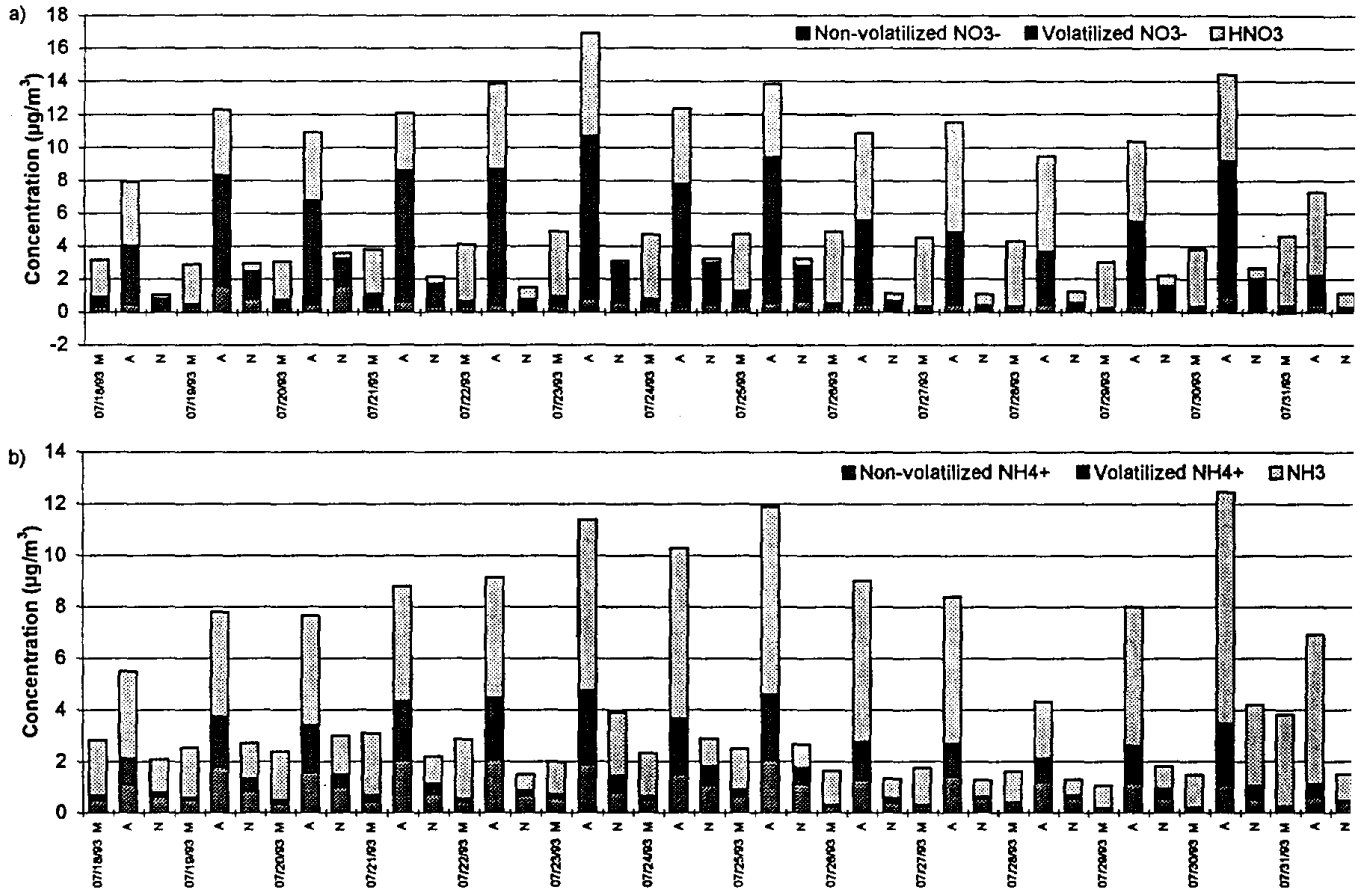


Figure 4-5. Summary of CO₂ and NO fluxes for the soils at Barton Flats, Plot 2.

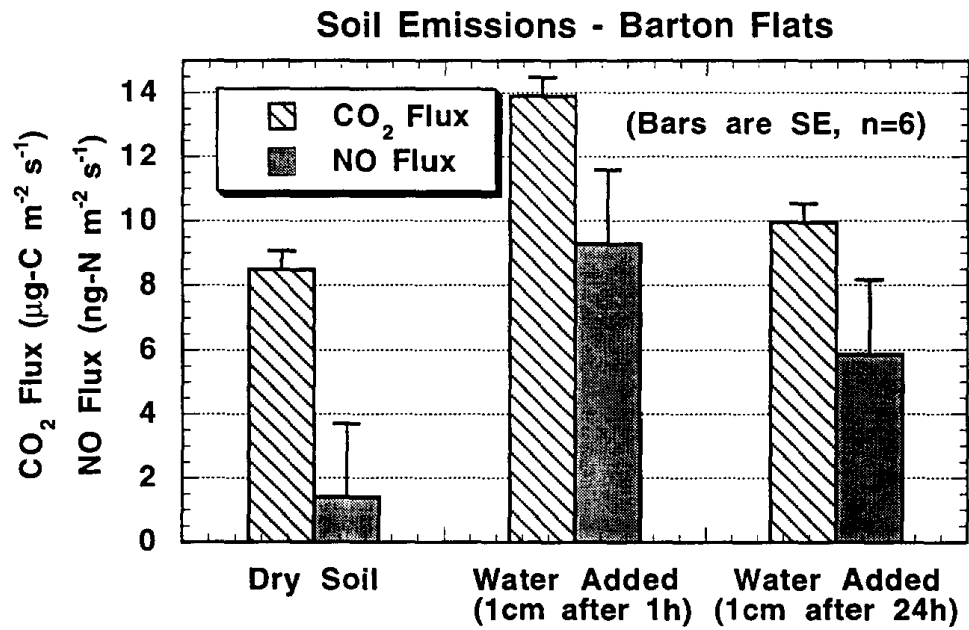


Figure 4-6. Deposition of nitrate to foliage of ponderosa pine seedlings located at the forest floor of Plots 1,2,and 3, roof of the monitoring station and tower top (Plot 2) during the July 23-30, 1993 period of the intensive study.

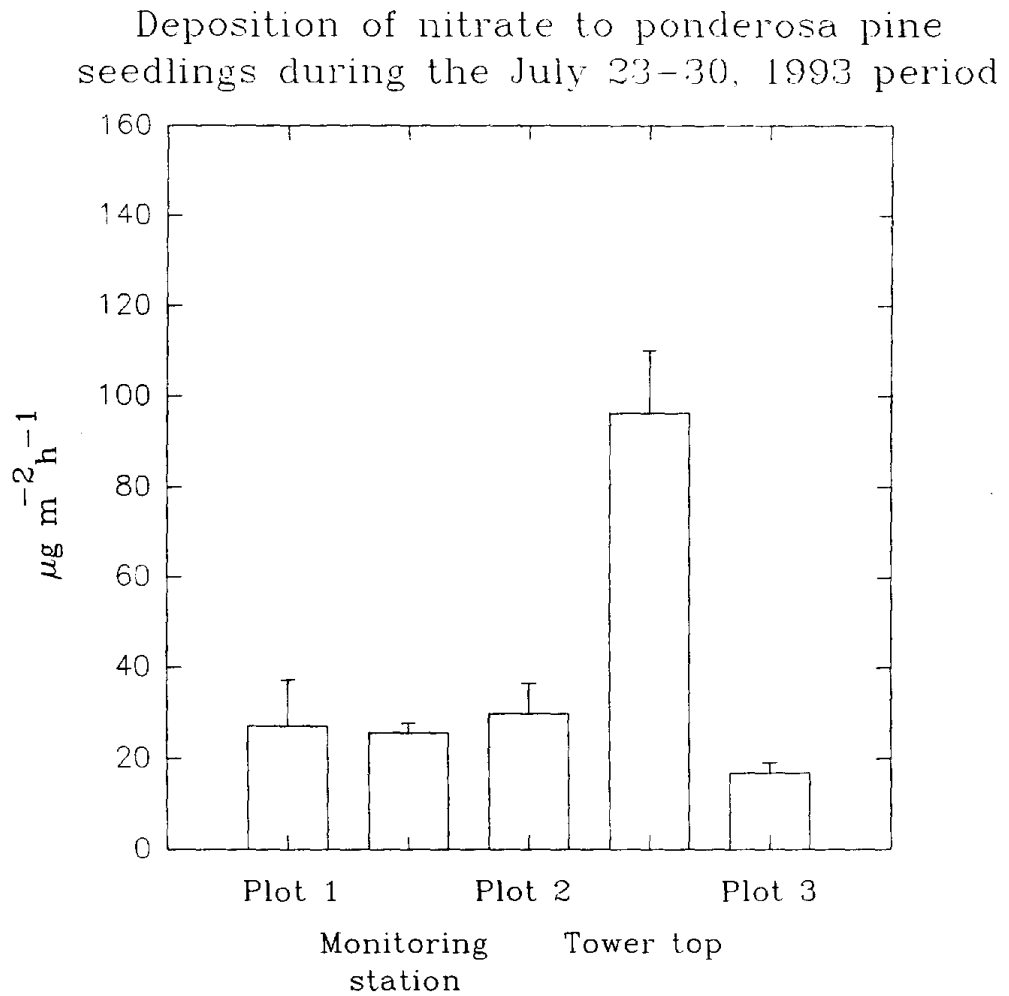


Figure 4-7. Deposition of ammonium to foliage of ponderosa pine seedlings located at the forest floor of Plots 1, 2 and 3, roof of the monitoring station and tower top (Plot 2) during the July 23 - 30, 1993 period of the intensive study.

Deposition of ammonium to ponderosa pine seedlings during the July 23-30, 1993 period

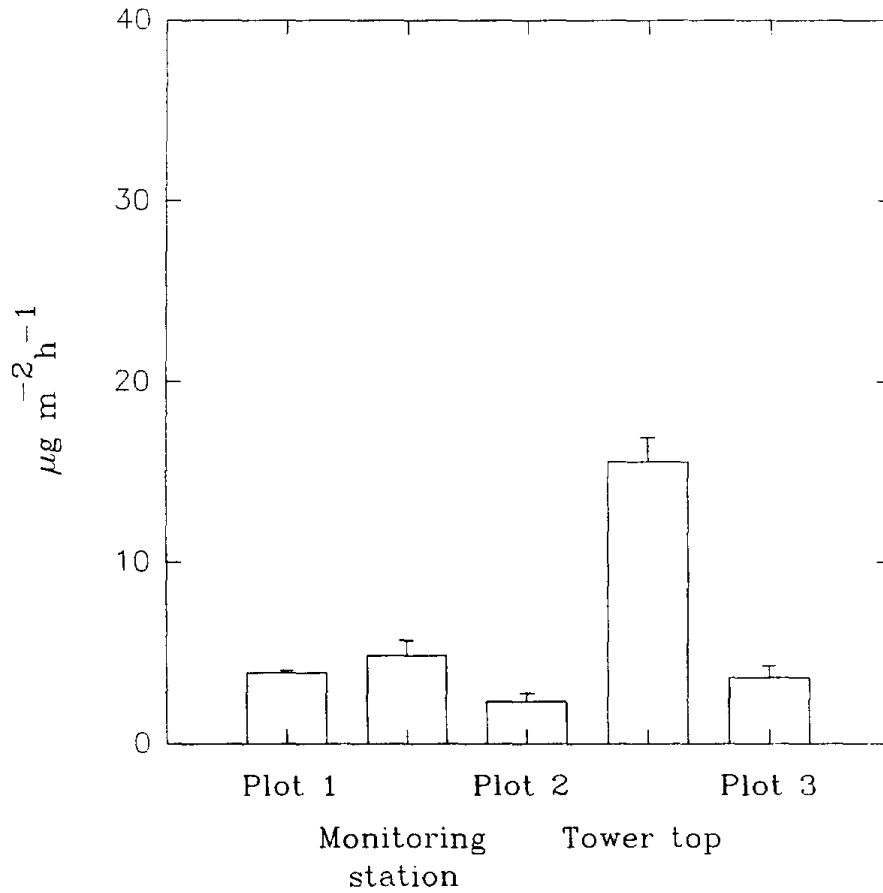


Figure 4-8. Deposition of sulfate to foliage of ponderosa pine seedlings located at the forest floor of Plots 1, 2 and 3, roof of the monitoring station and tower top (Plot 2) during the July 23 - 30, 1993 period of the intensive study.

Deposition of sulfate to ponderosa pine seedlings during the July 23-30, 1993 period

